

MORPHOLOGY, CYTOLOGY AND ULTRASTRUCTURE  
OF SELECTED SPECIES OF ENDOGONACEAE  
(ENDOGONALES: ZYgomycetes)

By

JACK L. GIBSON

A DISSERTATION PRESENTED TO THE GRADUATE SCHOOL  
OF THE UNIVERSITY OF FLORIDA  
IN PARTIAL FULFILLMENT OF THE REQUIREMENTS  
FOR THE DEGREE OF DOCTOR OF PHILOSOPHY

UNIVERSITY OF FLORIDA

1985

#### ACKNOWLEDGEMENTS

I wish to express my gratitude to Dr. James W. Kimbrough, chairman of the supervisory committee, for his guidance, patience and unfailing support throughout the course of this study. I also gratefully acknowledge the assistance and support of Dr. Henry C. Aldrich, member of the supervisory committee, and the staff of the Electron Microscopy Lab for valuable technical assistance and for the use of their facilities and equipment.

I am especially grateful to Dr. Gerald L. Benny for friendship, encouragement, and much valuable advice throughout this study. The assistance, encouragement, and many stimulating discussions about mycorrhizae with Dr. Norman C. Schenck, member of the supervisory committee, are also gratefully acknowledged.

Furthermore, I would like to thank Drs. Dana G. Griffin, III, and Walter S. Judd for their willingness to serve on the Supervisory Committee and for their support. Gratitude is also extended to the Department of Botany and the Florida Extension Service for financial support in the form of a graduate research assistantship over the course of this study.

LIST OF FIGURES

	<u>Page</u>
Fig. 1.1. <u>Endogone pisiformis</u> . Typical sporocarps on substrate of rotten wood. . . . .	23
Fig. 1.2. <u>Endogone pisiformis</u> . Squash mount of young sporocarp . . . . .	23
Fig. 1.3. <u>Endogone pisiformis</u> . Transverse section of sporocarp in Melzer's reagent . . . . .	23
Fig. 1.4. <u>Endogone pisiformis</u> . Zygosporangia enclosed by tapering peridial hyphae . . . . .	23
Fig. 1.5. <u>Endogone pisiformis</u> . Peridial hyphae stained with Melzer's reagent . . . . .	23
Fig. 1.6. <u>Endogone pisiformis</u> . Branching of peridial hyphae. . . . .	25
Fig. 1.7. <u>Endogone pisiformis</u> . Peridial hyphae in transverse section. . . . .	25
Fig. 1.8. <u>Endogone pisiformis</u> . Peridial hyphae relative to zygosporangia. . . . .	25
Fig. 1.9. <u>Endogone pisiformis</u> . Zygosporangia and peridial hyphae of sporocarp. . . . .	25
Fig. 1.10. <u>Endogone pisiformis</u> . Young zygosporangium with apposed gametangia . . . . .	25
Fig. 1.11. <u>Endogone pisiformis</u> . More mature stage in zygosporangium development. . . . .	25
Fig. 1.12. <u>Endogone pisiformis</u> . Mature zygospore within zygosporangium. . . . .	25
Fig. 1.13. <u>Endogone pisiformis</u> . Mature zygospore enclosed by zygosporangium . . . . .	27
Fig. 1.14. <u>Endogone pisiformis</u> . Several zygospores embedded in thin-walled glebal hyphae. . . . .	27
Fig. 1.15. <u>Endogone pisiformis</u> . Zygospore and more darkly stained zygosporangial wall. . . . .	27
Fig. 1.16. <u>Endogone pisiformis</u> . Zygosporangial wall continuous with gametangial wall. . . . .	27

Fig. 1.17. <u>Endogone pisiformis</u> . Gametangial remnants with concave gametangial septa. . . . .	27
Fig. 1.18. <u>Endogone pisiformis</u> . Early deposition of zygosporangium wall within zygosporangium. . . . .	29
Fig. 1.19. <u>Endogone pisiformis</u> . Gametangial attachment of young zygosporangium . . . . .	29
Fig. 1.20. <u>Endogone pisiformis</u> . Silver deposition on zygosporangial wall . . . . .	29
Fig. 1.21. <u>Endogone pisiformis</u> . Zygosporangium of intermediate maturity . . . . .	29
Fig. 1.22. <u>Endogone pisiformis</u> . Spore cytoplasm including lipid globules. . . . .	29
Fig. 1.23. <u>Endogone pisiformis</u> . Mature zygosporangium enclosed by zygosporangium. . . . .	29
Fig. 1.24. <u>Endogone pisiformis</u> . Layering of zygosporangium wall . . . . .	31
Fig. 1.25. <u>Endogone pisiformis</u> . Transition zone between zygosporangial and zygosporangium walls. . . . .	31
Fig. 1.26. <u>Endogone pisiformis</u> . Silver proteinate staining of zygosporangial surface material . . . . .	31
Fig. 1.27. <u>Endogone pisiformis</u> . Transition between zygosporangium wall and cytoplasm. . . . .	31
Fig. 1.28. <u>Endogone pisiformis</u> . Mature zygosporangium stained with barium permanganate. . . . .	31
Fig. 1.29. <u>Endogone pisiformis</u> . Zygosporangial and zygosporangium walls stained with barium permanganate. . . . .	31
Fig. 1.30. <u>Endogone pisiformis</u> . Median section of zygosporangium base . . . . .	33
Fig. 1.31. <u>Endogone pisiformis</u> . Secondary zygosporangial wall continuous with gametangial remnant . . . . .	33
Fig. 1.32. <u>Endogone pisiformis</u> . Continuity of primary zygosporangium and wall of gametangial remnant. . . . .	33
Fig. 1.33. <u>Endogone pisiformis</u> . Perforations in gametangial septum. . . . .	33
Fig. 1.34. <u>Endogone pisiformis</u> . Higher magnification of gametangial perforations. . . . .	33

Fig. 1.35. <u>Endogone pisiformis</u> . Glebal hypha showing early development of septum . . . . .	33
Fig. 1.36. <u>Endogone pisiformis</u> . Septum of glebal hypha with solitary pore. . . . .	33
Fig. 1.37. <u>Endogone pisiformis</u> . Higher magnification of septal pore . . . . .	33
Fig. 1.38. <u>Endogone pisiformis</u> . Clustered wall perforations in glebal hypha . . . . .	33
Fig. 1.39. <u>Endogone pisiformis</u> . Cytoplasmic constituents of glebal hypha. . . . .	35
Fig. 1.40. <u>Endogone pisiformis</u> . Nucleus of glebal hypha. . . . .	35
Fig. 1.41. <u>Endogone pisiformis</u> . Protein bodies of glebal hypha . . . . .	35
Fig. 1.42. <u>Endogone pisiformis</u> . Delimitation between unstained and silver-stained lipid globules . . . . .	35
Fig. 2.1. <u>Gigaspora margarita</u> . Whole mount of crushed azygospore. . . . .	61
Fig. 2.2. <u>Gigaspora margarita</u> . Azygospore fractured longitudinally. . . . .	61
Fig. 2.3. <u>Gigaspora margarita</u> . Azygospore base showing smooth wall and collapsed bulbous suspensor . . . . .	61
Fig. 2.4. <u>Gigaspora margarita</u> . Thin outer and thick inner layers of crushed azygospore wall . . . . .	61
Fig. 2.5. <u>Gigaspora margarita</u> . Higher magnification of azygospore wall . . . . .	61
Fig. 2.6. <u>Gigaspora margarita</u> . Thick inner layer of wall divided into several sublayers. . . . .	61
Fig. 2.7. <u>Gigaspora margarita</u> . Darkly stained outer wall layer and less intensely stained inner wall . . . . .	61
Fig. 2.8. <u>Gigaspora margarita</u> . Probable polyphosphate granules within spore cytoplasm. . . . .	61
Fig. 2.9. <u>Gigaspora margarita</u> . Cytoplasmic contents of azygospore. . . . .	63
Fig. 2.10. <u>Gigaspora margarita</u> . Higher magnification of spore wall. . . . .	63

Fig. 2.11. <i>Gigaspora margarita</i> . Higher magnification of outer wall layers . . . . .	63
Fig. 2.12. <i>Gigaspora margarita</i> . Higher magnification of inner wall layers . . . . .	63
Fig. 2.13. <i>Gigaspora margarita</i> . Several rippled layers of inner wall . . . . .	63
Fig. 2.14. <i>Gigaspora margarita</i> . Details of outer wall layer. . . . .	63
Fig. 2.15. <i>Gigaspora margarita</i> . Azygospore wall stained with barium permanganate . . . . .	63
Fig. 2.16. <i>Gigaspora margarita</i> . Higher magnification of barium permanganate-stained azygospore wall. . . . .	63
Fig. 2.17. <i>Gigaspora margarita</i> . Details of spore wall stained with barium permanganate. . . . .	65
Fig. 2.18. <i>Gigaspora margarita</i> . Azygospore stained with silver proteinate . . . . .	65
Fig. 2.19. <i>Gigaspora margarita</i> . Silver-stained azygospore wall . .	65
Fig. 2.20. <i>Gigaspora margarita</i> . Silver deposited on outer portion of outer wall layer . . . . .	65
Fig. 2.21. <i>Gigaspora margarita</i> . Thickened area of innermost wall layer. . . . .	65
Fig. 2.22. <i>Gigaspora margarita</i> . Fully developed thickening of innermost wall layer . . . . .	65
Fig. 2.23. <i>Gigaspora margarita</i> . Closely spaced thickenings of innermost wall layer . . . . .	65
Fig. 2.24. <i>Gigaspora margarita</i> . Various organelles of spore cytoplasm . . . . .	65
Fig. 2.25. <i>Gigaspora margarita</i> . Cytoplasm adjacent to azygospore wall . . . . .	67
Fig. 2.26. <i>Gigaspora margarita</i> . Irregularly shaped, granular nuclei within spore cytoplasm . . . . .	67
Fig. 2.27. <i>Gigaspora margarita</i> . Partially disrupted nuclear envelope. . . . .	67
Fig. 2.28. <i>Gigaspora margarita</i> . Nucleus with single nucleolus and discontinuous envelope. . . . .	67

Fig. 2.29. <i>Gigaspora margarita</i> . Portion of spore cytoplasm with few nuclei . . . . .	67
Fig. 2.30. <i>Gigaspora margarita</i> . Nucleus with nucleolus and smooth, continuous envelope . . . . .	67
Fig. 2.31. <i>Gigaspora heterogama</i> . Whole mount of crushed azygospore. . . . .	69
Fig. 2.32. <i>Gigaspora heterogama</i> . Base of crushed azygospore. . . . .	69
Fig. 2.33. <i>Gigaspora heterogama</i> . Surface ornamentation and bulbous suspensor at spore base . . . . .	69
Fig. 2.34. <i>Gigaspora heterogama</i> . Azygospore wall in surface view .	69
Fig. 2.35. <i>Gigaspora heterogama</i> . Cupulate ornaments of spore surface . . . . .	69
Fig. 2.36. <i>Gigaspora heterogama</i> . Azygospore wall in optical section . . . . .	69
Fig. 2.37. <i>Gigaspora heterogama</i> . Broken spore with portion of membranous inner layer exposed . . . . .	69
Fig. 2.38. <i>Gigaspora heterogama</i> . Membranous inner wall partially separated from outer wall . . . . .	71
Fig. 2.39. <i>Gigaspora heterogama</i> . Sublayering of membranous inner wall. . . . .	71
Fig. 2.40. <i>Gigaspora heterogama</i> . Outer wall broken open. . . . .	71
Fig. 2.41. <i>Gigaspora heterogama</i> . Sublayering of outer wall . . . . .	71
Fig. 2.42. <i>Gigaspora heterogama</i> . Membranous inner wall separated from outer wall . . . . .	71
Fig. 2.43. <i>Gigaspora heterogama</i> . Various layers of outer wall. . . . .	71
Fig. 2.44. <i>Gigaspora heterogama</i> . Higher magnification of outer wall. . . . .	71
Fig. 2.45. <i>Gigaspora heterogama</i> . Higher magnification of membranous inner wall . . . . .	71
Fig. 2.46. <i>Gigaspora heterogama</i> . parallel orientation of fibrillar material of outer wall. . . . .	71
Fig. 2.47. <i>Gigaspora heterogama</i> . Inner membranous wall containing two germ chambers. . . . .	73

Fig. 2.48. <u>Gigaspora heterogama</u> . Position of germ chamber within inner layer of membranous wall . . . . .	73
Fig. 2.49. <u>Gigaspora heterogama</u> . Higher magnification of membranous wall and germ chambers . . . . .	73
Fig. 2.50. <u>Gigaspora heterogama</u> . Radial and tangential walls and cytoplasm of germ chambers. . . . .	73
Fig. 2.51. <u>Gigaspora pellucida</u> . Whole mount of azygospore. . . . .	75
Fig. 2.52. <u>Gigaspora pellucida</u> . Smooth surface and bulbous suspensor of azygospore . . . . .	75
Fig. 2.53. <u>Gigaspora pellucida</u> . Crushed azygospore showing walls and bulbous suspensor . . . . .	75
Fig. 2.54. <u>Gigaspora pellucida</u> . Higher magnification of bulbous suspensor . . . . .	75
Fig. 2.55. <u>Gigaspora pellucida</u> . Base of azygospore in surface view. . . . .	75
Fig. 2.56. <u>Gigaspora pellucida</u> . Membranous wall separated from outer wall . . . . .	75
Fig. 2.57. <u>Gigaspora pellucida</u> . Outer wall of azygospore appearing as a single layer . . . . .	77
Fig. 2.58. <u>Gigaspora pellucida</u> . Outer wall divided into two layers. . . . .	77
Fig. 2.59. <u>Gigaspora pellucida</u> . Crushed outer wall separated into three layers . . . . .	77
Fig. 2.60. <u>Gigaspora pellucida</u> . Darkly stained outer wall and less intensely stained inner wall . . . . .	77
Fig. 2.61. <u>Gigaspora pellucida</u> . Outer wall separated from inner wall by double membrane-like partition . . . . .	77
Fig. 2.62. <u>Gigaspora pellucida</u> . Higher magnification of fine, double membrane-like partition and walls. . . . .	77
Fig. 2.63. <u>Gigaspora pellucida</u> . Separation of outer and inner walls . . . . .	77
Fig. 2.64. <u>Gigaspora pellucida</u> . Higher magnification of outer wall lamellae . . . . .	79
Fig. 2.65. <u>Gigaspora pellucida</u> . Densely stained outer and greatly expanded membranous inner walls . . . . .	79

Fig. 2.66. <i>Gigaspora pellucida</i> . Azygospore wall showing increased thickness due to microfibrillar expansion . . . . .	79
Fig. 2.67. <i>Gigaspora pellucida</i> . Outer wall and germ chambers of chlamydospores. . . . .	79
Fig. 2.68. <i>Gigaspora pellucida</i> . Germ chambers within disrupted zone of membranous wall . . . . .	79
Fig. 2.69. <i>Gigaspora pellucida</i> . Higher magnification of germ chamber. . . . .	79
Fig. 2.70. <i>Gigaspora pellucida</i> . Spore wall post stained with silver proteinate . . . . .	79
Fig. 2.71. <i>Gigaspora pellucida</i> . Deposition of silver on outer spore wall. . . . .	79
Fig. 2.72. <i>Gigaspora gigantea</i> . Cross section of whole azygospore .	81
Fig. 2.73. <i>Gigaspora gigantea</i> . Base of azygospore with bulbous suspensor . . . . .	81
Fig. 2.74. <i>Gigaspora gigantea</i> . Opening in base of azygospore wall to bulbous suspensor . . . . .	81
Fig. 2.75. <i>Gigaspora gigantea</i> . Crushed azygospore showing outer wall. . . . .	81
Fig. 2.76. <i>Gigaspora gigantea</i> . Outer wall of crushed spore separated from inner wall . . . . .	81
Fig. 2.77. <i>Gigaspora gigantea</i> . darkly stained outer and less intensely stained inner walls. . . . .	81
Fig. 2.78. <i>Gigaspora gigantea</i> . Thin innermost wall layer of spore. . . . .	81
Fig. 2.79. <i>Gigaspora gigantea</i> . Microfibrillar orientation of outer wall. . . . .	81
Fig. 2.80. <i>Gigaspora gigantea</i> . Outer and inner wall sublayering and texture . . . . .	81
Fig. 2.81. <i>Gigaspora gigantea</i> . Characteristic thickening of innermost wall layer . . . . .	81
Fig. 2.82. <i>Gigaspora gregaria</i> . Whole mount of crushed azygospore. . . . .	83
Fig. 2.83. <i>Gigaspora gregaria</i> . Thick, plastic section of azygospore wall . . . . .	83

Fig. 2.84. <u>Gigaspora gregaria</u> . Higher magnification of outer wall. . . . .	83
Fig. 2.85. <u>Gigaspora gregaria</u> . Continuity of spore and suspensor inner walls . . . . .	83
Fig. 2.86. <u>Gigaspora gregaria</u> . Ornamentation layer and electron opaque inner layer of outer wall . . . . .	83
Fig. 2.87. <u>Gigaspora gregaria</u> . Fibrillar nature of surface ornamentation layer . . . . .	83
Fig. 2.88. <u>Gigaspora gregaria</u> . Deposition of silver on ornamentation layer and outer portion of outer wall . . . .	83
Fig. 2.89. <u>Gigaspora gregaria</u> . Higher magnification showing silver deposition on outer wall . . . . .	83
Fig. 3.1. <u>Glomus intraradices</u> . Whole mount of chlamydospores. . .	103
Fig. 3.2. <u>Glomus intraradices</u> . Fractured chlamydospore showing outer wall. . . . .	103
Fig. 3.3. <u>Glomus intraradices</u> . Lipid globules and inner wall of fractured chlamydospore . . . . .	103
Fig. 3.4. <u>Glomus intraradices</u> . Higher magnification of chlamydospore surface . . . . .	103
Fig. 3.5. <u>Glomus intraradices</u> . Inner wall sublayering of fractured chlamydospore. . . . .	103
Fig. 3.6. <u>Glomus intraradices</u> . Thick, plastic section of chlamydospore showing wall structure. . . . .	103
Fig. 3.7. <u>Glomus intraradices</u> . Lipid globules enclosed by multilayered inner wall . . . . .	105
Fig. 3.8. <u>Glomus intraradices</u> . Transverse section of chlamydospore . . . . .	105
Fig. 3.9. <u>Glomus intraradices</u> . Inner wall partially separated from outer wall . . . . .	105
Fig. 3.10. <u>Glomus intraradices</u> . Wall structure of senescent chlamydospore . . . . .	105
Fig. 3.11. <u>Glomus intraradices</u> . Outer wall of degraded chlamydospore . . . . .	105
Fig. 3.12. <u>Glomus intraradices</u> . Higher magnification of senescent chlamydospore . . . . .	105

Fig. 3.13. <i>Glomus intraradices</i> . Septal perforations of intraradical hypha . . . . .	107
Fig. 3.14. <i>Glomus intraradices</i> . Nonperforate and perforate septa of intraradical hypha . . . . .	107
Fig. 3.15. <i>Glomus intraradices</i> . Higher magnification of septal perforations . . . . .	107
Fig. 3.16. <i>Glomus intraradices</i> . Higher magnification of nonperforate septum . . . . .	107
Fig. 3.17. <i>Glomus intraradices</i> . chlamydospores within root . . . . .	107
Fig. 3.18. <i>Glomus intraradices</i> . Chlamydospores and hyphae within root . . . . .	109
Fig. 3.19. <i>Glomus intraradices</i> . Hyphae oriented longitudinally within root cortex. . . . .	109
Fig. 3.20. <i>Glomus intraradices</i> . Arbuscules within root cortical cells . . . . .	109
Fig. 3.21. <i>Glomus intraradices</i> . Higher magnification of colonized root. . . . .	109
Fig. 3.22. <i>Glomus intraradices</i> . Collapsed arbuscule within cortical cell . . . . .	109
Fig. 3.23. <i>Glomus intraradices</i> . Finely branched and collapsed arbuscules within cortical cells. . . . .	111
Fig. 3.24. <i>Glomus intraradices</i> . Arbuscular branches within cortical cell . . . . .	111
Fig. 3.25. <i>Glomus intraradices</i> . Granular matrix between wall of arbuscular branch and host plasmalemma. . . . .	111
Fig. 3.26. <i>Glomus intraradices</i> . Tannin body of colonized cortical cell . . . . .	111
Fig. 3.27. <i>Glomus intraradices</i> . Mass of collapsed arbuscular material enclosed by tonoplast. . . . .	111
Fig. 3.28. <i>Glomus intraradices</i> . Higher magnification of collapsed arbuscular branches . . . . .	111
Fig. 3.29. <i>Glomus constrictum</i> . Whole mount of chlamydospore. . . . .	113
Fig. 3.30. <i>Glomus constrictum</i> . Constriction of hyphal connection at chlamydospore base. . . . .	113

Fig. 3.31. <u>Glomus constrictum</u> . Outer surface of fractured chlamydospore . . . . .	113
Fig. 3.32. <u>Glomus constrictum</u> . Uniform, single wall of chlamydospore . . . . .	113
Fig. 3.33. <u>Glomus constrictum</u> . Spore wall split into two sublayers . . . . .	113
Fig. 3.34. <u>Glomus constrictum</u> . Lamellate appearance of chlamydospore wall . . . . .	113
Fig. 3.35. <u>Glomus constrictum</u> . Chlamydospore wall in optical section . . . . .	113
Fig. 3.36. <u>Glomus constrictum</u> . Spore cytoplasm enclosed by lamellate wall . . . . .	115
Fig. 3.37. <u>Glomus constrictum</u> . Microfibrillar pattern of spore wall . . . . .	115
Fig. 3.38. <u>Glomus constrictum</u> . Bands of spore wall microfibrils . . . . .	115
Fig. 3.39. <u>Glomus constrictum</u> . Cluster of nuclei within chlamydospore cytoplasm . . . . .	115
Fig. 3.40. <u>Glomus constrictum</u> . Double membrane-bound nucleus within spore cytoplasm . . . . .	115
Fig. 3.41. <u>Glomus etunicatum</u> . Whole mount of chlamydospore . . . . .	117
Fig. 3.42. <u>Glomus etunicatum</u> . Wall of crushed chlamydospore . . . . .	117
Fig. 3.43. <u>Glomus etunicatum</u> . Outer wall of spore separated from inner wall . . . . .	117
Fig. 3.44. <u>Glomus etunicatum</u> . Crushed chlamydospore showing separation of walls . . . . .	117
Fig. 3.45. <u>Glomus etunicatum</u> . Higher magnification of separated spore walls . . . . .	117
Fig. 3.46. <u>Glomus etunicatum</u> . Coarse, fibrous texture of outer spore wall . . . . .	119
Fig. 3.47. <u>Glomus etunicatum</u> . Uneven surface and sublayering of outer spore wall . . . . .	119
Fig. 3.48. <u>Glomus etunicatum</u> . Higher magnification of outer wall . . . . .	119

Fig. 3.49. <u>Glomus etunicatum</u> . Multilayered inner wall of mature spore . . . . .	119
Fig. 3.50. <u>Glomus etunicatum</u> . Higher magnification of outer lamellae of inner spore wall . . . . .	119
Fig. 3.51. <u>Glomus etunicatum</u> . Higher magnification of inner wall showing less distinct lamellae . . . . .	119
Fig. 3.52. <u>Sclerocystis coremioides</u> . Sporocarps with peridia of interwoven hyphae . . . . .	121
Fig. 3.53. <u>Sclerocystis coremioides</u> . Higher magnification of sporocarp surface . . . . .	121
Fig. 3.54. <u>Sclerocystis coremioides</u> . Central plexus of sporocarp .	121
Fig. 3.55. <u>Sclerocystis coremioides</u> . Thick, plastic section of sporocarp . . . . .	121
Fig. 3.56. <u>Sclerocystis coremioides</u> . Higher magnification of sporocarp . . . . .	121
Fig. 3.57. <u>Sclerocystis coremioides</u> . Colonies of bacteria within sporocarp . . . . .	123
Fig. 3.58. <u>Sclerocystis coremioides</u> . Higher magnification of bacterial colonies . . . . .	123
Fig. 3.59. <u>Sclerocystis coremioides</u> . Dense colonies of bacteria within the central plexus . . . . .	123
Fig. 3.60. <u>Sclerocystis coremioides</u> . Fused chlamydospore walls .	123
Fig. 3.61. <u>Sclerocystis coremioides</u> . Higher magnification of chlamydospore wall . . . . .	123
Fig. 3.62. <u>Sclerocystis coremioides</u> . Multiperforate septum of sporocarpic hypha . . . . .	123
Fig. 3.63. <u>Sclerocystis coremioides</u> . Higher magnification of septal perforations . . . . .	123
Fig. 4.1. <u>Glaziella aurantiaca</u> . Two typical dried sporocarps .	140
Fig. 4.2. <u>Glaziella aurantiaca</u> . Sporocarp showing several lobes .	140
Fig. 4.3. <u>Glaziella aurantiaca</u> . Sporocarp showing individual spores . . . . .	140
Fig. 4.4. <u>Glaziella aurantiaca</u> . Sporocarp wall in cross section .	140

Fig. 4.5. <i>Glaziella aurantiaca</i> . Sporocarp wall in cross section showing spore cytoplasm . . . . .	140
Fig. 4.6. <i>Glaziella aurantiaca</i> . Interwoven hyphae of middle layer of sporocarp wall. . . . .	142
Fig. 4.7. <i>Glaziella aurantiaca</i> . Higher magnification of sporocarp wall. . . . .	142
Fig. 4.8. <i>Glaziella aurantiaca</i> . Pseudoparenchymatous pockets of sporocarp wall . . . . .	142
Fig. 4.9. <i>Glaziella aurantiaca</i> . Pocket of densely stained pseudoparenchyma. . . . .	142
Fig. 4.10. <i>Glaziella aurantiaca</i> . Sporocarp wall showing position of pseudoparenchyma-lined locule . . . . .	142
Fig. 4.11. <i>Glaziella aurantiaca</i> . Textura angularis of outer pseudoparenchymatous zone. . . . .	142
Fig. 4.12. <i>Glaziella aurantiaca</i> . Young ascus enclosed by pseudoparenchyma in sporocarp wall. . . . .	142
Fig. 4.13. <i>Glaziella aurantiaca</i> . Young ascus dislodged from center of locule. . . . .	144
Fig. 4.14. <i>Glaziella aurantiaca</i> . Basal attachment of young ascus . . . . .	144
Fig. 4.15. <i>Glaziella aurantiaca</i> . Cross section of young ascus in pseudoparenchyma-lined locule. . . . .	144
Fig. 4.16. <i>Glaziella aurantiaca</i> . Two young, clavate asci within middle wall layer. . . . .	144
Fig. 4.17. <i>Glaziella aurantiaca</i> . Locule enclosed by pseudoparenchyma. . . . .	144
Fig. 4.18. <i>Glaziella aurantiaca</i> . Wall of mature ascus. . . . .	144
Fig. 4.19. <i>Glaziella aurantiaca</i> . Mature spore enclosed between outer and inner pseudoparenchymatous zones. . . . .	146
Fig. 4.20. <i>Glaziella aurantiaca</i> . Outer wall of spore fused to sporocarpic hyphae. . . . .	146
Fig. 4.21. <i>Glaziella aurantiaca</i> . Outer wall of mature spore. . . . .	146
Fig. 4.22. <i>Glaziella aurantiaca</i> . Sporocarpic hyphae separated from spore surface. . . . .	146

Fig. 4.23. <i>Glaziella aurantiaca</i> . Two ascomycetous septa of sporocarpic hyphae. . . . .	146
Fig. 4.24. <i>Glaziella aurantiaca</i> . Very young septum . . . . .	148
Fig. 4.25. <i>Glaziella aurantiaca</i> . Moderately young septum . . . . .	148
Fig. 4.26. <i>Glaziella aurantiaca</i> . Median section of mature septum. . . . .	148
Fig. 4.27. <i>Glaziella aurantiaca</i> . Nonmedian section of mature septum. . . . .	148
Fig. 4.30. <i>Glaziella aurantiaca</i> . Membrane-bound Woronin body associated with septal wall . . . . .	148
Fig. 4.31. <i>Glaziella aurantiaca</i> . Higher magnification of septal plug . . . . .	148
Fig. 4.32. <i>Glaziella aurantiaca</i> . Transverse section of spore wall. . . . .	148
Fig. 4.33. <i>Glaziella aurantiaca</i> . Spore wall transition zone. . . . .	148
Fig. 4.34. <i>Glaziella aurantiaca</i> . Collapsed spore . . . . .	150
Fig. 4.35. <i>Glaziella aurantiaca</i> . Fractured spore . . . . .	150
Fig. 4.36. <i>Glaziella aurantiaca</i> . Membranous partition of transition zone . . . . .	150
Fig. 4.37. <i>Glaziella aurantiaca</i> . Transverse section of outer spore wall and associated sporocarpic hyphae. . . . .	150
Fig. 4.38. <i>Glaziella aurantiaca</i> . Inner and outer walls of spore separated by transition zone. . . . .	150
Fig. 4.39. <i>Glaziella aurantiaca</i> . Membranous partition of transition zone . . . . .	152
Fig. 4.40. <i>Glaziella aurantiaca</i> . Hyphae of middle wall layer . . . . .	152
Fig. 4.41. <i>Glaziella aurantiaca</i> . Silver proteinate staining of septum of sporocarpic hypha. . . . .	152
Fig. 4.42. <i>Glaziella aurantiaca</i> . Unstained septal wall lined with densely stained membranous material. . . . .	152
Fig. 4.43. <i>Glaziella aurantiaca</i> . Intensely stained membranous fragments . . . . .	152

Fig. 4.44. <u>Glaziella aurantiaca</u> . Glycogen deposits within spore cytoplasm . . . . .	152
Fig. 4.45. <u>Glaziella aurantiaca</u> . Individual rosettes of glycogen. . . . .	152
Fig. 4.46. <u>Glaziella aurantiaca</u> . Higher magnification of glycogen rosettes . . . . .	152

## TABLE OF CONTENTS

	<u>Page</u>
ACKNOWLEDGEMENTS . . . . .	ii
LIST OF FIGURES . . . . .	iii
ABSTRACT . . . . .	xviii
GENERAL INTRODUCTION . . . . .	1
CHAPTER I    A LIGHT AND ELECTRON MICROSCOPE STUDY OF THE SPOROCARPS OF <u>ENDOGONE PISIFORMIS</u> . . . . .	6
Introduction . . . . .	6
Materials and Methods . . . . .	9
Results . . . . .	12
Discussion . . . . .	18
CHAPTER II    LIGHT AND ELECTRON MICROSCOPIC STUDIES OF THE AZYGOSPORES OF SELECTED SPECIES OF <u>GIGASPORA</u> . . . . .	36
Introduction . . . . .	36
Materials and Methods . . . . .	39
Results . . . . .	44
Discussion . . . . .	51
CHAPTER III    LIGHT AND ELECTRON MICROSCOPE EXAMINATION OF THE CHLAMYDOSPORES OF SELECTED SPECIES OF <u>GLOMUS</u> AND <u>SCLEROCYSTIS</u> . . . . .	84
Introduction . . . . .	84
Materials and Methods . . . . .	87
Results . . . . .	88
Discussion . . . . .	94
CHAPTER IV    GLAZIELLALES ORD. NOV. AND GLAZIELLACEAE FAM. NOV.: NEW TAXA BASED UPON LIGHT AND ELECTRON MICROSCOPIC OBSERVATIONS OF <u>GLAZIELLA AURANTIACA</u> . . . . .	124
Introduction . . . . .	124
Materials and Methods . . . . .	126
Results . . . . .	129
Discussion . . . . .	134
CHAPTER V    GENERAL CONCLUSIONS . . . . .	153
BIBLIOGRAPHY . . . . .	157
BIOGRAPHICAL SKETCH . . . . .	166

Abstract of Dissertation Presented to the Graduate School  
of the University of Florida in Partial Fulfillment of the  
Requirements for the Degree of Doctor of Philosophy

MORPHOLOGY, CYTOLOGY AND ULTRASTRUCTURE OF SELECTED SPECIES  
OF ENDOGONACEAE (ENDOGONALES: ZYgomycetes)

By

Jack L. Gibson

May 1985

Chairman: J. W. Kimbrough

Major Department: Botany

Morphological and cytological features of vegetative and reproductive structures of selected species of Endogonaceae were examined with light (LM) and electron microscopy (EM), compared with previously published data, and evaluated for possible taxonomic significance. A total of 11 species of the genera Endogone, Gigaspora, Glomus, Sclerocystis, and Glaziella were examined.

The data indicate that zygosporangia of Endogone pisiformis develop from the fusion of paired, apposed gametangia. A primary zygosporangium is disrupted by an expanding secondary zygosporangium, within which the zygospore develops. Zygosporangial and zygospore walls contrast in staining properties with both LM and EM. Gametangial septa are multiperforate, and glebal hyphae possess infrequent septa with single, central perforations. Abundant glycogen and two kinds of lipid globules exist in the sporoplasm.

Bands of apparent arched microfibrils are present in the inner wall of G. margarita and the outer wall of G. pellucida, but not in other Gigaspora species examined. Wall structure of G. gigantea is

similar to that of G. margarita. In G. pellucida and G. heterogama germination chambers develop within a layer of the membranous inner wall, rather than at a preexisting partition. The inner membranous walls of G. heterogama, G. pellucida, and G. gregaria have a complex substructure. Wall structure does not correlate with spore pigmentation as a basis for the infrageneric division of Gigaspora. The outer wall of some Gigaspora species is similar in staining properties, and is possibly homologous, to the zygosporangium of Endogone pisiformis.

The ephemeral outer wall of G. intraradices and G. etunicatum chlamydospores is apparently degraded by bacterial activity. The inner wall of G. intraradices has approximately four separable layers while that of G. etunicatum has numerous, inseparable bands of microfibrils similar to those of the single wall of G. constrictum. Colonies of bacteria occur within the central plexus and peridium of sporocarps of Sclerocystis coremioides. The chlamydospore walls appear to fuse with surrounding elements. Both Glomus and Sclerocystis possess multiperforate septa.

Sporocarpic hyphae of Glaziella aurantiaca possess typical ascomycetous septa with plugged, central pores associated with Woronin bodies. Nomarski LM indicates that the "chlamydospores" are actually ascospores arising from unisored asci. Spore wall ultrastructure is discussed, and the new order Glaziellales is proposed to accommodate this taxon.

## GENERAL INTRODUCTION

The Endogonaceae are primarily hypogeous, frequently sporocarpic zygomycetes that traditionally have been placed in the Mucorales (Thaxter, 1922; Gerdemann and Trappe, 1974). Recently, however, the family was raised to ordinal rank when Benjamin (1979) validated the Endogonales, a monotypic order originally proposed by Moreau (1953). Although the Endogonaceae were generally considered to be closely related to the Mortierellaceae by earlier authors (Bucholtz, 1912; Thaxter, 1922; Zycha et al. 1969), Gerdemann and Trappe (1974) believe that zygospore formation in Endogone is more similar to the Piptocephalidaceae, and that its true affinities may lie with that family. The Endogonales, therefore, may have closer affinities to this particular family of the Mucorales rather than to the Mortierellaceae, as originally believed.

The family was first monographed by Thaxter (1922) and included the genera Endogone, Sclerocystis, Sphaerocreas, and Glaziella. Later Zycha (1935) synonymized Sphaerocreas with Endogone, leaving only three genera in the family. The generic concepts of the Endogonaceae were revised by Gerdemann and Trappe (1974), who recognized a total of seven genera, Endogone, Sclerocystis, Glomus, Gigaspora, Acaulaspore, Modicella, and Glaziella.

Subsequent to the monograph of Gerdemann and Trappe (1974), two additional genera have been proposed and one transferred out of the family. Complexipes was erected by Walker (1979) for one species that commonly forms ectendomycorrhizae on pines, but was later determined to be the anamorphic state of a discomycete (Danielson, 1982).

Entrophospora was described by Ames and Schneider (1979) to accommodate a taxon in which a unique type of spore development was found. Although the type species of Entrophospora is apparently not known to form mycorrhizae, typical VA mycorrhizal development has recently been reported for a newly described species (Schenck *et al.* 1984). Modicella, the position of which has been in doubt for some time (Thaxter, 1922), was recently transferred to the Mortierellaceae (Mucorales) by Trappe and Schenck (1982). Currently, the family consists of seven genera and approximately 100 species (Trappe and Schenck, 1982).

The various genera of the Endogonaceae are separated on the basis of mode of spore formation. Separation of species, however, is based primarily on spore characteristics which include presence or absence of sporocarps, spore size, color, wall thickness, number of walls, hyphal connection characters, etc. (Trappe, 1982; Trappe and Schenck, 1982). The importance of spore wall characters in the delimitation of species has been strengthened with the increasing number of species described, and this aspect of the taxonomy of the family is discussed by Walker (1983). Several taxonomic accounts with keys have been published, including recent ones by Gerdemann and Trappe (1974), Becker and Hall (1976), Nicolson and Schenck (1979), Hall and Fish (1979), Walker and Trappe (1981), Schenck and Smith (1982), Trappe (1982), Hall (1984), and Schenck *et al.* (1984).

The Endogonaceae are recognized today as a family of great ecological and economic importance, since many species form the vesicular-arbuscular (VA) type of endomycorrhizae that are known to

occur in most herbaceous and in many woody plant species (Nicolson, 1967; Gerdemann, 1975). Before the extensive occurrence of this type of mycorrhiza was realized, the family was of interest only to a relatively few mycologists and plant pathologists. However, the revelation that certain genera of the Endogonaceae form this widespread association, primarily by the early work of Mosse (1953, 1956, 1957) and Gerdemann (1955, 1964), stimulated a tremendous surge of interest and research from a number of scientific disciplines (Schenck, 1983). Also of importance in stimulating research were the discoveries that species of the fungi can be grown with a plant symbiont in "pot culture" and that the association is generally beneficial to the colonized plants (Nicolson, 1967).

The potential benefits that these fungi offer to agriculture and forestry are numerous. Applications of VA mycorrhizal fungi to crop plants and nurseries have resulted in enhanced growth, drought resistance, transplant survivability, resistance to pathogens, etc. (Menge, 1983).

The family, although relatively small, has a long history of taxonomic confusion, primarily resulting from the fact that the sexual stage (occurrence of zygospores) has been identified only for the genus Endogone. Additionally, the relative rarity with which they are collected and the fact that, until recently (Berch and Fortin, 1983a), there have been no confirmed reports of their culture on common laboratory media have added to the difficulty in studying these fungi. Thaxter (1922) alluded to this taxonomic ambiguity in such remarks as, "the true relationships of the group to other families of fungi have

long been a matter of conjecture, as evident from the terms--asci, sporangia, cysts, vesicles, etc.--which have been applied by various authors to the chlamydospores alone" (p. 293) and "the inclusion in a single genus of the zygosporic and chlamydosporic types, has hitherto been based entirely on a general resemblance in habit and habitat, and a similarity in the appearance of the two types of spores" (p. 293). Also, Gerdemann and Trappe (1974), even after having revised the generic concepts, still expressed some doubt about the taxonomic coherence of the family in stating "the complete life cycles of most species are still in doubt. A number of diverse elements are included in the Endogonaceae and quite possibly certain groups of species will eventually be transferred to other families" (p. 1).

Ultrastructural examinations of the Endogonaceae are infrequent. Most of these studies are limited to the fungal structures within the root (i.e., the mycorrhizae), and these have been reviewed by Harley and Smith (1983) and Scannerini and Bonfante-Fasolo (1983). However, a few studies have focused on spore structure. Bonfante-Fasolo and Scannerini (1976) studied the development and ultrastructure of the zygospores of Endogone lactiflua Berk. & Broome. The first ultrastructural studies of VA mycorrhizal fungal spores were done by Mosse (1970a-c) on a species currently classified as Acaulospora laevis Gerd. & Trappe. Later, Sward (1981a-c) examined the ultrastructure of spores of Gigaspora margarita Becker & Hall. Most recently, the fine structure of the spores of Glomus epigaeum Daniels & Trappe were examined by Bonfante-Fasolo and Vian (1984).

The present study was undertaken to examine the morphology, cytology and ultrastructure of various vegetative and reproductive structures of selected species of Endogonaceae, and to compare the data obtained with those of previously published studies and evaluate their possible significance to the general taxonomic arrangement of the family. The genera Acaulospora and Entrophospora were unfortunately excluded from the present study, primarily as a result of time limitations, but hopefully will be included in future investigations.

CHAPTER I  
A LIGHT AND ELECTRON MICROSCOPE STUDY OF THE SPOROCARPS  
OF ENDOGONE PISIFORMIS

Introduction

Endogone Link ex Fr. is the type genus of the family Endogonaceae and, as such, has received considerable attention from various researchers. Bucholtz (1912) first showed sexual reproduction by the fusion of gametangia and thus the zygomorphic nature of the taxon. Endogone is the only genus of the Endogonaceae for which the teleomorph has been established, the remainder apparently producing asexual spores. Thaxter (1922) included chlamydosporic and sporangial species in his concept of the genus. Later, Gerdemann and Trappe (1974) limited Endogone to those species of Endogonaceae producing true zygosporangia.

The genus Endogone also differs from other genera of the Endogonaceae in its mycorrhizal status. Whereas the other genera form arbuscular or vesicular-arbuscular (VA) type endomycorrhizae, two species of Endogone have been reported to form somewhat atypical ectomycorrhizae, either with conifers (Fassi, 1965; Fassi et al., 1969; Fassi and Palenzona, 1969; Chu-Chou and Grace, 1979) or species of Eucalyptus (Warcup, 1975). The remaining species of Endogone are presumed to be ectomycorrhizal, primarily because of their hypogeous habit and ectomycorrhizal host associations, are of unknown mycorrhizal status, or else exhibit some saprobic ability (Gerdemann and Trappe, 1974).

Several questionable or unconfirmed reports of the isolation and growth of Endogone in axenic culture have been made (Kanouse, 1936;

Bakerspigel, 1958; Gerdemann and Trappe, 1974; Warcup, 1975).

Recently, however, Berch and Fortin (1983a) presented strong evidence for the axenic culture on common laboratory media of an Endogone sp., although zygospores never formed.

The germination of Endogone zygospores was only very recently reported (Berch and Fortin, 1982, 1983b), in spite of numerous unsuccessful attempts by various researchers over the years (Bucholtz, 1912; Thaxter, 1922; Kanouse, 1936; Gerdemann and Trappe, 1974). The zygospores of Endogone incrassata Thaxter, from field-collected sporocarps, were observed to germinate by germ tube emergence through the gametangial attachment point (Berch and Fortin, 1982). By contrast, the zygospores of Endogone pisiformis germinate by the initial formation of an intrawall germ chamber and subsequent complete penetration of the wall by the germ tube (Berch and Fortin, 1983b). This mode of germination is reminiscent of certain species of Gigaspora and Acaulospora (as is discussed in Chapter III).

The ecological status of Endogone pisiformis has been of much interest to various workers. The general conclusion is that E. pisiformis is an apparent saprobe and is neither parasitic on, nor obligately associated with, the Sphagnum sp. on which it is commonly found in eastern North America (Atkinson, 1918; Thaxter, 1922; Gerdemann and Trappe, 1974; Parke and Linderman, 1980; Berch and Fortin, 1983a). A primary factor in this conclusion is the occurrence of the same species in western North America and other areas on substrates that preclude any possible biotrophic mode of existence (Gerdemann and Trappe, 1974).

As mentioned in the General Introduction, the taxonomic relationships of the other genera of Endogonaceae to Endogone are tenuous and admittedly based arbitrarily on superficial similarities of habit and morphology (Thaxter, 1922; Gerdemann and Trappe, 1974). This situation results primarily from lack of information regarding the teleomorphic stages of these other genera placed in the family. The determination of their true relationship to Endogone depends upon acquiring more information on these stages.

Very few studies have dealt with the ultrastructure of Endogone. Bonfante-Fasolo and Scannerini (1977) studied, at both the light and electron microscopic levels, the morphological and cytological features of the mycorrhiza synthesized between Pinus strobus L. and Endogone flammicorona Trappe & Gerdemann. In a separate study they examined the development and structure of the zygospores of E. flammicorona (Bonfante-Fasolo and Scannerini, 1976) and demonstrated the presence of a thin outer primary (zygosporangial) wall and a thick inner (zygospore) wall. They also described the development of the hyphal mantle (i.e., "flaming crown") that, in part, distinguishes this species from E. lactiflu Berk. & Broome (Trappe and Gerdemann, 1972). They showed that the characteristic hyphal mantle of the mature spores results from the differential thickening of the secondary walls of hyphae appressed to the outer (zygosporangial) wall. Apparently, those areas of the hyphal walls contiguous with the outer wall undergo a rapid thickening and thus, at maturity, appear to flare out from the surface of the wall, giving the typical "flaming crown" appearance.

The present study was undertaken to examine sporocarpic tissues of Endogone pisiformis at both the light and electron microscope levels in order to gain more information about the structure and development of the constituent zygosporae and enveloping hyphae.

#### Materials and Methods

##### Source of Materials

Freshly collected sporocarps of E. pisiformis were used for both light and electron microscope examinations. The material was obtained from Dr. G. L. Benny, University of Florida, and is currently deposited in the University of Florida Mycological Herbarium (FLAS-53822: U.S.A., North Carolina, Macon County, Highlands, Highlands Biological Station, Botanic Garden, 3,800 ft. elev., on rotten wood, G. L. Benny, July 6, 1977).

##### Light Microscopy (LM)

Whole sporocarps were rinsed in three changes of deionized water and allowed to soak in 40% aqueous mucilage for approximately 1 hr at room temperature before being frozen and sectioned in mucilage with a Cryostat microtome (-20 C). Transverse sections approximately 12  $\mu\text{m}$  thick were mounted in lacto-phenol cotton blue or Melzer's reagent and examined with a Nikon compound light microscope equipped with Nomarski differential-interference contrast optics.

##### Scanning Electron Microscopy (SEM)

Transverse sections of small pieces of the dried sporocarp were made with a razor blade under a dissecting microscope. These sections were placed on stubs with double-sticky cellophane tape, coated with

gold in a Hummer Jr. sputter coater, and observed with a Hitachi S-450 scanning electron microscope.

#### Transmission Electron Microscopy (TEM)

Small, hand-sectioned pieces of the fresh sporocarps were fixed at room temperature in 2% paraformaldehyde, 2.5% glutaraldehyde and 2 mM calcium chloride in 0.1 M sodium cacodylate buffer (pH 7.2). The material was rinsed in 0.1 M sodium cacodylate buffer, postfixed in 1% osmium tetroxide in 0.1 M cacodylate buffer, and then dehydrated in an ethanol series, which included en bloc staining with saturated uranyl acetate in 70% ethanol for ca. 2 hr at room temperature. The ethanol dehydration series was followed by acetone (Benny and Aldrich, 1975). The material was then embedded in ERL 4206 resin (Spurr, 1969) and ultrathin sectioned on a Sorvall MT-2 ultramicrotome with a diamond knife. The sections were collected on one-hole, formvar-coated copper grids, stained for 10 min in 2% (w/v) aqueous uranyl acetate followed by 10 min in Reynolds' (1963) lead citrate, and examined at 75 kV on an Hitachi HU-11C or Philips EM-301 transmission electron microscope.

#### Cytochemistry

The barium permanganate post staining method of Hoch (1977) was employed in an attempt to visualize, in better detail, the wall structure of hyphae and spores, or to obtain differential staining of the spore wall layers. Material prepared for TEM was ultrathin sectioned in the same manner as described above. A drop of aqueous 1% barium permanganate was placed on the sections supported by formvar-coated copper grids. The stain was washed away after ca. 30 sec with a gentle stream of deionized water. To remove possible contaminants, a

drop of 0.05% citric acid was placed on the sections for ca. 30 sec, after which they were rinsed again with deionized water. The sections were then stained with aqueous uranyl acetate for 2 min, rinsed with deionized water, and stained with Reynolds' (1963) lead citrate. Both the uranyl acetate and lead citrate were placed, dropwise, directly on the sections, since staining times were relatively brief. The sections were then given a final deionized water rinse and dried for examination with TEM.

In order to localize carbohydrates in the sporocarpic tissue and spores, the silver proteinate stain was employed (Thiéry, 1967; McLaughlin, 1974). Material prepared for TEM was used, however, with the exclusion of the uranyl acetate en bloc treatment during the ethanol dehydration. Ultrathin sections were obtained as described above but were collected from the boat unmounted with the use of small plastic rings in which the sections floated on the surface of a drop of liquid held in the center of the ring (Marinozzi, 1961). These sections were treated as follows: 1) incubated on 1% aqueous periodic acid for 30 min at room temperature; 2) washed on deionized water, once briefly and three times for 10 min each; 3) incubated on 1% thiosemicarbazide in 10% aqueous acetic acid for 24 hr at room temperature; 4) washed on 10% aqueous acetic acid, twice briefly and three times for 20 min each; 5) washed on 5% aqueous acetic acid for 5 min; 6) washed on 1% aqueous acetic acid for 5 min; 7) washed on deionized water two times for 5 min each; 8) incubated on 1% aqueous silver proteinate for 30 min at room temperature in the dark; 9) washed on deionized water, three times briefly and once for 10 min.

After this treatment the sections were mounted onto formvar-coated copper grids, dried, and observed with TEM. Control sections were treated as above, however, excluding the 1% periodic acid oxidation step.

### Results

#### General Features of the Sporocarps

The fresh sporocarps of *E. pisiformis* examined are pulvinate to somewhat reniform and approximately 1-2.5 x 2-5 mm in diameter (Fig. 1.1). They were typically hollow at maturity with a 1-2 mm opening at the base and produced numerous, fine hyphal connections to the substrate. The sporocarps were bright yellow-orange when fresh and moist but faded to dull pale-orange upon drying.

#### Light Microscopy (LM) and Scanning Electron Microscopy (SEM)

Under the dissecting microscope the surface of the sporocarps is lightly tomentose, a condition more evident in the dried state. The tomentum results from the presence of what Thaxter (1922) refers to as "peculiarly differentiated hyphae forming the superficial tomentum" (fig. 7, p. 344). These hyphae form a loose, interwoven peridium surrounding the zygospores and glebal hyphae (Figs. 1.3, 1.4). The peridial hyphae forming the tomentum are hyaline but become dark red-brown (dextrinoid) in Melzer's reagent (Figs. 1.3, 1.5). Also, they are thick walled (Figs. 1.5-1.9), long tapered (Fig. 1.4), aseptate, and frequently branched (Fig. 1.6).

The peridium encloses the interior of the sporocarp, which consists of a gleba of thin-walled hyphae and zygosporangia (Figs. 1.2-1.4). In young sporocarps immature stages of zygosporangium

formation can be detected (Fig. 1.2). The young zygosporangia develop as buds from the tips of apposed suspensors (Fig. 1.10). Apparently, plasmogamy is brought about by the disintegration of the walls between the apposed gametangia at their tips. The gametangia are delimited from the suspensors by the formation of gametangial septa (Figs. 1.10-1.12, 1.17). These septa are convex when initially formed and the gametangia possess cytoplasm (Fig. 1.10), but subsequently they become concave as the zygosporangia mature (Figs. 1.11, 1.17) and the gametangial cytoplasm is completely transferred to the young zygosporangium.

Although the zygospores develop independently within the zygosporangia, the walls of these two structures remain closely associated (Figs. 1.13-1.16). The zygosporangial wall is continuous with the walls of the gametangia (Figs. 1.13, 1.16, 1.17) and stains more intensely with azure-methylene blue (AMB) (Richardson *et al.*, 1960) than the zygospore wall (Figs. 1.14, 1.15, 1.17). The zygosporangial and zygospore walls were both particularly well differentiated with Normarski differential-interference contrast LM and thus development of the zygospore wall could be followed from a very young stage (Fig. 1.16).

The cytoplasm of mature zygospores consists primarily of lipid globules of fairly uniform size. In some mature, plastic-embedded, AMB-stained zygospores, median sections frequently revealed an indistinct region of densely stained material that may represent a fusion nucleus (Fig. 1.15). However, no definitive evidence was found to substantiate the nuclear condition either with LM or TEM.

Transmission Electron Microscopy (TEM)

The silver proteinate stain was useful in differentiating the zygosporangial wall from that of the zygospore, the former staining densely, while the latter remained essentially unstained. Controls deleting the periodic acid oxidation step showed no deposition of silver, or only sparse, random clumping of silver across the entire section, indicating no specificity.

The young zygosporangium is irregularly lobed to ovoid in shape and possesses a wall of fairly uniform consistency and electron opacity (Fig. 1.18). The zygosporangial wall is continuous with that of the attached gametangia and is very similar in staining properties. (Fig. 1.19). Also, it is closely adherent to the wall of the enclosed zygospore (Figs. 1.18, 1.19). This stage of zygosporangial development, at the EM level, is roughly comparable to that shown on the lower left side of Fig. 1.16 (arrows). At this stage the young zygospore is very thin walled and possesses the same irregular shape as the enveloping mother zygosporangium (Figs. 1.18, 1.19).

As the zygosporangium matures, perhaps the most obvious changes result from further deposition of zygospore wall material and a corresponding increase in zygospore wall thickness. Also notable is the change in shape of the zygosporangium and enclosed zygospore from somewhat irregularly lobed at the very young stages (Figs. 1.18, 1.19), to more or less spherical at or near maturity (Figs. 1.21, 1.23). These changes in shape correspond with increases in thickness

of the zygosporangium wall and perhaps represent a "ballooning out" of the maturing spores.

Another notable change in the zygosporangium during their development involves the occurrence of glycogen deposits within the spore cytoplasm between the lipid globules. When treated with silver proteinate, glycogen appears as densely stained clusters that are more irregular in shape and outline than the surrounding lipid globules (Figs. 1.18, 1.20). The amount of glycogen appears to decrease as the zygosporangium matures, and little or none is detectable in the fully mature zygosporangium (Fig. 1.23).

The predominant sporoplasmonic constituent appears to be lipid, which exists as well-defined, spherical globules. There are apparently two forms of lipid globule present, based upon physical and staining properties. One kind apparently has an affinity for the silver proteinate stain and is relatively small in size, while the other appears to have no affinity for the silver stain, is decidedly larger, and very frequently appears perforate in section (Figs. 1.18-1.23, 1.42).

Although the wall of the mature zygosporangium is intimately associated with that of the zygosporangium, there appear to be distinct differences between these two walls. As pointed out previously in considering the early stages of zygosporangial formation, one of the most obvious differences is the affinity of the silver proteinate for the zygosporangial wall (Figs. 1.24-1.26). At higher magnification the silver is observed as fine grains deposited uniformly across the wall of the zygosporangium (Fig. 1.26). The outer

surface of the zygosporangium is rather indistinct and intergrades into a mass of irregular fibrils that also appear to possess some deposition of silver (Fig. 1.26). The inner surface of the zygosporangium borders the outer (primary) layer of the zygospore (Figs. 1.24-1.26). This layer consists of two thin, densely stained zones separated by a somewhat wider zone that is relatively unstained with silver (Figs. 1.24-1.26). This layer is also evident with the barium permanganate post stain (Figs. 1.28, 1.29). Upon initial observation this thin layer appears to be the inner layer of the zygosporangium. However, the presence of this layer across the suspensor connection at the spore base indicates that it is continuous with the wall of the zygospore (Figs. 1.30, 1.31, 1.34) and apparently represents the primary wall of the zygospore. The thick, electron translucent secondary wall of the zygospore, as previously mentioned, does not stain with silver proteinate and, in the mature state, appears to be divided into an outer and inner layer with the inner layer generally thicker (Figs. 1.24, 1.25). This subdivision is evident both with the silver proteinate and barium permanganate post stains (Figs. 1.28, 1.29). The demarcation between the zygospore wall and the sporoplasm is quite well defined (Figs. 1.24, 1.27).

The suspensor attachment, including the gametangial remnants, is evident in median longitudinal sections of zygosporangia (Figs. 1.30, 1.31). In these sections the primary layer of the zygospore wall is visible traversing the zygosporangial wall at the junction of the gametangia (Figs. 1.30, 1.31), as are the remnants of the primary zygosporangial wall. The primary zygosporangial wall apparently

ruptures relatively early in the development of the zygosporangium as the secondary wall rapidly increases in thickness (Figs. 1.30, 1.31). Also, the primary wall of the zygosporangium is continuous with the outermost (primary) wall of the gametangia and, likewise, the secondary wall of the zygosporangium is continuous with the innermost (secondary) wall of the gametangia (Fig. 1.31). This correspondence between the zygosporangial and gametangial walls is evident also in young zygosporangia (Fig. 1.19). Apparently, in the development of the zygosporangium of E. pisiformis, the primary wall of the zygosporangium develops as an extension of the primary fusion wall of the apposed gametangia. However, within this wall layer a secondary wall develops very early and also is continuous with the gametangia; it is the expansion of this secondary wall that apparently mechanically disrupts the primary wall resulting in the microfibrillar remnants evident in Figs. 1.19, 1.30, 1.31 and 1.34.

The mature gametangial septa, as mentioned previously, are concave (Figs. 1.30-1.32). At higher magnifications they can be seen to possess numerous, fine perforations (Figs. 1.33, 1.34). These perforations completely traverse the primary wall of the septa, but do not appear to penetrate the secondary wall layer (Fig. 1.34).

The relatively thin-walled hyphae of the gleba are only infrequently septate, and no such multiperforate septal structures were observed in these (Figs. 1.35-1.37). The initial stage of septum formation in these hyphae involves the typical centripetal growth of the hyphal wall (Fig. 1.35). The mature septa frequently appear to have a single, central pore which, however, was detected only in the

barium permanganate post stained sections. Furthermore, perforations not necessarily associated with septa frequently occur in the walls of these glebal hyphae (Fig. 1.38). These perforations occur in clusters, each consisting of several irregular channels through the wall.

The cytoplasm of the glebal hyphae has a typical complement of organelles including nuclei, mitochondria, endoplasmic reticulum, ribosomes and vacuoles (Fig. 1.39). The nuclei appear to possess clusters of mostly peripheral heterochromatin (Fig. 1.39, 1.40). Also present in the cytoplasm of the glebal hyphae are peculiar structures which are electron opaque and have fine, parallel striations. These apparently represent protein storage bodies (Figs. 1.41). The two types of lipid commonly found in the sporoplasm (Fig. 1.42) have not been found in the glebal hyphae of the sporocarps.

#### Discussion

In the zygomycete literature frequently the term zygospore has been used erroneously to refer to the entire zygosporangium as well as the enclosed zygospore (Gerdemann and Trappe, 1970, 1974; Trappe and Gerdemann, 1972; Bonfante-Fascolo and Scannerini, 1976). Recently, however, the distinction between these two structures has been clearly demonstrated and their independent origins emphasized (Benny and O'Donnell, 1978; O'Donnell *et al.*, 1978; Jeffries and Young, 1983). Berch and Fortin (1982) recently pointed out this distinction in their study of zygospore germination in Endogone pisiformis.

In this study the data from both light and electron microscopy show that in Endogone pisiformis the wall of the zygosporangium is continuous with the wall of the gametangium, and the zygospore wall

has an independent origin within the zygosporangium. The data also reveal interesting features of both the young and mature zygosporangia which have not been shown previously. Apparently an ephemeral primary zygosporangium is formed very soon after fusion of the apposed gametangia. The wall of this primary zygosporangium is initially continuous with the primary wall of the gametangia, but is subsequently completely disrupted by the expansion of the secondary zygosporangium, leaving the remnants of the primary zygosporangia as disrupted microfibrillar material at the base. The mature zygosporangium then is actually the secondary zygosporangium, and it is within this structure that the zygospore develops.

The occurrence of perforations in the gametangial septa is another feature of E. pisiformis that has been reported for other zygomycetes (O'Donnell et al., 1976, 1977b) and is considered a "hallmark" of gametangial septa of Mucorales (Alexopoulos and Mims, 1979, p. 193). These perforations have also been reported in the septa of vegetative hyphae of various zygomycetes (O'Donnell et al., 1977a; Jeffries and Young, 1983). This fact is interesting, especially in conjunction with the occurrence of apparent solitary perforations in the septa and clusters of perforations in the walls of the vegetative hyphae of E. pisiformis. The significance of these solitary septal perforations being especially visible in barium permanganate post stained sections is not known.

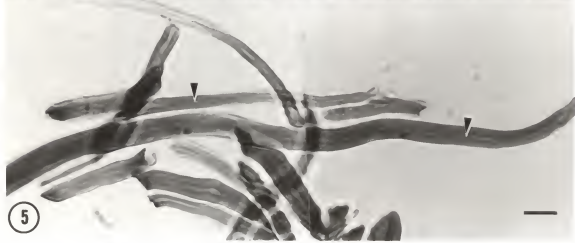
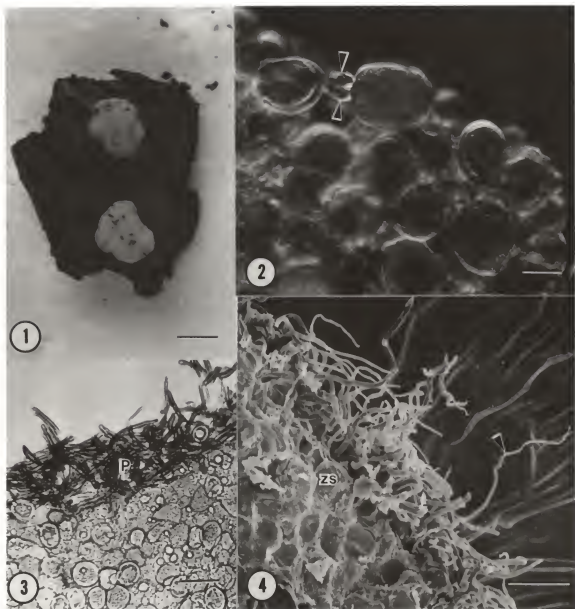
The data here showing independent zygosporangial and zygospore walls, fusion of gametangia, and multiperforate gametangial septa support the early studies of Bucholtz (1912) in establishing the true

nature of the zygospores of Endogone pisiformis. However, additional ultrastructural studies of other species of Endogone are needed. Studies of species that differ in some regard from E. pisiformis would be of special interest. An example is E. incrassata in which the "outer" spore wall is described as thicker than the "inner" wall (Gerdemann and Trappe, 1970). This outer wall of the zygospore may actually be the zygosporangial wall or might possibly represent an outer zygospore wall, if the zygosporangium was ephemeral and thus nonexistent at the mature spore stage.

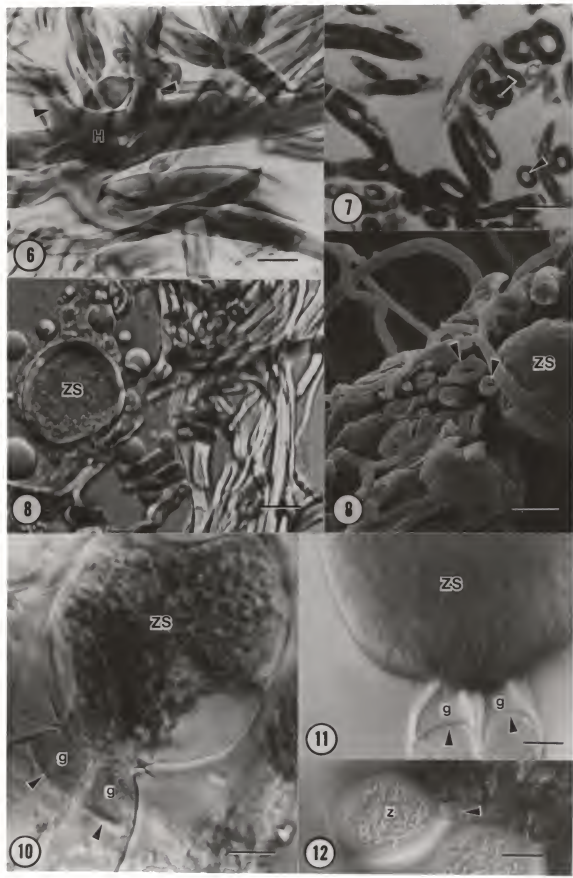
One of the most pressing problems in developing a more natural classification system of the Endogonaceae is in obtaining sufficient information about the other genera included in the family in order to establish greater confidence in their affinities to Endogone. As pointed out earlier, these other genera are included in the family primarily because of superficial similarities of morphology and habit and lack of information regarding their teleomorphic nature. The identification of the teleomorphic states of these genera, if they exist, would be the ideal solution to this taxonomic ambiguity. However, additional information regarding the general biology of these genera, as well as that of Endogone, can also be of great value in understanding the relationships of the genera. For example, the elucidation of the mode of germination of E. pisiformis by Berch and Fortin (1983b) as very similar to that of certain Gigaspora and Acaulospora species may suggest a closer relationship between Endogone and these two genera than was previously believed, based upon spore morphology alone.

The relationship between the azygosporic genera of Endogonaceae and the genus Endogone is of special significance. The azygosporic status of Gigaspora, Acaulospora, and Entrophospora is presumptive, since their spores only resemble zygospores. Additional data are needed on the development of these spores in order to determine if they represent teleomorphic stages and are thus closely related to Endogone. The chlamydosporic genera perhaps represent a greater challenge, since no sexual stage, real or presumed, has been associated with them, and comparative developmental studies of this spore type with Endogone may be less valuable.

- Figs. 1.1-1.5. *Endogone pisiformis*. Fig. 1.1. Macrophotography. Fig. 1.2. Nomarski differential-interference contrast light microscopy. Figs. 1.3, 1.5. Light microscopy (LM). Fig. 1.4. Scanning electron microscopy (SEM).
- Fig. 1.1. Two typical sporocarps on substrate of rotten wood. (bar= 2.0 mm).
- Fig. 1.2. Squash mount of young sporocarp showing numerous zygosporangia, one with gametangia evident (arrowheads). (bar= 50  $\mu$ m).
- Fig. 1.3. Cryostat transverse section of sporocarp mounted in Melzer's reagent showing mass of zygosporangia and glebal tissue enclosed by loose peridium (P) of interwoven, dextrinoid hyphae. (bar= 100  $\mu$ m).
- Fig. 1.4. Section of sporocarp showing mass of zygosporangia enclosed by tapering peridial hyphae (arrowhead). (bar= 50  $\mu$ m).
- Fig. 1.5. Higher magnification of peridial hyphae stained with Melzer's reagent showing thick walls and narrow lumen (arrowheads). (bar= 20  $\mu$ m).

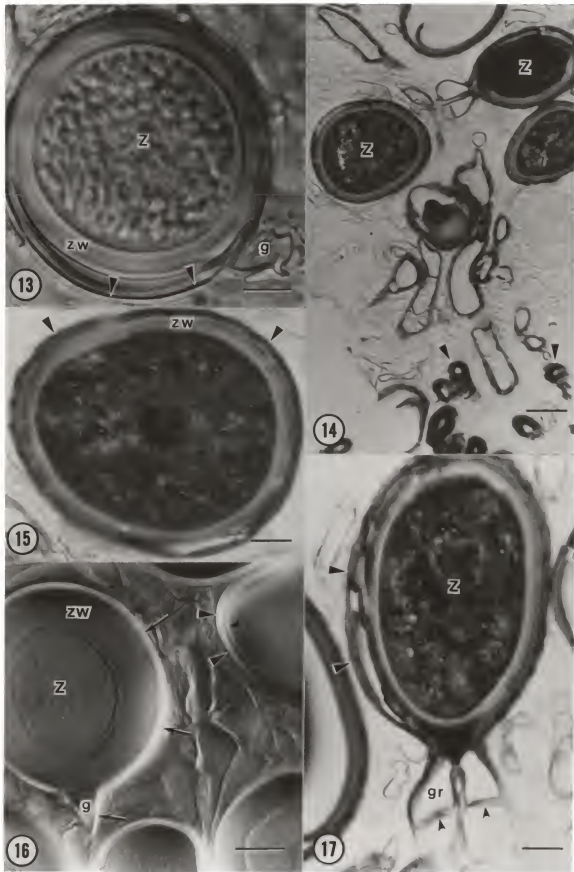


- Figs. 1.6-1.12. *Endogone pisiformis*. Figs. 1.6, 1.8, 1.10-1.12. Nomarski differential-interference contrast LM. Fig. 1.7. LM. Fig. 1.9. SEM.
- Fig. 1.6. Higher magnification of dextrinoid, interwoven peridial hyphae showing two branches (arrowheads) of a main hyphal axis (H). (bar= 25  $\mu$ m).
- Fig. 1.7. Thick, plastic section of sporocarp showing several peridial hyphae in transverse section. Note thick walls and narrow lumen (arrowheads). (bar= 20  $\mu$ m).
- Fig. 1.8. Cryostat transverse section of sporocarp showing interwoven peridial hyphae relative to an enclosed zygosporangium (ZS). (bar= 50  $\mu$ m).
- Fig. 1.9. Transverse section of sporocarp showing zygosporangium (ZS) and the thick walls and narrow lumen (arrowheads) of peridial hyphae. (bar= 50  $\mu$ m).
- Fig. 1.10. Squash mount of sporocarp showing young zygosporangium (ZS) forming at tip of two apposed gametangia (g). Note confluence of dense cytoplasm from gametangia into zygosporangium and convex nature of gametangial septa (arrowheads). (bar= 10  $\mu$ m).
- Fig. 1.11. More mature stage in zygosporangium development showing empty gametangia (g), thin-walled, expanding zygosporangium (ZS), and concave gametangial septa (arrowheads). (bar= 10  $\mu$ m).
- Fig. 1.12. Mature zygospore (Z) within zygosporangium showing intact suspensor connection and gametangial septum in outline (arrowhead). Note uniform consistency of zygospore lipid contents. (bar= 50  $\mu$ m).



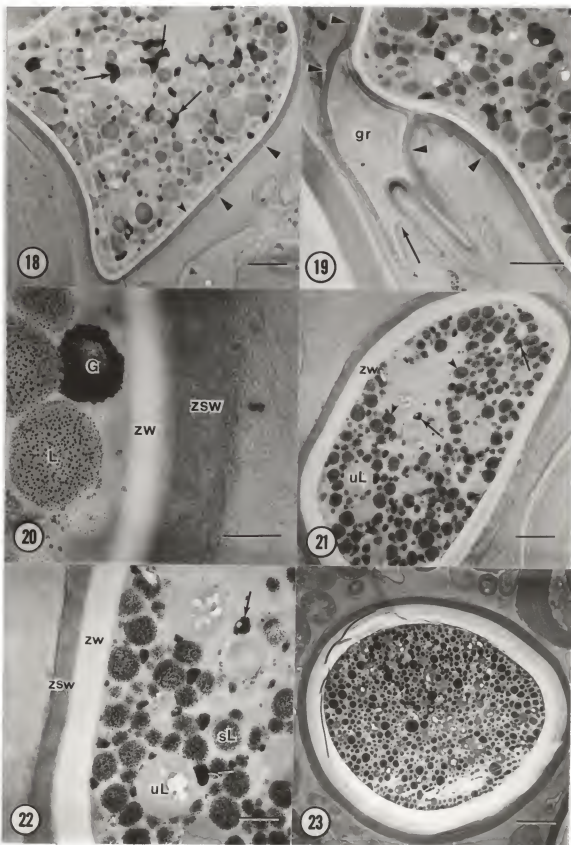
Figs. 1.13-1.17. Endogone pisiformis. Fig. 1.13. LM of Cryostat section. Figs. 1.14, 1.15, 1.17. LM of thick, plastic sections. Fig. 1.16. Nomarski differential-interference contrast LM of Cryostat section.

- Fig. 1.13. Mature zygospore (Z) containing lipid globules of fairly uniform size and with relatively thick, homogeneous, single wall (ZW) enclosed by relatively thin-walled zygosporangium (arrowheads). (bar= 20  $\mu\text{m}$ ).
- Fig. 1.14. Transverse section of sporocarp showing several zygospores (Z) embedded in thin-walled glebal hyphae and several peridial hyphae (arrowheads) evident at periphery of sporocarp. (bar= 50  $\mu\text{m}$ ).
- Fig. 1.15. Higher magnification of zygospore showing zygospore wall (ZW) distinguishable from darker-stained zygosporangium wall (arrowheads). Note possible fusion nucleus in center of zygospore. (bar= 20  $\mu\text{m}$ ).
- Fig. 1.16. Transverse section of sporocarp showing somewhat oblique section of mature zygospore (Z) and zygospore wall (ZW) and showing zygosporangial wall (arrows) continuous with gametangial connection (g). Note nearby younger zygosporangium with the zygospore wall (small arrowheads) just beginning to form within zygosporangial wall (large arrowheads). (bar= 20  $\mu\text{m}$ ).
- Fig. 1.17. Higher magnification of mature zygospore (Z) enclosed within partially broken zygosporangial wall (large arrowheads) showing gametangial remnants (gr) and concave gametangial septa (small arrowheads). (bar= 20  $\mu\text{m}$ ).

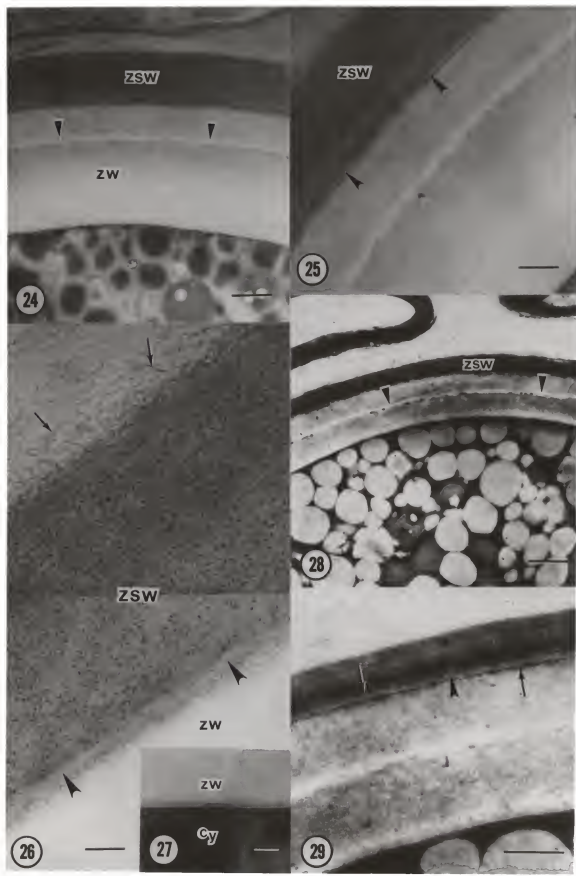


Figs. 1.18-1.23. Endogone pisiformis. Figs. 1.18-1.23. TEM with silver proteinate post stain.

- Fig. 1.18. Very young zygosporangium showing early deposition of electron translucent zygospore wall (small arrowheads) closely adherent to darkly stained wall of zygosporangium (large arrows). Note deposits of possible glycogen (arrows) in sporoplasm (double arrows) and irregular shape of zygosporangium. (bar= 2.0  $\mu\text{m}$ ).
- Fig. 1.19. Young zygosporangium showing attachment of gametangial remnant (gr). Note concave gametangial septum (arrow) and continuity of darkly stained zygosporangial wall with that of gametangium (arrowheads). (bar= 2.0  $\mu\text{m}$ ).
- Fig. 1.20. Higher magnification of portion of Fig. 1.18 showing silver deposition on zygosporangial wall (ZSW) contrasting with relatively unstained wall (ZW) of inclosed zygospore. Note possible glycogen (G) and silver-stained lipid globules (L) in spore cytoplasm. (bar= 0.5  $\mu\text{m}$ ).
- Fig. 1.21. Zygosporangium of more or less intermediate maturity approaching the spherical shape of mature zygospores. Note increased thickness of zygospore wall (ZW), stained (small arrows) and unstained (uL) lipid globules and possible glycogen deposits (arrows) in sporoplasm. (bar= 2.0  $\mu\text{m}$ ).
- Fig. 1.22. Higher magnification of Fig. 1.21 showing zygospore wall (ZW) and zygosporangial wall (ZSW) as well as possible glycogen deposits (arrows) among characteristically perforate, unstained (uL) and silver-stained lipid globules (sL) in sporoplasm. (bar= 1.0  $\mu\text{m}$ ).
- Fig. 1.23. More or less fully mature zygospore exhibiting thick, electron translucent wall enclosed by densely stained zygosporangium. (bar= 5  $\mu\text{m}$ ).



- Figs. 1.24-1.29. Endogone pisiformis. Figs. 1.24-1.29. TEM. Figs. 1.24-1.27. TEM with silver proteinate post stain. Figs. 1.28, 1.29. TEM with barium permanganate post stain.
- Fig. 1.24. Transverse section of mature zygosporangium showing zygosporangial wall (ZSW) enclosing zygospore wall (ZW). Note division (arrows) of latter into two apparent layers. (bar= 1.0  $\mu\text{m}$ ).
- Fig. 1.25. Higher magnification of Fig. 1.24 showing zygosporangial wall (ZSW) and two-layered zygospore wall. Note narrow, unstained region of zygosporangial wall adjacent to zygospore wall (arrowheads). (bar= 0.5  $\mu\text{m}$ ).
- Fig. 1.26. Higher magnification of zygosporangial wall (ZSW) showing narrow, unstained layer (arrowheads) adjacent to inner zygospore wall (ZW). Note uniform deposition of silver on former wall extending into fibrous material on spore surface (arrows). (bar= 0.2  $\mu\text{m}$ ).
- Fig. 1.27. Transverse section of zygosporangium showing transition between zygospore wall (ZW) and spore cytoplasm (Cy). (bar= 0.2  $\mu\text{m}$ ).
- Fig. 1.28. Transverse section of mature zygosporangium showing densely stained zygosporangial wall (ZSW) and unstained zone of zygospore wall (arrowheads) corresponding with zone of division shown in Figs. 1.24. (bar= 1.0  $\mu\text{m}$ ).
- Fig. 1.29. Higher magnification of Fig. 1.28 showing relatively unstained zone (arrowhead) between two very thin, darkly stained zones (arrows) of the primary layer of the zygospore wall. Note also thin, unstained inner zone of zygospore wall. (bar= 0.5  $\mu\text{m}$ ).



Figs. 1.30-1.38. Endogone pisiformis. Figs. 1.30-1.38. TEM of material variously post stained. Fig. 1.30. Uranyl acetate/lead citrate. Figs. 1.31-1.34. Silver proteinate. Figs. 1.35-1.38. Barium permanganate.

Fig. 1.30. Median section of zygosporangium base showing gametangial remnants (gr) and concave gametangial septa (large arrowheads). Note remnants of primary zygosporangial wall (arrows) and primary layer of zygospore wall spanning gametangial connection (small arrowheads). (bar= 2.0  $\mu\text{m}$ ).

Fig. 1.31. Zygosporangium base showing secondary zygosporangial wall (SZW) continuous with inner wall (brackets) of gametangial remnant (gr) and disrupted primary zygosporangial wall (PZW) continuous with outer gametangial wall (\*). Note also primary zygospore layer (small arrowheads) and gametangial septum (large arrowhead). (bar= 1.0  $\mu\text{m}$ ).

Fig. 1.32. Higher magnification of Fig. 1.31 showing secondary zygosporangial wall (SZW) continuous with inner wall (bracket) of gametangial remnant (gr) and disrupted primary zygosporangial wall (PZW) continuous with outer wall (\*) of gametangial remnant. Note primary layer of zygospore (small arrowheads) continuous across gametangial connection. (bar= 0.5  $\mu\text{m}$ ).

Fig. 1.33. Gametangial remnant (gr) showing numerous perforations (arrows) of gametangial septum. (bar= 0.5  $\mu\text{m}$ ).

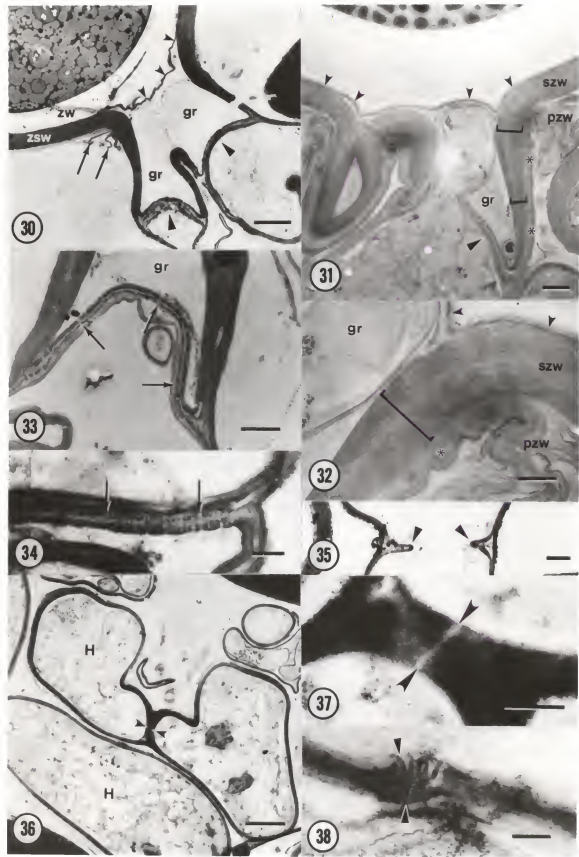
Fig. 1.34. Higher magnification of gametangial septum showing numerous perforations (arrows). (bar= 0.25  $\mu\text{m}$ ).

Fig. 1.35. Transverse section of glebal hypha showing early stage in development of septum (arrowheads). (bar= 0.5  $\mu\text{m}$ ).

Fig. 1.36. Hyphae (H) of sporocarp including a septum with solitary pore (arrowheads). (bar= 2.0  $\mu\text{m}$ ).

Fig. 1.37. Higher magnification of Fig. 1.36 showing densely stained septum and solitary pore (arrowheads) in greater detail. (bar= 0.5  $\mu\text{m}$ ).

Fig. 1.38. Transverse section of wall of glebal hypha showing clustered wall perforations (arrowheads). (bar= 0.5  $\mu\text{m}$ ).



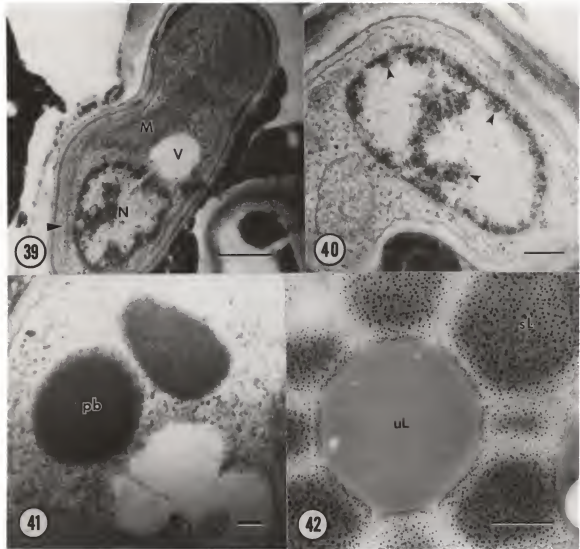
Figs. 1.39-1.42. *Endogone pisiformis*. Figs. 1.39-1.42. TEM. Figs. 1.39-1.41. Uranyl acetate and lead citrate post stained. Fig. 1.42. Silver proteinate post stained.

Fig. 1.39. Transverse section of glebal hypha showing nucleus (N), mitochondrion (M), ER (arrowhead), ribosomes, and vacuole (V). (bar= 0.5  $\mu\text{m}$ ).

Fig. 1.40. Higher magnification of glebal hypha showing nucleus with primarily peripheral clusters of heterochromatin (arrows). (bar= 0.2  $\mu\text{m}$ ).

Fig. 1.41. Higher magnification of glebal hypha showing two apparent protein bodies (pb) with fine, parallel striations. (bar= 0.1  $\mu\text{m}$ ).

Fig. 1.42. Transverse section of mature zygosporae showing delimitation between an unstained lipid globule (uL) and surrounding silver-stained lipid globules (sL). (bar= 0.5  $\mu\text{m}$ ).



CHAPTER II  
LIGHT AND ELECTRON MICROSCOPIC STUDIES OF THE AZYGOSPORES  
OF SELECTED SPECIES OF GIGASPORA

Introduction

The genus Gigaspora was erected by Gerdemann and Trappe (1974), in their monograph of the Endogonaceae, for three species that were first placed in the genus Endogone by Nicolson and Gerdemann (1968), and two newly described taxa. The spores of Gigaspora resemble those of Endogone in size, wall structure, and in the texture of the lipid contents; however, the formation of the spores differs from Endogone and the other currently recognized genera of the Endogonaceae. The spore develops at the tip of a large, swollen suspensor-like cell from which a slender hypha projects to the base of the spore. This hypha is reminescent of a suspensor, but there is no apparent fusion with the spore, and thus no definitive evidence exists for a sexual process in the spore formation of Gigaspora. Consequently, these spores are generally regarded as azygospores (Gerdemann and Trappe, 1974), since they resemble zygospores, form on a single suspensor, and may develop parthenogenetically, although they were originally designated as zygospores by Nicolson and Gerdemann (1968).

Gigaspora is also distinctive in producing endomycorrhizae without vesicles in the root cortex, contrasting with the other endomycorrhiza-forming genera of Endogonaceae which produce both vesicles and arbuscules. The genus does, however, produce vesicle-like auxiliary cells in the soil outside the root (Trappe and Schenck, 1984). These auxiliary cells are thin walled, frequently ornamented, single or in clusters on coiled hyphae, filled with lipids, and have

been likened to the asexual sporulating structures of some Mucorales (Zycha et al. 1969; Gerdemann and Trappe, 1974). However, since they are not cut off from the subtending hypha by septa and possess abundant lipid material, it is assumed that they represent temporary storage reservoirs for azygospore formation (Gerdemann and Trappe, 1974).

Gerdemann and Trappe (1974), in their initial treatment of Gigaspora, presented a key to five species. Subsequently, many additional species have been described (Becker and Hall, 1976; Hall, 1977; Nicolson and Schenck, 1979; Ferrer and Herrera, 1980; Bhattacharjee and Mukerji, 1982; Schenck and Smith, 1982; Koske et al., 1983; Hall and Abbott, 1984). Trappe (1982) listed 18 species of Gigaspora in his synoptic key to the genus.

Ultrastructural investigations of Gigaspora, as for the other genera of Endogonaceae, have been extremely infrequent. This situation is unfortunate, especially in light of the importance of wall characteristics in the delimitation of species within the genus (Trappe, 1982). As stated in the General Introduction, Walker (1983) recently proposed the use of a detailed diagrammatic representation of wall structure for species of VA mycorrhizal fungi. These diagrammatic representations, which he termed murographs, are based upon the wall layering of crushed spores (to minimize the effects of distortions due to light refraction) as observed at the light microscope level. They are very similar to a wall diagram originally presented by Mosse (1970c) for Acaulospora laevis Gerdemann & Trappe, which was

formulated from her investigations of the wall ultrastructure of this species.

Old et al. (1973) first examined the spore ultrastructure of a Gigaspora species. They used scanning and transmission electron microscopy to examine the azygospores of a then unnamed species of "Endogone," later described as Gigaspora nigra Redhead (Nicolson and Schenck, 1979).

In their study they found the wall ultrastructure of G. nigra to be quite complex with the most conspicuous feature being the dark outer wall which consists of an outer layer with a regular pattern of pores enclosing an inner layer of open spiral meshwork. The light brown inner wall, by contrast, is nonperforate and consists of at least four distinct layers, including a very thin layer with radial striations as was shown for A. laevis by Mosse (1970c). Furthermore, the inner wall layers of G. nigra appear to be structurally similar to those of A. laevis as described by Mosse (1970c), although the outer wall structure is quite different for these two taxa.

Old et al. (1973) also detected the presence of a germ plate and germ chambers within the inner wall near the base of the azygospores of G. nigra. This type of germination was also shown for A. laevis in the ultrastructural studies of Mosse (1970a,c) and subsequently has been found to occur in several species of Gigaspora with light microscopy.

Sward (1981a,b,c), in the only other study of spore wall ultrastructure in a Gigaspora species, examined azygospores of G. margarita Becker & Hall. His comprehensive ultrastructural examination

of this species included dormant spore structure (1981a), changes in spore structure accompanying germination (1981b), and details of the germination process (1981c). Regarding the wall structure of mature azygospores, Sward (1981a) found four main wall layers, one of which showed some degree of sublayering. He found the germination of G. margarita azygospores to differ markedly from that previously reported for G. nigra and A. laevis, since there was an absence of intrawall germ chambers. Instead, he found that germ tubes penetrate all wall layers directly and develop between localized thickenings of the innermost wall layer near the base of the azygospores. This mode of germination has also been noted with light microscopy for other species of Gigaspora.

The purpose of this study is to examine the azygospores of several species of Gigaspora with light and electron microscopy in order to obtain more information on the structure of these spores, especially the comparative structure of the spore wall and mode of germination. The data obtained will be compared with that of the type genus Endogone and with the data on Gigaspora from previous ultrastructural studies of the genus.

#### Materials and Methods

##### Source of Material

Freshly collected azygospores of G. margarita, G. heterogama (Nicol. & Gerd.) Gerd. & Trappe, G. gigantea (Nicol. & Gerd.) Gerd. & Trappe, and G. gregaria Nicol. & Schenck were provided by Dr. N. C. Schenck, Dept. of Plant Pathology, University of Florida. These azygospores were obtained from pot cultures grown in a greenhouse. The

spores were isolated by wet sieving and decanting (Gerdemann and Nicolson, 1963) followed by the sucrose centrifugation method of Jenkins (1964). Azygospores of G. pellucida were obtained from rhizosphere soil of a Panicum sp. collected at Sugarfoot Hammock (approximately 0.5 mi west of I-75 on S.W. 20th Ave., Gainesville, Florida). These spores were isolated from the soil by the methods outlined above for the other species under study.

In this study obviously immature, senescent, or parasitized azygospores were generally excluded, since an attempt was made to examine the comparative structure of mature spores from several different taxa. Therefore, only the mature stage in azygospore ontogeny is reported, except as indicated in the results.

#### Light Microscopy (LM)

Whole and crushed mounts of azygospores were observed directly with a Nikon compound light microscope. Additionally, 0.5  $\mu\text{m}$  sections of plastic-embedded material, prepared for electron microscopy as described below, were made. These sections (thick, plastic sections) were stained with a 1:1 mixture of 1% (aq.) azure blue and 1% (aq.) methylene blue (Richardson *et al.*, 1960) and observed with a Nikon compound light microscope equipped with Nomarski differential-interference contrast optics.

#### Scanning Electron Microscopy (SEM)

Groups of approximately 10-15 azygospores, isolated as above for light microscopy, were transferred with micropipettes to the surface of a microscope slide covered with a thin (ca. 1-2 mm) layer of solidified 1% water agar. The slides with the spores were transferred

to 15 x 100 mm plastic, disposable Petri dishes containing a small vessel (ca. 0.5 ml) filled with 4% osmium tetroxide (Quattlebaum and Carner, 1980). The Petri dishes were then sealed securely with several layers of stretched Parafilm, placed in a vented hood, and the azygospores fixed for approximately 96 hours by the osmium tetroxide vapors that developed within the dishes.

At the end of the fixation period the slides were carefully removed from the dishes and the excess osmium discarded. At this time the excess portions of the water agar were trimmed off the slides with a razor blade in order to minimize the desiccation period. The slides were then placed in a desiccator with fresh anhydrous calcium sulfate desiccant (Drierite) for approximately 36 hr in order to sufficiently dry the specimens for gold coating. After the period of desiccation the water agar was reduced to a thin, cellophane-like film to which the spores adhered. This agar film with the adherent spores was carefully transferred with fine forceps to the surface of stubs covered with double-sticky cellophane tape. At this point some of the spores were fractured with a sharp razor blade while being viewed with a stereo dissecting microscope. The stubs were then sputter-coated with gold in a Hummer Jr. sputter coater, and observed with a Hitachi S-450 scanning electron microscope.

#### Transmission Electron Microscopy (TEM)

Groups of approximately 10-15 azygospores, isolated as above for light microscopy, were transferred with micropipettes to the surface of glass microscope slides. The excess water was allowed to dry at room temperature. These groups of spores were then covered with a thin

layer (ca. 2 mm) of molten (warm) 1% water agar, which immediately solidified with the spores embedded within. The layer of agar was then cut with a razor blade into ca. 5 mm strips, each containing 2-5 azygospores. These agar strips were removed from the slide and fixed for 3 hours at room temperature in 1.5% paraformaldehyde, 3.0% glutaraldehyde, 1.5% acrolein, and 2 mM calcium chloride in 0.1 M sodium cacodylate buffer (pH 7.2). The material was rinsed in 0.1 M sodium cacodylate buffer, postfixed in 2.0% osmium tetroxide in 0.1 M cacodylate buffer, and then dehydrated in an ethanol series, which included en bloc staining with saturated uranyl acetate in 70% ethanol for ca. 2 h at room temperature. The ethanol dehydration series was followed by acetone. The material was then embedded in ERL 4206 resin (Spurr, 1969) and ultrathin-sectioned on a Sorvall MT-2 ultramicrotome with a diamond knife. The sections were collected on one-hole, formvar-coated copper grids, stained for 10 min in 2% (w/v) aqueous uranyl acetate followed by 10 min in Reynolds' (1963) lead citrate, and examined at 75 kV on an Hitachi HU-11C or Philips EM-301 transmission electron microscope.

#### Cytochemistry

The barium permanganate post staining method of Hoch (1977) was employed in an attempt to visualize, in better detail, the wall structure of spores, or to obtain differential staining of the spore wall layering. Material prepared for TEM was ultrathin sectioned in the same manner as described above. A drop of aqueous 1% barium permanganate was placed on the sections supported by formvar-coated copper grids. The stain was washed away after ca. 30 sec with a gentle

stream of deionized water. To remove possible contaminants, a drop of 0.05% citric acid was placed on the sections for ca. 30 sec, after which they were rinsed again with deionized water. The sections were then stained with aqueous uranyl acetate for 2 min, rinsed with deionized water, and stained with Reynolds' (1963) lead citrate. Both the uranyl acetate and lead citrate were placed, dropwise, directly on the sections, since staining times were relatively brief. The sections were then given a final deionized water rinse and dried for examination with TEM.

In order to localize possible carbohydrates in the walls of the azygospores, the silver proteinate stain was employed (Thiéry, 1967). Material prepared for TEM was used, however, with the exclusion of the uranyl acetate en bloc treatment during the ethanol dehydration. Thin sections were obtained as described above, but were collected from the boat unmounted with small plastic rings in which the sections floated on the surface of a drop of liquid held in the center (Marinozzi, 1961). These sections were treated as follows: 1) incubated on 1% aqueous periodic acid for 30 min at room temperature; 2) washed on deionized water, once briefly and three times for 10 min each; 3) incubated on 1% thiosemicarbazide in 10% aqueous acetic acid for 24 hr at room temperature; 4) washed on 10% aqueous acetic acid, twice briefly and three times for 20 min each; 5) washed on 5% aqueous acetic acid for 5 min; 6) washed on 1% aqueous acetic acid for 5 min; 7) washed on deionized water two times for 5 min each; 8) incubated on 1% aqueous silver proteinate for 30 min at room temperature in the dark; 9) washed on deionized water, three times briefly and once for

10 min. After this treatment the sections were mounted onto formvar-coated copper grids, dried, and observed with TEM. Control sections were treated as above, however, excluding the 1% periodic acid oxidation step.

### Results

#### Gigaspora margarita

Mature azygospores are white to slightly yellowish, opaque, and approximately 250–350 µm in diameter. The spores generally have a single wall (Fig. 2.1), which is smooth except for occasional surface debris, and they possess a typical swollen suspensor-like connection (Figs 2.2, 2.3). The wall of crushed azygospores appears single at low magnification when observed with LM (Fig. 2.1), but at higher magnification there appears to be a thin outer wall layer and a thick inner layer (Fig. 2.4). The inner wall layer often appears multilayered or lamellate (Fig. 2.5). Thick, plastic sections stained with AMB show a conspicuous, darkly stained outer layer and a thick, relatively less intensely stained inner layer (Figs. 2.7, 2.8). When observed with SEM the wall appears multilayered. However, the outer layer is distinct and is constant in thickness, while there is much variation in the number and thickness of the inner wall sublayers (Fig. 2.6).

TEM of azygospores reveals, in some instances, a wall of more or less uniform composition (Figs. 2.9–2.12), and relatively good preservation of spore cytoplasm (Fig. 2.9). At low magnification little wall detail is apparent (Fig. 2.9), but at higher magnification four wall layers of approximately equal thickness are discernible

(Figs 2.10-2.12). In addition, a very thin, electron dense innermost layer is evident (Figs. 2.10, 2.12).

By contrast, TEM of other preparations of G. margarita show thin sublayers consisting of coarse ripples within the thick inner layer (Figs. 2.13, 2.14). Lying just below the outer wall layer (I) in these sections is a thin layer that shows finer rippling or striations (Fig. 2.14).

Sections treated with barium permanganate were relatively more darkly stained than with the regular lead citrate and uranyl acetate post stain (Figs. 2.15-2.17). In these the outer layer is generally quite evident, but there is little detectable sublayering in the thick, inner wall layer. The thin, innermost layer, however, is always distinct (Figs. 2.16, 2.17).

Thin sections post stained with silver proteinate reveal the distinction between the outer and inner wall layers quite well (Figs. 2.18-2.20). At lower magnification (Figs. 2.18, 2.19) the outer layer has a more or less uniform granular texture, and the thick inner layer has little sublayering. However, at higher magnification (Fig. 2.20) a deposition of fine silver grains is present in the outermost zone of the outer layer (I) (Fig. 2.20). Also, the inner wall layer possesses bands, each consisting of an arcuate pattern of fine microfibrils (Fig. 2.20). The width of these bands appears to decrease from outside inward. The thin, electron opaque innermost wall, however, is not well stained in these preparations (Fig. 2.19).

Swollen areas of the electron opaque, innermost wall are frequently observed near the base of azygospores (Figs. 2.21-2.23).

These first appear as slightly bulging, localized areas adjacent to the plasmalemma (Fig. 2.21), but increase in thickness (Fig. 2.22) and often appear in pairs (Fig. 2.23).

The cytoplasm of G. margarita is well preserved with the acrolein-glutaraldehyde-paraformaldehyde primary fixation. A standard complement of sporoplasmic organelles is present, including numerous nuclei, mitochondria, ER, and lipid globules (Figs. 2.9, 2.13, 2.24-2.30). Intensely stained, electron opaque granules are visible in both LM (Figs. 2.7, 2.8) and TEM (Figs. 2.9, 2.24, 2.25, 2.29). They are generally quite electron opaque, variable in size, and are always enclosed within vacuoles (Figs. 2.9, 2.25). These structures apparently represent polyphosphate granules as described by White and Brown (1979).

Clusters of nuclei, in proximity to the wall opposite the bulbous suspensor, were present in some of the azygospores examined (Figs. 2.13, 2.26). These nuclei have very coarse, granular contents, are generally quite irregular in outline, and appear to have discontinuous envelopes. (Figs. 2.26, 2.28). By contrast, other azygospores examined possessed nuclei dispersed within the sporoplasm (Figs. 2.9, 2.29). These nuclei are very regular in shape, have less granular contents, and possess smooth, continuous envelopes (Fig. 2.30).

#### Gigaspora heterogama

Mature azygospores are light to dark brown, 150-250  $\mu\text{m}$  in diam. and generally possess a laterally attached bulbous suspensor (Figs. 2.31-2.33). When observed using LM the azygospore surface appears echinulate (Figs. 2.32, 2.34, 2.36). When viewed with SEM, the surface

ornamentation consists of evenly distributed, stalked and frequently cupulate structures (Figs. 2.33, 2.35, 2.37).

The azygospore wall is comprised of a thick outer wall and a thin, membranous inner wall that readily separate from each other (Figs. 2.37, 2.38). At higher magnification the inner membranous wall appears multilayered (Fig. 2.39). The thick outer wall, in some preparations, also appears to be divided into a dark outer and relatively light inner layer (Figs. 2.38-2.39), but in others it appears as a single thick wall with a thin outer layer supporting the surface ornamentations (Figs. 2.40, 2.41).

When observed with TEM, the outer wall has three distinct sublayers. The outermost layer (I) is very thin and appears to be continuous with the surface ornaments (Figs. 2.42-2.44). The next wall layer (II) is relatively thin and appears to have a fibrillar pattern that is more or less parallel with the spore surface (Figs. 2.43, 2.44, 2.46). The innermost layer (III) of the outer wall is the thickest and possesses a uniform granular texture, except for the presence of fine, parallel striations which apparently represent microchatter resulting from ultrathin sectioning.

The membranous inner wall, at the TEM level, appears quite complex in structure (Figs. 2.42, 2.43, 2.45). This wall consists of outer (i) and inner (ii) layers separated by a "double membrane-like" partition (Figs. 2.43, 2.45). Also, there appears to be a thin, electron opaque innermost layer (Figs. 2.43, 2.45), very similar to that of G. margarita (cf. Figs. 2.10, 2.12). The inner wall layer (ii)

frequently has a sublayering of variable, alternating light and dark bands (Figs. 2.43, 2.45).

Germ chambers within the membranous inner wall were observed in G. heterogama (Figs. 2.47-2.50). These chambers appear to develop within the inner layer (ii) (Figs. 2.48, 2.49). Each germ chamber is filled with cytoplasmic material and develops its own radial and tangential walls (Fig. 2.50).

#### Gigaspora pellucida

The azygospores of G. pellucida are hyaline, globose to oblong, smooth-surfaced, and approximately 80-200 µm in diam. at the greatest dimension (Figs. 2.51, 2.52). The spore wall consists of a thick, brittle outer wall which separates from the thin, membranous inner wall (Figs. 2.53, 2.54, 2.56). At higher magnification a distinct pore can be detected in the wall between the spore and the swollen suspensor connection (Figs. 2.54, 2.55).

The membranous inner wall readily separates from the brittle outer wall in crush mounts of azygospores (Figs. 2.56-2.58). The outer wall often appears as a single, thick wall (Fig. 2.57) but may separate into two (Fig. 2.58) or three (Fig. 2.59) layers. Thick, plastic sections reveal a thick, uniform, darkly stained outer wall and a thin, less intensely stained inner wall (Fig. 2.60).

In TEM the outer and inner walls are quite distinct (Fig. 2.61). The outer wall consists of numerous thin lamellae and is separated from the membranous inner wall by a thin, double membrane-like partition (Fig. 2.63). The membranous inner wall, on the other hand, consists of two distinct layers of approximately equal thickness and a

thin, electron opaque innermost layer (Fig. 2.62). The outer wall and membranous inner wall separate at the double membrane-like partition (Fig. 2.62). At higher magnification the lamellae of the outer wall can be seen as bands of microfibrils in an arcuate pattern (Fig. 2.64).

Germination chambers also develop within the membranous inner wall of the azygospores of this species (Figs. 2.65-2.71). In germinating spores the membranous wall increases markedly in thickness (Fig. 2.65). In TEM this increased thickness is seen to result from an expansion of the outer layer (i) (Fig. 2.66). This expansion apparently is due to the disorganization of part of the wall material of this layer into a loose matrix of both granular and fibrous components (Figs. 2.66, 2.69). The germ chambers develop within this disorganized zone of the outer layer (i) (Figs. 2.67-2.69).

The silver proteinate stain is deposited primarily on the outer wall of the azygospores of G. pellucida (Fig. 2.70). The deposition of silver grains, however, is not uniform across the wall; there appears to be greater accumulation on the outer layers and the very innermost layers of this wall (Fig. 2.70). By contrast, the inner membranous layer has very little stain deposited (Fig. 2.71). The use of barium permanganate post stain resulted in a generally darker wall staining and was, otherwise, similar to the regular uranyl acetate and lead citrate post stain.

#### Gigaspora gigantea

The azygospores of this species are large (approximately 250-450  $\mu\text{m}$  in diam.) and have a distinctive greenish-yellow color. Plastic-

embedded azygospores, thick-sectioned and stained with AMB, have a darkly stained outer layer and a thicker, less intensely stained inner layer (Figs. 2.72, 2.73, 2.77). These layers are tightly bound but can be separated when the spores are put under firm pressure and the walls crushed (Figs. 2.75, 2.76).

When observed with TEM, the azygospore wall is composed of an outer layer, in which the fibrillar texture runs parallel with the spore surface, and an inner layer which is relatively thicker and more electron opaque (Figs. 2.78, 2.79). At higher magnification the outer layer can be seen to possess a thin, nonfibrous outermost layer consisting of two zones, one electron opaque and the other translucent (Fig. 2.80, bracket). The inner layer, at higher magnification, has a fibrillar pattern running approximately perpendicular to that of the outer layer (Fig. 2.80). The electron opaque innermost layer (Fig. 2.78, open arrow) develops wall thickenings (Fig. 2.81) that are very similar to those reported for G. margarita. (cf. Figs. 2.21-2.23). The azygospore wall also has an opening to the bulbous suspensor that is occluded by a plug of what appears to be membrane-bound cytoplasmic material with an irregular surface facing toward the spore contents (Fig. 2.74).

#### Gigaspora gregaria

The azygospores of this species are approximatley 250-400 µm in diam., reddish-brown to dark brown and possess a surface layer of mound-shaped ornaments (Fig. 2.82). Thick, plastic sections of azygospores stained with AMB show an outer wall consisting of an almost continuous layer of mound-shaped ornaments supported by a very

darkly stained inner layer (Figs. 2.83, 2.84). The inner wall separates under pressure from the outer wall and is comprised of a thick outer layer and a thin, membranous inner layer (Fig. 2.84). Thick, plastic sections also show the inner wall of the spore to be continuous with the inner wall of the bulbous suspensor and, likewise, the outer wall of the spore continuous with the outer wall of the suspensor (Fig. 2.85).

When observed with TEM, the surface layer consists of more or less mound-shaped ornaments (Figs. 2.86, 2.87). The inner layer of the outer wall is electron opaque and continuous (Fig. 2.86, 2.87). The inner wall consists of a thick outer layer (Fig. 2.87) that has fine, radial striations similar to those in the outer wall of G. heterogama (cf. Figs. 2.43, 2.44, 2.50), and a somewhat thinner inner layer. At higher magnification the individual ornaments of the outer layer appear as thin, interwoven fibrillar material (Fig. 2.88). This fibrillar material and the outer portion of the underlying layer are the only parts of the azygospore wall to take up the silver stain (Fig. 2.89). With the barium permanganate post stain the azygospore wall differed from the normal uranyl acetate and lead citrate post stain only in that all the layers were more darkly stained.

#### Discussion

The genus Gigaspora is characterized by the formation of azygospores; these are defined as parthenogenetically formed zygospores and always develop from a single gametangium (Blakeslee, 1920; Benjamin and Mehrotra, 1963; Hawksworth et al., 1983). Benjamin and Mehrotra described two species of Mucor that are known to form

only azygospores, listed the species of Mucorales that produce azygospores with or without the concurrent production of zygospores, and discussed the significance of azygospore formation in the Mucorales. In addition to species that develop only azygospores under normal conditions (obligate azygosporogenesis), others may form them sporadically by changes in culture conditions or by interspecific or intergeneric matings (induced azygosporogenesis) (Benjamin and Mehrotra, 1963; O'Donnell *et al.*, 1977b). The azygosporic nature of these species is evident, since the azygospore develops from a single structure clearly identifiable as a gametangium and since the azygospore is morphologically very similar to the zygospores produced by the same species or genus.

The azygosporic nature of Gigaspora, however, is less clear than in species of Mucorales. Since true zygospores are not known to occur in Gigaspora, the azygospores can only be compared to the closest presumed relative to produce zygospores, i.e., the genus Endogone. Although there are distinct differences between Gigaspora and Endogone, such as the endocarpic and non-endomycorrhizal status of the latter contrasting with ectocarpic and obligate endomycorrhizal status of the former, there still appears to be a degree of similarity in the morphology of the spores, and since the swollen suspensor of Gigaspora resembles a gametangium of Endogone, it can only be assumed that this structure functions as a gametangium and that the resulting spores represent azygospores.

The hyphal protuberance, which projects back obliquely from the bulbous suspensor to the base of the azygospore and which is

frequently found in species of Gigaspora, was originally suggested as a possible reduced gametangium (Nicolson and Gerdemann, 1968). This hyphal projection is usually septate, and one cell may act as a gametangium. However, fusion of this structure with the spore wall has never been reported, and thus no actual evidence for its function as a gametangium exists. Furthermore, protuberances of greater or lesser complexity occur on the suspensors of several genera of zygomycetes including Fennellomyces (Misra *et al.*, 1979), Phycomyces (O'Donnell *et al.*, 1976), Absidia and Radiomyces (Mistry, 1977), and in none of these have the appendages been shown to have any apparent sexual function, but rather are assumed to play a role in zygosporangium dispersal (Benjamin, 1979; Bessey, 1950).

The wall ultrastructure of G. margarita presented in this study is somewhat at odds with that shown by Sward (1981a). He described four wall layers in his ultrastructural examination of G. margarita. The evidence in this study indicates that he studied azygospores similar to those shown in Figs. 2.13 and 2.14. These sections contain thin zones of coarse ripples which are assumed to be artifactual, since they appear to be in regions of the ultrathin sections that have torn, rather than sliced, in the ultrathin sectioning of the plastic-embedded material. The rippling of these layers shown in Figs. 2.13 and 2.14 is somewhat coarser than that reported by Sward (1981a, Fig. 2.5). However, the second outermost layer reported by Sward (II) appears to correspond to the more finely rippled layer (r) in Fig. 2.14 of this study. Also, the very thick third layer in Sward's study appears to correspond to the three inner layers (II-IV) of this study

shown in Fig. 2.10. These layers can be seen with the silver proteinate post stained sections (Fig. 2.20) to correspond with the bands of arcuate microfibrils. These patterns of apparent arcuate microfibrils are responsible for "layers" II through IV of Figs. 2.10-2.12 and also perhaps for the sublayering of the third layer reported by Sward (1981a).

From the data presented in this study, the actual structure of the wall of G. margarita is represented in Fig. 2.20, which shows a thin outer wall layer with microfibrils in an orientation parallel to the spore surface, and a much thicker inner layer with the microfibrils existing in an apparent arcuate orientation in bands. The occurrence of these bands of apparent arcuate microfibrils explains why there seems to be sublayering in the thick inner wall layer in the normal post stained preparations, since the number and thickness of the bands correspond with that of the sublayers. It also explains the LM observation of a lamellate appearance to the thick inner wall of the azygospores. Bonfante-Fasolo and Vian (1984) recently have shown the occurrence of these bands of arcuate microfibrils in the wall ultrastructure of Glomus epigaeum Daniels & Trappe, a chlamydosporic species of Endogonaceae in which the spores possess a single laminated wall. They point out that these bands, as well as the arcuate orientation of the microfibrils, are an optical effect of the sectioning process. Apparently, the microfibrils are neither curved, as the arches indicate, nor in bands; instead, they are deposited onto the wall in parallel bundles that are offset from each other by small angles. Deposition of microfibrils that results in 180 degrees of

rotation results in what appears to be one band upon sectioning. Thus, the wall is actually a single unit (wall) composed of varying numbers of rotations of microfibrillar deposition (Bonfante-Fasolo and Vian, 1984).

The reason for the presence of rippled sublayers in some sections, as shown in this study and in Sward's (1981a) study, must still be explained. It is felt that the rippling produced in the layers, as shown in Figs. 2.13 and 2.14, perhaps represents a difference in the age of the azygospores. The possibility exists that, as the spores mature, the wall chemistry changes in such a way that certain zones, possibly as represented by the rippled areas, become less amenable to fixation, embedding, or some other preparatory process of EM, resulting in the rippling observed. Although an attempt was made to use only mature spores for this study, some variation in the maturity of the spores perhaps occurred and, accordingly, may have resulted in these differences.

Good preservation of the cytoplasm of the azygospores for TEM occurred only in G. margarita. The clusters of nuclei in the cytoplasm of this species, as shown in Figs. 2.26 and 2.13, are assumed to be the "nuclear centers" described by Sward (1981a), which are clusters of nuclei in proximity to the wall distal to the suspensor connection. The significance of the differences observed between these nuclei and those that occur isolated in the cytoplasm is not known, except that they may possibly represent different metabolic or mitotic states.

In spite of the lack of preservation of the cytoplasm of the majority of species examined, the wall structure appeared to be better

preserved. The structure of the walls falls into two broad categories, those with an inner membranous wall (G. heterogama, G. pellucida, and G. gregaria) and those lacking this wall (G. margarita and G. gigantea). This separation into two groups also correlates with the two different modes of germination found in these species. Direct penetration of germ tubes through the azygospore wall between mound-shaped thickenings of the innermost wall layer occurs in G. margarita (Sward, 1981a) and G. gigantea (Nicolson and Gerdemann, 1968). By contrast, preliminary formation of intrawall germ chambers with subsequent formation of germ tubes that then penetrate the remaining wall layers occurs in G. heterogama and G. pellucida, as is shown in this study, and as has been observed in the spores of G. gregaria (N. C. Schenck, pers. comm.).

The association of the membranous wall and germination chambers is not surprising, since the germ chambers always develop within this wall. Specifically, the germ chambers develop within a sublayer of the inner membranous wall as is shown for G. heterogama and G. pellucida in this study. This, however, is somewhat surprising, as one might expect the separation of this wall, to accommodate these chambers, to occur at a preexisting partition, such as the double membrane-like partition of G. heterogama or the separation between the inner and outer layers of G. pellucida. Furthermore, the germ chambers of both G. nigra (Old *et al.*, 1973) and A. laevis (Mosse, 1971b) appear to form within a layer, rather than at any existing partition or division in the membranous walls of these species, as far as can be determined from the micrographs presented in their studies.

Of interest also in the structure of the inner membranous wall is the area of disorganization noted in the wall layer containing the germ chambers of G. pellucida. This zone appears to be unique to this species, since it was not found in the germinating spores of G. heterogama in this study, or in G. nigra (Old et al., 1973) or A. laevis (Mosse, 1971a,c). The significance of this area is not known. If the disruption of the microfibrillar structure is necessary to accommodate the expanding germ chambers, then one would expect to see this in the other species producing these chambers, which is not the case.

The species of Gigaspora all share a closely defined complex of characters. The large size of the spores and the swollen suspensor-like hyphal attachment with the peculiar hyphal protrusion separate this genus well from the other genera in the classification of the family. However, the infrageneric classification of the genus presents a special problem. Although Gigaspora is not officially divided into infrageneric taxa, traditionally it has been separated, especially in the construction of taxonomic keys, into the dark-spored and light-spored species. This separation is perhaps suitable as an artificial character, but the wall ultrastructure and mode of germination perhaps are more important in reflecting the phylogeny of the species included in the genus. This more natural grouping does not correlate with the separation based upon spore pigmentation, an excellent example from this study being the hyaline-spored G. pellucida being allied with the dark-spored G. heterogama on the basis of similarity of wall

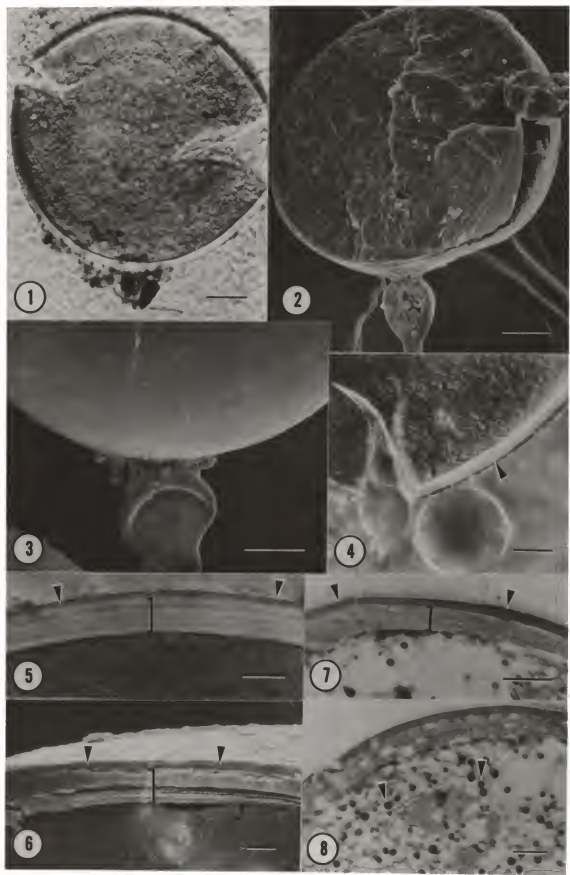
ultrastructure and germination mode, rather than with the light-spored species, G. margarita and G. gigantea.

Perhaps the most pressing taxonomic difficulty with Gigaspora lies, not with its infrageneric classification, but rather with its position relative to the other genera of the family, especially the type genus Endogone. This problem is associated with the "presumed" azygosporic status of the genus. Evidence from this study indicates that the outer wall of several of the Gigaspora species examined may be homologous to the zygosporangium of Endogone (Chapter I), since these two structures appear to be similar in staining properties. At the light microscope level, the outer wall of G. margarita (Fig. 2.7) and the zygosporangium of Endogone pisiformis (Fig. 1.15) stain very similarly with AMB. Also, the thick outer wall of G. pellucida (Figs. 2.60, 2.65) and the outer walls of G. gigantea (Figs. 2.73, 2.77) and G. gregaria (Figs. 2.84, 2.85) stain very darkly with AMB similar to the zygosporangium of Endogone pisiformis (Fig. 1.15). Likewise, with silver proteinate at the TEM level, the outer walls of G. margarita (Fig. 2.20, bracket), G. pellucida (Figs. 2.70, 2.71), and G. gregaria (Figs. 2.88, 2.89) all are stained as is the zygosporangium of Endogone pisiformis (Figs. 1.20, 1.24-1.26), although the staining of the former is not as uniform as is that of the zygosporangium of Endogone.

The above evidence indicates that Gigaspora may be closely related to Endogone, especially in conjunction with the recent findings of Berch and Fortin (1983b) that intrawall germ chambers develop in the zygospores of Endogone pisiformis similar to those

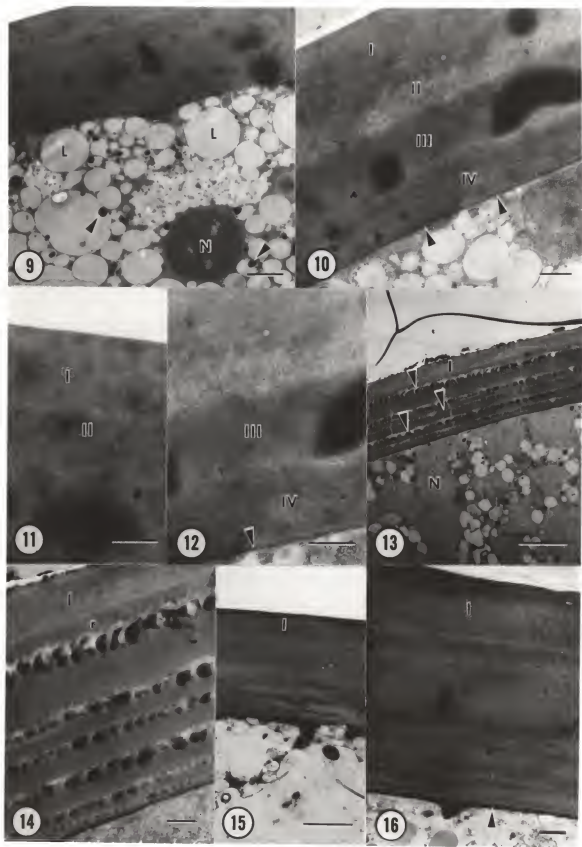
known to occur in azygospores of Gigaspora. An examination of the very early stages of azygospore formation including nuclear behavior would be of great benefit in helping to solve this problem. If the spores are determined to be azygospores (or even true zygosporcs), then the affinity of the genus with the genus Endogone, and placement in the Endogonaceae, would be greatly strengthened.

- Figs. 2.1-2.8. *Gigaspora margarita*. Figs. 2.1, 2.4, 2.5, 2.7, 2.8, Light Microscopy (LM). Figs. 2.2, 2.3, 2.6, Scanning Electron Microscopy (SEM).
- Fig. 2.1. Whole mount of crushed azygospore. (bar= 50  $\mu\text{m}$ ).
- Fig. 2.2. Azygospore fractured longitudinally showing spore contents and attachment of bulbous suspensor. (bar= 50  $\mu\text{m}$ ).
- Fig. 2.3. Higher magnification of azygospore base showing smooth wall and collapsed bulbous suspensor (bar= 50  $\mu\text{m}$ ).
- Fig. 2.4. Portion of crushed azygospore showing relatively thin outer layer (arrowhead) and thicker inner layer of wall. (bar= 50  $\mu\text{m}$ ).
- Fig. 2.5. Higher magnification of azygospore wall showing thin, dark outer layer (arrowheads) and relatively thick, lamellate inner layer (bracket). (bar= 10  $\mu\text{m}$ ).
- Fig. 2.6. Azygospore wall showing relatively thin outer layer (arrowheads) and thicker inner layer (bracket) divided into several sublayers. (bar= 10  $\mu\text{m}$ ).
- Fig. 2.7. Thick, plastic section of azygospore showing thin, darkly stained outer layer (arrowheads) and relatively thicker, less intensely stained inner wall (bracket). (bar= 20  $\mu\text{m}$ ).
- Fig. 2.8. Thick, plastic section as in Fig. 2.7, except showing numerous darkly stained, vacuole-enclosed, apparent polyphosphate granules (arrowheads) within spore cytoplasm. (bar= 20  $\mu\text{m}$ ).



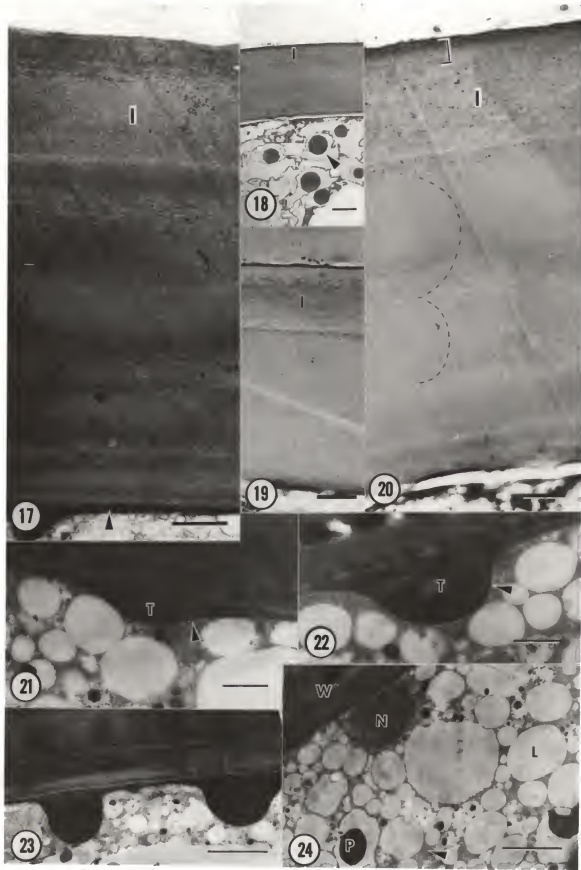
Figs. 2.9-2.16. Gigaspora margarita. Transmission Electron Microscopy (TEM).

- Fig. 2.9. Azygospore showing wall and some enclosed cytoplasmic contents including lipid globules (L), apparent polyphosphate granules (arrowheads), and a nucleus (N). (bar= 1.0  $\mu$ ).
- Fig. 2.10. Higher magnification of wall showing somewhat indistinct wall layers (I-IV, from outside inward) and a very thin, electron opaque innermost layer (arrowheads). (bar= 0.5  $\mu$ ).
- Fig. 2.11. Higher magnification of outer wall layers (I and II). (bar= 0.5  $\mu$ m).
- Fig. 2.12. Higher magnification of inner wall layers (III and IV) including a relatively thin innermost layer (arrow). (bar= 0.5  $\mu$ m).
- Fig. 2.13. Portion of azygospore wall showing a distinct outermost layer (I), several rippled layers of inner wall (arrowheads), and a portion of cytoplasm containing numerous nuclei (N) with granular contents. (bar= 2.0  $\mu$ m).
- Fig. 2.14. Higher magnification of Fig. 2.13 showing wall details including outer layer (I) and thin, rippled layer (r). (bar= 0.5  $\mu$ m).
- Fig. 2.15. Portion of azygospore wall post stained with barium permanganate showing darkly stained wall with little detectable sublayering, except for outer layer (I). (bar= 2.0  $\mu$ m).
- Fig. 2.16. Higher magnification of portion of azygospore wall stained with barium permanganate showing conspicuous outer layer (I) and relatively thick inner layer with inconspicuous sublayering, except the thin, electron opaque innermost layer (arrowhead). (bar= 0.5  $\mu$ m).



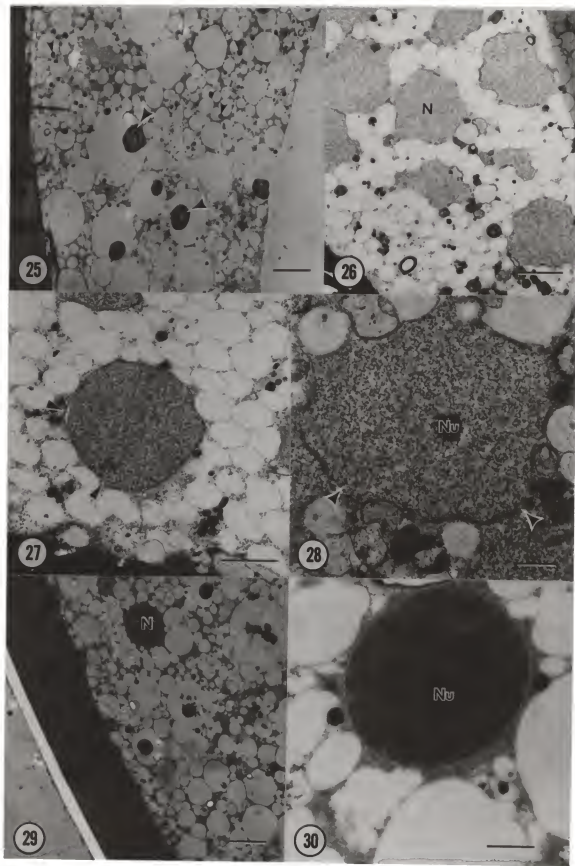
Figs. 2.17-2.24. Gigaspora margarita. TEM.

- Fig. 2.17. Higher magnification of Fig. 2.16 showing mottled area of staining in outermost wall layer (I) adjacent to spore surface and indistinct sublayering of remainder of azygospore wall, except the innermost layer (arrowhead). (bar= 0.5  $\mu\text{m}$ ).
- Fig. 2.18. Azygospore post stained with silver proteinate showing outer (I) and inner wall layers enclosing a portion of cytoplasm which includes several darkly stained possible polyphosphate granules (arrowheads). (bar= 2.0  $\mu\text{m}$ ).
- Fig. 2.19. Higher magnification of wall in Fig. 2.18 showing conspicuous inner and outer (I) wall layers. (bar= 1.0  $\mu\text{m}$ ).
- Fig. 2.20. Higher magnification of wall as in Fig. 2.19 showing outer layer (I) with fine silver grains deposited near outer surface (bracket), but otherwise with a homogeneous, granular texture and thick inner wall layer. Note inner layer consists of bands of fine microfibrils arranged in an arcuate pattern (dashed lines). (bar= 0.5  $\mu\text{m}$ ).
- Fig. 2.21. Thickened area (T) of electron opaque innermost wall layer bordering on plasmalemma (arrowhead) of azygospore. (bar= 0.5  $\mu\text{m}$ ).
- Fig. 2.22. A more fully developed thickening (T) of innermost wall layer adjacent to plasmalemma (arrowhead). (bar= 0.5  $\mu\text{m}$ ).
- Fig. 2.23. Two closely spaced thickenings (T) of innermost wall layer. (bar= 1.0  $\mu\text{m}$ ).
- Fig. 2.24. Portion of cytoplasm adjacent to spore wall (W) showing various organelles including a nucleus (N), mitochondrion (arrowhead), possible polyphosphate granules (P), and lipid globules (L). (bar= 1.0  $\mu\text{m}$ ).

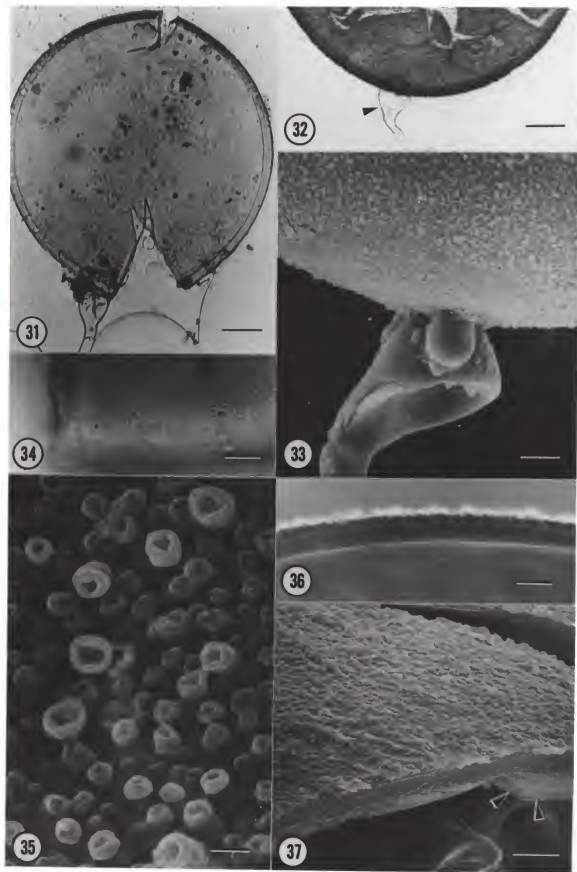


Figs. 2.25-2.30. Gigaspora margarita. TEM.

- Fig. 2.25. Portion of cytoplasm adjacent to wall showing several large (large arrowheads) and numerous smaller (small arrowheads) electron opaque, vacuole-enclosed possible polyphosphate granules. (bar= 2.0  $\mu\text{m}$ ).
- Fig. 2.26. Area of cytoplasm near spore wall showing several irregularly shaped, granular nuclei (N). (bar= 2.0  $\mu\text{m}$ ).
- Fig. 2.27. Nucleus from same area as Fig. 2.26 showing partially disrupted nuclear envelope (arrowheads) consisting of double membrane. (bar= 1.0  $\mu\text{m}$ ).
- Fig. 2.28. Higher magnification of nucleus as in Fig. 2.26 with single nucleolus (Nu) and envelope that is discontinuous (arrowheads). (bar= 0.5  $\mu\text{m}$ ).
- Fig. 2.29. Portion of spore cytoplasm with only infrequent nuclei (N). (bar= 2.0  $\mu\text{m}$ ).
- Fig. 2.30. Higher magnification of nucleus as in Fig. 2.29 showing smooth, continuous envelope and less granular contents, including a nucleolus (Nu). (bar= 0.5  $\mu\text{m}$ ).



- Figs. 2.31-2.37. Gigaspora heterogama. Figs. 2.31, 2.32, 2.34, 2.36, LM. Figs. 2.33, 2.35, 2.37, SEM.
- Fig. 2.31. Whole mount of crushed azygospore in distilled water. (bar= 50  $\mu\text{m}$ ).
- Fig. 2.32. Base of crushed azygospore showing rough surface and bulbous suspensor connection (arrowhead). (bar= 50  $\mu\text{m}$ ).
- Fig. 2.33. Azygospore base showing fine surface ornamentation and bulbous suspensor. (bar= 10  $\mu\text{m}$ ).
- Fig. 2.34. Azygospore wall in surface view showing the roughened appearance due to ornamentation. (bar= 20  $\mu\text{m}$ ).
- Fig. 2.35. Higher magnification of azygospore surface showing numerous cupulate ornaments. (bar= 1.0  $\mu\text{m}$ ).
- Fig. 2.36. Azygospore wall in optical section showing fairly indistinct sublayering and roughened surface. (bar= 20  $\mu\text{m}$ ).
- Fig. 2.37. Azygospore wall broken open, exposing a portion of membranous inner layer (arrowheads). (bar= 5.0  $\mu\text{m}$ ).



Figs. 2.38-2.46. Gigaspora heterogama. Figs. 2.38-2.41. LM. Figs. 2.42-2.46. TEM.

Fig. 2.38. Azygospore showing membranous inner wall (arrowheads) partially separated from outer wall (W). (bar= 50  $\mu$ m).

Fig. 2.39. Higher magnification of Fig. 2.38 showing sublayering of membranous inner wall (arrowheads). (bar= 25  $\mu$ m).

Fig. 2.40. Portion of rigid outer wall broken open showing a thin outermost layer (arrowheads) visible on each side of break. (bar= 25  $\mu$ m).

Fig. 2.41. Thick, plastic section of outer wall showing indistinct sublayering including thin outermost layer (arrowheads). (bar= 10  $\mu$ m).

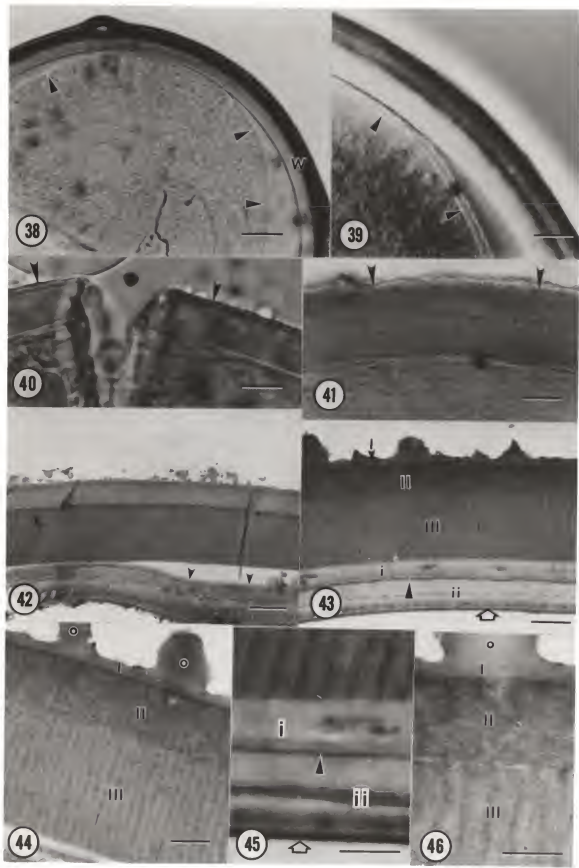
Fig. 2.42. Azygospore wall showing membranous inner wall (arrowheads) separating from thick outer wall. (bar= 2.0  $\mu$ m).

Fig. 2.43. Section of wall showing various layers (I, II and III, from outside inward) of outer wall, membranous inner wall comprised of two layers (i and ii) separated by a double membrane-like partition (large arrowhead), and thin, electron opaque innermost layer (small arrowhead). (bar= 1.0  $\mu$ m).

Fig. 2.44. Higher magnification of outer wall showing outermost layer (I) giving rise to spore ornaments (o), middle layer (II) with fibrillar orientation parallel to spore surface, and thick inner layer (III) with fine parallel striations. (bar= 0.5  $\mu$ m).

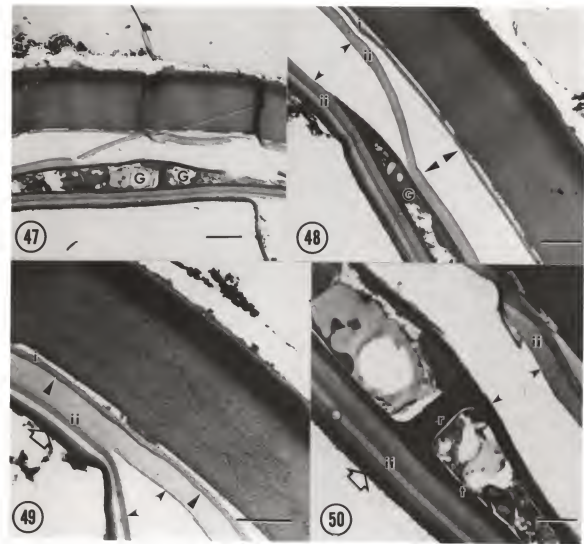
Fig. 2.45. Higher magnification of membranous inner wall showing outer (i) and inner (ii) layers separated by thin, double membrane-like partition (arrowhead). Note alternating light and dark bands of inner layer (ii) and thin, electron opaque innermost layer (open arrow). (bar= 0.5  $\mu$ m).

Fig. 2.46. Higher magnification of outer wall showing parallel orientation of fibrillar material of middle layer (II), portion of inner striate layer, and outermost layer (I) including base of protruding ornament (o). (bar= 0.5  $\mu$ m).



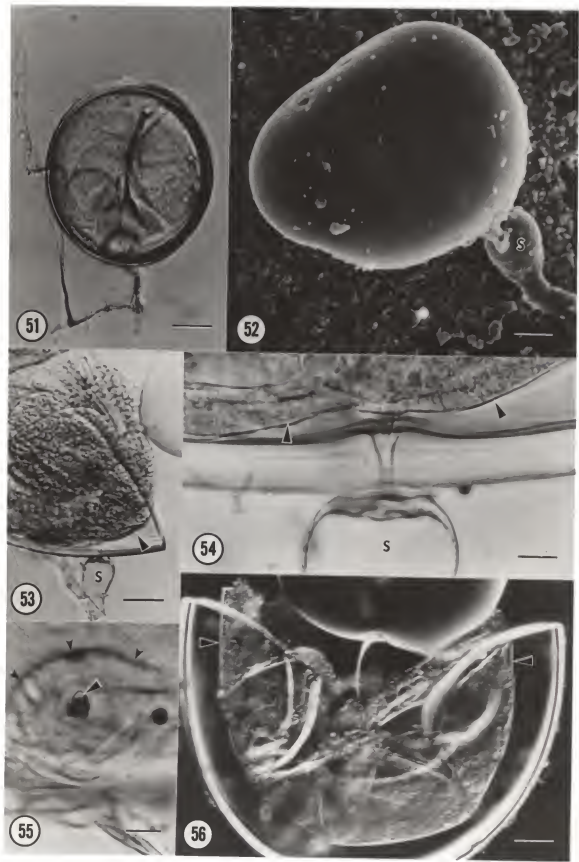
Figs. 2.47-2.50. Gigaspora heterogama. TEM

- Fig. 2.47. Portion of inner membranous wall, broken away from outer wall, containing two germ chambers (G). (bar= 3  $\mu\text{m}$ ).
- Fig. 2.48. Germ chamber showing its position within inner layer (ii) of inner membranous wall. Note that this layer (ii) has split apart (small arrowheads) at end of germ chamber and that the double membrane-like partition has also split (large arrowheads) separating outer layer (i) from inner layer (ii). (bar= 2.0  $\mu\text{m}$ ).
- Fig. 2.49. Higher magnification of same wall as in Fig. 2.48 showing inner membranous wall layer (ii) in which germ chambers develop partially split open (small arrowsheads). Note double membrane-like partition (large arrowheads) separating inner layer (ii) from thin outer layer (i) and electron opaque innermost layer (open arrow). (bar= 2.0  $\mu\text{m}$ ).
- Fig. 2.50. Higher magnification of germ chambers showing radial (r) and tangential (t) walls of each chamber and enclosed cytoplasmic contents. Note chambers embedded in layer ii, which has split (arrowheads), and electron opaque innermost layer (open arrow). (bar= 1.0  $\mu\text{m}$ ).



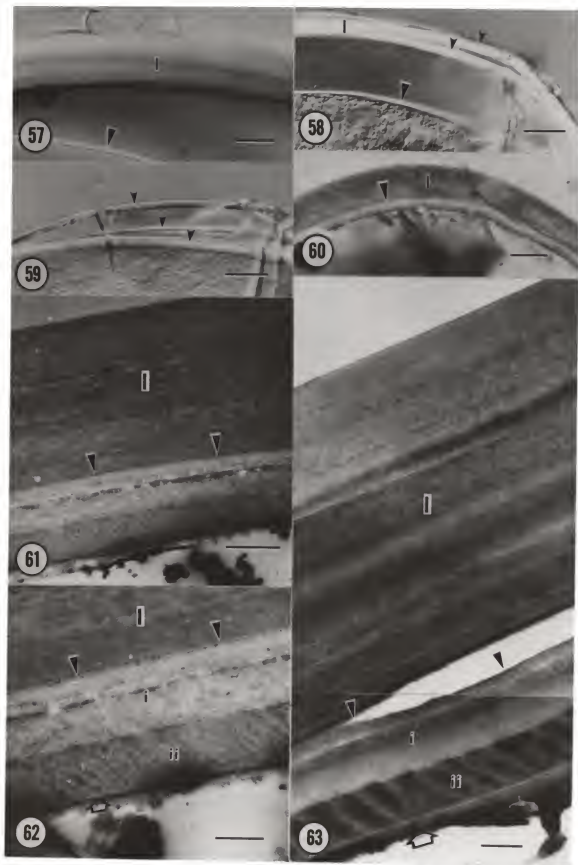
Figs. 2.51-2.56. Gigaspora pellucida. Figs. 2.51, 2.53-2.56, LM. Fig. 2.52, SEM.

- Fig. 2.51. Whole mount of azygospore in distilled water. (bar= 50  $\mu\text{m}$ ).
- Fig. 2.52. Oblong azygospore showing smooth surface and bulbous suspensor (S). (bar= 20  $\mu\text{m}$ ).
- Fig. 2.53. Crushed azygospore showing inner membranous wall (arrowhead) separated from brittle outer wall at bulbous suspensor connection (S). (bar= 50  $\mu\text{m}$ ).
- Fig. 2.54. Higher magnification of bulbous suspensor attachment (S) showing separation of membranous wall (arrowheads) from outer wall and a pore through the wall into suspensor (S). (bar= 10  $\mu\text{m}$ ).
- Fig. 2.55. Base of azygospore in surface view showing bulbous suspensor (small arrowheads) and pore (large arrowhead). (bar= 20  $\mu\text{m}$ ).
- Fig. 2.56. Whole mount of crushed azygospore showing thin, pliable, membranous inner wall (arrowheads) completely separated from thick, brittle outer wall. (bar= 50  $\mu\text{m}$ ).



Figs. 2.57-2.63. Gigaspora pellucida. Figs. 2.57-2.60. LM. Figs. 2.61-2.63. TEM.

- Fig. 2.57. Outer wall of azygospore, which appears as a single layer, separated from inner membranous wall (arrowhead). (bar= 20  $\mu\text{m}$ ).
- Fig. 2.58. Azygospore showing outer wall separated from membranous inner wall (large arrowhead) and divided into two layers (small arrowheads). (bar= 50  $\mu\text{m}$ ).
- Fig. 2.59. Crushed outer wall separated into three distinct layers (arrowheads). (bar= 50  $\mu\text{m}$ ).
- Fig. 2.60. Thick, plastic section of azygospore showing darkly stained outer wall (I) contrasting with less intensely stained, membranous inner wall (arrowhead). (bar= 20  $\mu\text{m}$ ).
- Fig. 2.61. Azygospore showing thick, lamellate outer wall (I) separated from membranous inner wall by thin, double membrane-like partition (arrowheads). (bar= 1.0  $\mu\text{m}$ ).
- Fig. 2.62. Higher magnification of Fig. 2.61 showing fine, double membrane-like partition (arrowheads) and membranous inner wall with thick, relatively electron translucent outer layer (i), and striate inner layer (ii). Note thin, electron opaque innermost layer (open arrow) adjacent to sporoplasm. (bar= 0.5  $\mu\text{m}$ ).
- Fig. 2.63. Azygospore showing outer wall (I) partially separated from inner membranous wall layers (i and ii). Note expanded and somewhat vacuolate appearance of innermost layer (open arrow) of membranous wall. (bar= 0.5  $\mu\text{m}$ ).



Figs. 2.64-2.71. Gigaspora pellucida. Figs. 2.64, 2.66, 2.68-2.71, TEM. Figs. 2.65, 2.67, LM.

Fig. 2.64. Higher magnification of outer wall showing each lamella as a band of microfibrils in apparent arcuate orientation (dashed lines). (bar= 0.2  $\mu\text{m}$ ).

Fig. 2.65. Thick, plastic section of azygospore wall showing densely stained outer wall (I) and greatly expanded membranous inner wall (II). (bar= 20  $\mu\text{m}$ ).

Fig. 2.66. Portion of azygospore wall as in Fig. 2.65, but in ultrathin section, showing increased wall thickness due to area of apparent microfibrillar expansion and disruption (d) within outer layer (i) of inner membranous wall. Note also inner (ii) and innermost (open arrow) layers of this wall. (bar= 2.0  $\mu\text{m}$ ).

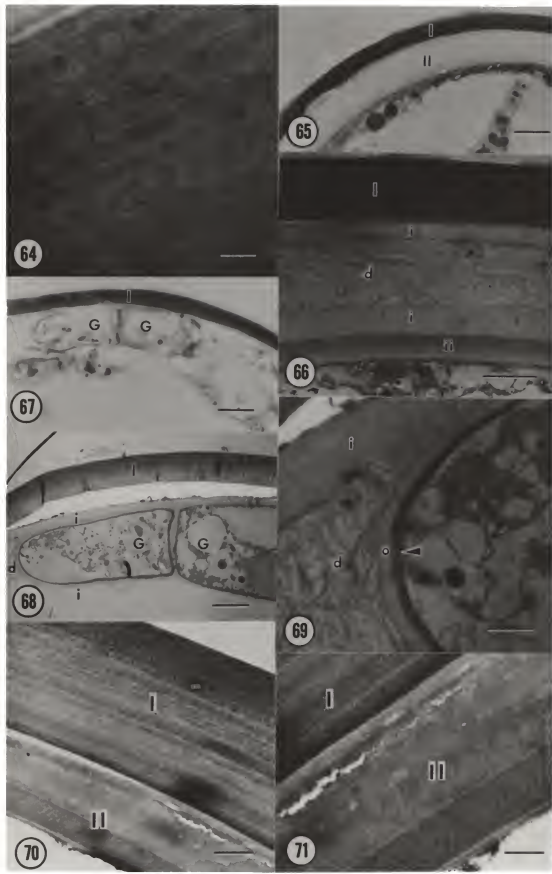
Fig. 2.67. Thick, plastic section of wall showing outer wall (I) and germ chambers (G) within inner membranous wall. (bar= 20  $\mu\text{m}$ ).

Fig. 2.68. Ultrathin section of wall as in Fig. 2.67 showing outer wall (I) and two germ chambers (G) within area of microfibrillar disruption (d) in outer layer (i) of membranous wall. (bar= 2.0  $\mu\text{m}$ ).

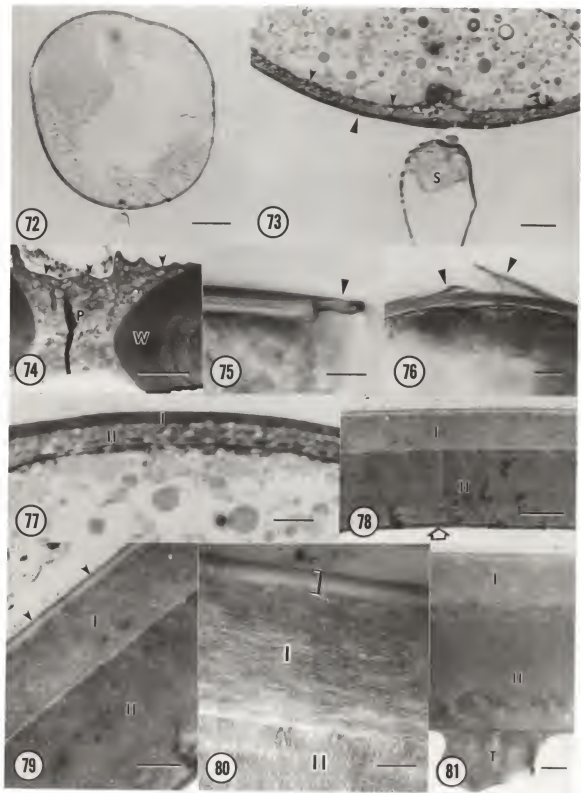
Fig. 2.69. Higher magnification of part of germ chamber within disorganized area (d) in outer layer (i) showing outer (o) and inner (arrowhead) walls of chamber. (bar= 0.5  $\mu\text{m}$ ).

Fig. 2.70. Azygospore wall post stained with silver proteinate showing stain restricted to outer wall (I), especially to outermost lamellae, and little stain in inner wall (II). (bar= 1.0  $\mu\text{m}$ ).

Fig. 2.71. Higher magnification of portion of wall as in Fig. 2.70 showing outer wall (I) with deposition of fine silver grains and little deposition on inner membranous wall (II). (bar= 0.5  $\mu\text{m}$ ).

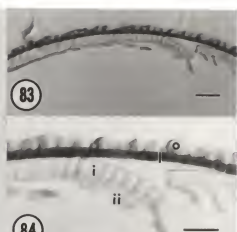


- Figs. 2.72-2.81. Gigaspora gigantea. Figs. 2.72, 2.73, 2.75-2.77, LM.  
Figs. 2.74, 2.78-2.81, TEM.
- Fig. 2.72. Thick, plastic section of azygospore. (bar= 50  $\mu\text{m}$ ).
- Fig. 2.73. Higher magnification of Fig. 2.72 showing base of azygospore with bulbous suspensor attachment (S) and darkly stained outer wall (large arrowhead) contrasting with thicker, less intensely stained inner wall (small arrowheads). (bar= 20  $\mu\text{m}$ ).
- Fig. 2.74. Opening in base of azygospore wall (W) to bulbous suspensor attachment occluded by plug (P) of cytoplasmic material with irregular surface (arrowheads) facing toward spore contents. (bar= 2.0  $\mu\text{m}$ ).
- Fig. 2.75. Crushed azygospore showing portion of outer wall (arrowhead) separated from inner wall at break. (bar= 20  $\mu\text{m}$ ).
- Fig. 2.76. Outer wall (arrowheads) of crushed azygospore separated from thicker inner wall. (bar= 25  $\mu\text{m}$ ).
- Fig. 2.77. Thick, plastic section of azygospore showing darkly stained outer wall (I) and thicker, less intensely stained inner wall (II). (bar= 10  $\mu\text{m}$ ).
- Fig. 2.78. Azygospore wall showing outer wall (I) and thicker, relatively more electron opaque, inner wall (II) with very thin innermost layer (open arrow) adjacent to spore contents. (bar= 1.0  $\mu\text{m}$ ).
- Fig. 2.79. Higher magnification of wall showing inner wall (II) and outer wall (I), with microfibrils of the latter parallel to surface of spore (arrowheads). (bar= 0.5  $\mu\text{m}$ ).
- Fig. 2.80. Outer wall showing two thin, nonfibrous outer zones (bracket), of electron opaque and translucent nature respectively, enclosing much thicker layer of parallel microfibrils (I). Note approximate perpendicular orientation of microfibrils of inner layer (II) to those of outer wall. (bar= 0.3  $\mu\text{m}$ ).
- Fig. 2.81. Azygospore showing outer (I) and inner (II) walls with characteristic thickening (T) of innermost wall layer. (bar= 0.5  $\mu\text{m}$ ).



Figs. 2.82-2.89. Gigaspora gregaria. Figs. 2.82-2.85, LM. Figs. 2.86-2.89, TEM.

- Fig. 2.82. Whole mount of crushed azygospore in distilled water showing roughened surface resulting from mound-shaped ornaments. (bar= 50  $\mu$ m).
- Fig. 2.83. Thick, plastic section of azygospore wall. (bar= 25  $\mu$ m).
- Fig. 2.84. Higher magnification of Fig. 2.83 showing outer wall, comprised of outer ornamentation layer (o) and darkly stained inner layer (I), partially separated from inner wall which is comprised of thick outer layer (i), that has been somewhat rippled in sectioning, and thin inner layer (ii) that is partially fragmented. (bar= 20  $\mu$ m).
- Fig. 2.85. Thick, plastic section of azygospore showing inner wall of spore (layers i and ii) continuous with inner wall of bulbous suspensor (small arrowheads) and outer wall of spore (layers o and I) continuous with outer wall of suspensor (large arrowheads). (bar= 20  $\mu$ m).
- Fig. 2.86. Azygospore wall showing outer wall comprised of ornamentation layer (o) and electron opaque inner layer (I) and inner wall consisting of thick outer layer (i) and relatively thin, membranous layer (ii). (bar= 2.0  $\mu$ m).
- Fig. 2.87. Wall structure showing thin, fibrillar surface ornaments (o) and underlying electron opaque layer (I). Note striate appearance of outer layer (i) and underlying inner layer (ii) of inner wall. (bar= 1.0  $\mu$ m).
- Fig. 2.88. Azygospore, stained with silver proteinate, showing some deposition of stain on ornamentation layer (o) and outer zone of inner layer (I) in outer wall. (bar= 0.5  $\mu$ m).
- Fig. 2.89. Higher magnification of Fig. 2.88 showing silver deposition on ornamentation layer (o) and outer portion of underlying layer (I). (bar= 0.2  $\mu$ m).



CHAPTER III  
LIGHT AND ELECTRON MICROSCOPE EXAMINATION OF THE CHLAMYDOSPORES  
OF SELECTED SPECIES OF GLOMUS AND SCLEROCYSTIS

Introduction

The genera Glomus and Sclerocystis differ from the other taxa of Endogonaceae in producing chlamydospores. Glaziella was formerly considered chlamydosporic but appears to be an ascomycete with unispired ascii that resemble chlamydospores (see Chapter IV). Glomus and Sclerocystis were initially included in the Endogonaceae on the basis of a general resemblance of the chlamdospores and sporocarps to those of known zygosporic species of Endogone. The species of Glomus, furthermore, were generally assumed to represent anamorphic states of zygosporic species (Thaxter, 1922; Kanouse, 1936; Gerdemann and Trappe, 1974). This assumption was strengthened by reports of zygospores occurring in the sporocarps of two different Glomus species, G. fasciculatum (Thaxter) Gerdemann & Trappe (Thaxter, 1922) and G. microcarpum Tul. & Tul. (Godfrey, 1957a). However, Gerdemann and Trappe (1974) believe that these reports represent chance mixtures of Endogone zygospores and Glomus chlamydospores growing together, or possibly instances of hyperparasitism. The chlamydospores of both genera are borne terminally on single, undifferentiated hyphae, although rare instances of intercalary chlamydospores and more than one sporophore per spore have been reported for Glomus (Thaxter, 1922; Gerdemann and Trappe, 1974; Gerdemann and Bakshi, 1976).

The genus Glomus was initially erected by Tulasne and Tulasne (1845), but was later synonymized with Endogone (Tulasne and Tulasne, 1851), a disposition accepted by Thaxter (1922) in his monograph of

the Endogonaceae. However, Gerdemann and Trappe (1974), in their more recent treatment of the family, recognize the genus Glomus. Initially, only species of Glomus (as currently recognized) possessing spores in sporocarps (endocarpic) were known. However, Nicolson and Gerdemann (1968) later described species of Glomus that produce chlamydospores singly in the soil (ectocarpic). Subsequently, many additional ectocarpic species have been described, perhaps due, in part, to the use of the wet sieving and decanting method for isolation of individual spores from soil samples (Gerdemann and Nicolson, 1963). Trappe (1982) listed 45 species of Glomus in his synoptic key.

The genus Sclerocystis consists only of endocarpic species and differs from Glomus in that the spores are arranged in the sporocarps compactly in a single layer around a central core of sterile, interwoven hyphae. As with Glomus, a peridium may or may not be present. Chlamydospores of Sclerocystis generally are more elongate than in species of Glomus, with the long axis of the spores radially aligned in the sporocarps. This difference, as a basis for generic separation, is not very great, but Gerdemann and Trappe (1974) believe that Sclerocystis may represent a specialized sporocarpic arrangement, and perhaps an evolutionary advance, and, therefore, that the two genera should be maintained separately.

Sclerocystis was first described by Berkeley and Broome (1873) for the type species S. coremioides. Later, von Höhnel (1910) transferred two previously described taxa, Ackermania dussii Patouillard (1902) and A. coccogenes Patouillard (1902) to Sclerocystis. These three species then were included in the first

monograph of the Endogonaceae (Thaxter, 1922). Gerdemann and Trappe (1974) included one additional species (S. rubiformis Gerd. & Trappe) in their monograph. Subsequently, several new species have been described; Trappe (1982) listed eight species in his synoptic key.

There are relatively few ultrastructural studies of Glomus or Sclerocystis. Several studies have dealt with the ultrastructure of Glomus mycorrhizae (i.e., the colonized root), and these have recently been reviewed by Scannerini and Bonfante-Fasolo (1983). However, none of these studies has also dealt with the fine structure of chlamydospores. There are no previous studies of the wall structure of a species of Sclerocystis. Recently, however, Bonfante-Fasolo and Vian (1984) examined the wall ultrastructure of the chlamydospores of Glomus epigaeum Daniels and Trappe. They found the chlamydospores of this species to possess a complex wall structure, including a relatively thin outer wall consisting of parallel microfibrils and a thick inner wall consisting of layers of microfibrils in an apparently arched orientation. This is, so far as I know, the first report of such an organized microfibrillar arrangement in the cell wall of a fungus.

The purpose of this study is to examine the structure of selected species of Glomus and Sclerocystis with both light and electron microscopy, particularly the structure of the chlamydospores and sporocarps, in order to obtain additional comparative information regarding these structures and to assess their position within the Endogonaceae. The study also includes the morphology and ultrastructure of roots of bahia grass colonized with Glomus.

intraradices, since these structures were more or less inadvertently observed while examining root segments for the characteristic intraradical chlamydospores.

#### Materials and Methods

##### Source of Material

Freshly isolated chlamydospores of Glomus intraradices Schenck & Smith and root segments of bahia grass (Paspalum notatum L.) colonized by this species were provided by Dr. N. C. Schenck, Dept. of Plant Pathology, University of Florida, along with freshly collected chlamydospores of Glomus constrictum Trappe and Glomus etunicatum Becker & Gerdemann. The chlamydospores and colonized root segments were obtained from pot cultures using the methods previously described in Chapter II for species of Gigaspora. Sporocarps of Sclerocystis coremioides Berk. & Broome were obtained from Dr. J. M. Trappe, U. S. Forestry Service, Corvallis, Oregon. These sporocarps were growing epigeously in association with a Musa sp. in the Department of Botany greenhouse, Oregon State University, Corvallis, Oregon.

As stated previously for Gigaspora spp. in Chapter II, in this study an attempt was made to examine mature chlamydospores and sporocarps, except as indicated in the results.

##### Light Microscopy

Crushed or whole mounts of chlamydospores in distilled water were observed directly with a Nikon compound light microscope. In addition, 0.5  $\mu\text{m}$  sections were made of plastic-embedded chlamydospores, sporocarps, or colonized roots of bahia grass that were prepared for TEM as described below. These sections (thick, plastic sections) were

stained with azure and methylene blue (1:1 aqueous mixture) according to the method of Richardson *et al.* (1960), as previously described for Gigaspora spp. in Chapter II, and examined with a Nikon compound light microscope equipped with Nomarski differential-interference contrast optics.

#### Electron Microscopy and Cytochemistry

The chlamydospores of the Glomus species listed above were prepared for scanning and transmission electron microscopy (SEM and TEM, respectively) as previously described in Chapter II for Gigaspora species. Also, the barium permanganate and silver proteinate post staining procedures, as described for Gigaspora in the preceding chapter, were used for these chlamydospores.

S. coremioides, however, was prepared for SEM by: 1) fixation in cacodylate-buffered glutaraldehyde, 2) dehydration in graded ethanol, and 3) critical point drying followed by gold coating. However, the same TEM and cytochemical preparations as for the Glomus species listed above were employed for this species.

#### Results

##### Glomus intraradices

The chlamydospores of Glomus intraradices are yellowish gray-brown to greenish brown, predominantly globose to infrequently subglobose (Fig. 3.1), ca. 50-175  $\mu\text{m}$  in diameter, and generally produced singly or in clusters within the cortex of colonized roots (Figs. 3.17, 3.18). Young chlamydospores possess an ephemeral outer wall that is generally not present in older spores (Fig. 3.2). This outer wall is apparently degraded by soil microorganisms, as indicated

by irregular chambers, lysed areas, and colonies of bacteria within this wall layer (Figs. 3.2-3.4, 3.8, 3.9, 3.11). The inner wall of the chlamydospores is persistent, up to 15  $\mu\text{m}$  thick in mature spores, and is distinguished by the presence of several layers, or lamellae, when viewed with LM (Fig. 3.6). The multiple layers are also detectable in SEM at higher magnifications (Figs. 3.4, 3.5). The primary constituent of the spore cytoplasm appears to be lipid globules of various sizes with other cytoplasmic constituents enclosed between (Figs. 3.3, 3.5, 3.7, 3.8).

With the use of TEM the inner chlamydospore wall can be seen to consist of several layers (Figs. 3.7-3.9). Senescent chlamydospores, in which the inner wall layers separated from the outer layer and from themselves, were helpful in visualizing the inner wall structure. In these spores there appears to be a thick outer layer (Figs. 3.10, 3.11), the outer surface of which was frequently degraded, presumably by soil microbial activity (Fig. 3.11). Also, there are approximately four inner layers of about equal thickness and of relatively greater electron opacity than the outer layer (Figs. 3.11, 3.12). Little detail of microfibrillar arrangement was evident in the wall ultrastructure of these chlamydospores, and in no case was the apparent arcuate orientation of microfibrils, as shown in the preceding chapter for certain species of Gigaspora, observed. Furthermore, post staining with barium permanganate and silver proteinate provided no differential staining or enhanced detail of spore wall ultrastructure above that of the normal uranyl acetate and lead citrate post stain.

The intraradical hyphae of G. intraradices are oriented primarily longitudinally within the root cortex (Figs. 3.18, 3.19). With the use of TEM these hyphae can be seen to contain many vacuoles and large amounts of glycogen (Figs. 3.13-3.16). Few other cytoplasmic constituents were observed. Infrequent septa occur in these hyphae, especially near branching points, and these septa have fine, radial perforations (Figs. 3.13-3.15). However, mature septa in the main axis of the intraradical hyphae are without any obvious perforations (Figs. 3.14, 3.16).

Certain areas of the colonized bahia grass roots were observed to be slightly more yellowish than, but otherwise morphologically identical to, the remainder of the root. These discolored areas were found to be heavily colonized, with the inner cortical cells possessing abundant arbuscules (Figs. 3.20-3.23) and numerous tannin bodies (Figs. 3.21, 3.22). Various stages of arbuscular development were evident in these areas, from the highly branched stages to the compacted masses of collapsed arbuscular branches (Figs. 3.20-3.23).

When observed with TEM, the arbuscular branches are highly vacuolate and relatively thin walled (Fig. 3.24). At higher magnification a matrix of medium electron opacity is evident between the wall of the arbuscular branch and the plasmalemma of the cortical cell enclosing it (Fig. 3.25). Within the cortical cells, arbuscular branches appear to be progressively compressed into compact, tonoplast-bound masses (Figs. 3.27, 3.28), more than one of which may occur in a single cortical cell, along with highly branched, uncompressed portions of the arbuscule (Fig. 3.23). Apparently, quite

normal cytoplasm exists in these extensively colonized cortical cells including numerous mitochondria (Fig. 3.24). Furthermore, with TEM tannin bodies are evident only in the vacuole of the cortical cells (Fig. 3.24), although this particular position within the cell was not discernible with light microscopy alone (Fig. 3.22). The tannin bodies are quite variable in size (Fig. 3.24), are electron opaque, and are non-membrane bound (Fig. 3.26).

#### Glomus constrictum

The chlamydospores of Glomus constrictum are globose, medium to dark brown, approximately 150-300  $\mu\text{m}$  in diameter (Fig. 3.29), and possess a hyphal attachment that is frequently constricted near the spore base (Fig. 3.30). The spores generally have a smooth, shiny surface, but may possess scattered surface debris (Figs. 3.31, 3.33). The chlamydospores have a single, thick wall (Figs. 3.31, 3.32), but this may appear as two layers in LM (Trappe, 1977) and in SEM (Fig. 3.33). With LM the wall frequently appears to consist of numerous thin lamellae (Figs. 3.34, 3.35).

With the use of TEM, the single, thick wall can be seen to possess approximately 10-12 bands (Figs. 3.36, 3.37), each of which consists of microfibrils in an apparent arcuate orientation (Fig. 3.38). Between the arcuate bands are zones in which the microfibrils appear to come together into an approximate parallel orientation (Fig. 3.38, bracket). No obvious outer wall layer was evident in the chlamydospores, except for a very thin outermost zone (Fig. 3.38). With the spores of this species, as was the case for G. intraradices, neither the barium permanganate nor silver proteinate post staining

resulted in improved contrast or differential staining of the spore wall over that of the regular post stain.

The chlamydospore cytoplasm of G. constrictum was not particularly well preserved in the preparations for TEM. However, the typical predominant lipid complement was present with interspersed cytoplasmic constituents (Fig. 3.36). Several double membrane-bound structures were observed between the lipid globules of some spores and appear to be nuclei (Figs. 3.39, 3.40). In several instances these were observed in tetrads (Fig. 3.39), but no indication of nuclear division was observed.

#### Glomus etunicatum

Chlamydospores of Glomus etunicatum are globose to subglobose, approximately 75-175  $\mu\text{m}$  in diameter, yellowish brown to brown, smooth walled, but frequently roughened with adherent surface debris (Fig. 3.41).

The chlamydospores possess two walls. Young spores have an ephemeral outer wall which is apparently degraded and breaks away as the spore matures, exposing the smooth, persistent inner wall (Figs. 3.42-3.44). Also, the outer wall stains more intensely than the inner wall with AMB in the thick, plastic sections (Fig. 3.45).

When observed with TEM, the ephemeral outer wall has coarse, electron opaque fibrils embedded in a granular matrix in a parallel orientation to the spore surface (Figs. 3.46-3.48). The outer surface is irregular, as though by microbial degradation, and exhibits abundant adherent debris (Figs. 3.46-3.48). Furthermore, this wall appears to be divided into two layers, although this division is

fairly indistinct and no separation of these layers was observed (Figs. 3.47, 3.48).

With TEM the persistent inner wall, in some instances, appears of more or less uniform granular composition (Fig. 3.46). In other instances, the inner wall appears to have several bands (Fig. 3.49) similiar to those described earlier for G. constrictum (cf. Fig. 3.36). However, an arcuate pattern of microfibrils is not clearly evident, either in the outer (Fig. 3.50) or inner (Fig. 3.51) bands of this wall. Instead, the bands between the parallel-arranged (Fig. 3.50, p) zones of microfibrils appear to have numerous, more or less irregular open spaces, or lacunae, of various sizes (Fig. 3.50, arrowheads). However, as was the case for G. constrictum, the bands do appear to become less distinct from the spore surface inward (Figs. 3.49, 3.50, 3.51).

The cytoplasm of the chlamydospores of this species was not very well preserved by the procedures used for TEM and, therefore, was not observed at the TEM level. However, the thick, plastic sections indicated the usual predominant complement of lipid globules (Fig. 3.44). Also, the barium permanganate and silver proteinate post stains were not helpful in elucidating wall structure over that of the normal post staining.

#### Sclerocystis coremioides

The sporocarps of Sclerocystis coremioides are subglobose to pulvinate, basally flattened, tan to light brown, 350-600  $\mu\text{m}$  in diameter, and occur epigeously in loose aggregations (Fig. 3.52). They possess a peridium of sterile, interwoven hyphae (Figs. 3.52-3.54).

The chlamydospores are arranged radially in a single layer around a central plexus of sterile hyphae (Figs. 3.54, 3.55).

The individual chlamydospores are obovoid to ellipsoid, approximately 55 x 75  $\mu\text{m}$ , and are embedded in a mass of very thick-walled hyphae (Fig. 3.56). With the use of SEM, the cytoplasm of the spores can be seen to consist of lipid globules of various sizes (Fig. 3.56). However, the cytoplasm was not well preserved in the TEM preparations and thus was not observed in ultrathin sections.

Colonies of bacteria occur within the chambers formed by the hyphae in the peridium of the sporocarps (Fig. 3.57) and in the central plexus (Fig. 3.59). These colonies are frequently quite dense, especially in the plexus (Figs. 3.58, 3.59).

The chlamydospore walls intergrade with the walls of surrounding hyphae, making the interpretation of these walls difficult (Figs. 3.57, 3.60). The spores have a thin, electron opaque inner layer and a thick outer layer; the latter frequently fuses with the wall of appressed hyphae (Fig. 3.61).

Occasional septa were observed in certain relatively thin-walled hyphae of the central plexus. These septa have distinct perforations (Figs. 3.62, 3.63) which are, however, coarser than those reported earlier in the intraradical hyphae of G. intraradices (cf. Figs. 3.13, 3.15).

#### Discussion

Although the separation of the genera Glomus and Sclerocystis is based merely upon the arrangement of the chlamydospores within the sporocarp, this separation has been defended on the basis of a

possible advanced organization of sporocarp structure in Sclerocystis (Gerdemann and Trappe, 1974). Furthermore, for many years species of these two genera have been grown in pot culture, and in these there has been no report of the production of spores or sporocarps of the one genus with those of the other (N. C. Schenck, pers. comm.). While this fact does not constitute direct proof that these genera are distinct, it is at least circumstantial evidence that they represent different taxa. Therefore, their continued separation appears justified until new evidence to the contrary arises.

The sporocarps of Sclerocystis are extremely difficult to prepare for TEM, and this presents a barrier to obtaining further data on the ultrastructure of this genus. The data from the TEM of S. coremioides presented in this study are rudimentary, since the spore wall ultrastructure was difficult to interpret, due to the apparent fusion with contiguous walls. Preliminary attempts to examine the sporocarps and chlamydospores of S. rubriformis Gerd. & Trappe and S. sinuosa Gerd. & Bakshi with TEM were not successful. Certainly, additional EM studies on species of this genus are needed. Perhaps most helpful in elucidating the relationship between Sclerocystis and Glomus would be a comparison of endocarpic Glomus species with species of Sclerocystis. However, endocarpic Glomus species were not available in this study, since they are rarely reported in Florida (N. C. Schenck, pers. comm.) and are less common, in general, than ectocarpic species.

Certain aspects of spore wall structure revealed in this study are of interest. The apparent bands of arcuate microfibrils that were shown for G. epigaeum by Bonfante-Fasolo and Vian (1984) and for

Gigaspora species in Chapter II, are also shown here most clearly for Glomus constrictum (Figs. 3.36-3.38). As discussed in the preceding chapter, these bands of curved microfibrils are an apparent illusion, since the microfibrils are neither bent nor laid down in bands, but rather are straight and are laid down in parallel bundles that are progressively offset from each other by small angles. This ordered deposition of microfibrils is apparently a rather common phenomenon in the formation of the chitinous cuticle of arthropods and in the cell walls of higher plants, as was discussed in detail by Bonfante-Fasolo and Vian (1984).

Bands were also present in the inner wall of Glomus etunicatum, and, although these bands are superficially very similar to those of G. constrictum and to those of G. epigaeum as reported by Bonfante-Fasolo and Vian (1984), they lack the arcuate microfibrillar arrangement, having instead irregularly shaped lacunae. However, the thinner bands of microfibrils in parallel arrangement that lie between the arcuate bands in the aforementioned two species, are also present in G. etunicatum, making this species very similar to them in this aspect of wall structure. The possibility exists that, as a result of incomplete penetration of fixative and(or) resin into the wall in the TEM preparation, these lacunae represent artifacts, and that good preservation of the spore wall might have revealed bands of arched microfibrils, as is evident in the other species. Also, the individual inner wall layers of G. intraradices (Figs. 3.11, 3.12) are reminiscent of the apparent bands of microfibrils in the inner wall of G. constrictum (Figs. 3.36-3.38) and G. etunicatum (Fig. 3.49).

However, no microfibrillar pattern was discernible in these, and this aspect of comparative spore wall structure in this species must await further study.

Also of note in reference to G. etunicatum is the lack of bands in the inner wall of young chlamydospores (i.e., those possessing an ephemeral outer wall as shown in Fig. 3.46). Therefore, younger spore stages may have a wall structure very different from that of mature spores. Mosse (1970) found the ultrastructure of young azygospores of Acaulospora laevis Gerd. & Trappe to differ considerably from that of mature spores. Hers is the only developmental study of the spore wall ultrastructure of a species of Endogonaceae, and thus the need for additional studies is obvious.

An outer wall exists only in young spores of G. etunicatum and G. intraradices. Soil microorganisms apparently play a role in the degradation of this ephemeral wall. This is particularly evident from the TEM of G. intraradices, which shows portions of the wall lysed, presumably by the action of soil microorganisms. Also, the wall of G. etunicatum spores appears degraded in TEM, although this occurs primarily at the surface. MacDonald and Chandler (1981), in their ultrastructural study of Glomus caledonicum (Nicol. & Gerd.) Trappe & Gerd., reported bacteria in and on the chlamydospore walls and discussed the presence of these bacteria in relation to surface sterilization of spores and axenic culture of these fungi.

Soil microorganisms are involved in spore dormancy and germination. Several species of Glomus require a dormancy period before germination is possible (Godfrey, 1957b; Daniels and Graham,

1976; Hepper and Smith, 1976). Also, improved spore germination under unsterilized conditions, implicating soil microbial activity, has been noted by several researchers (Mosse, 1959; Daniels and Graham, 1976; Daniels and Trappe, 1980). However, no specific soil factor responsible for enhanced germination has been identified (Herrick, 1984), and the possibility of a nutritional, rather than microbial, factor must also be considered in germination experiments using sterilized soils (Daniels and Graham, 1976). Nevertheless, strong evidence exists for the presence of self-inhibitors in the spores of at least some species of Endogonaceae (Watrud *et al.*, 1978; Daniels and Trappe, 1980), and it is possible that soil microorganisms, such as those associated with the spore wall in the present study and in the ones cited, may in some way eliminate these self-inhibitors by their physical or chemical activities in or on the walls.

The ephemeral outer wall of the chlamydospores in the two species mentioned above contrasts with the absence of an outer wall in G. constrictum and with G. epigaeum (Bonfante-Fasolo and Vian, 1984), in which a well-defined outer wall exists, but which is persistent, neither breaking away from the inner wall, nor becoming degraded at maturity. Perhaps in some species of ectocarpic Endogonaceae, the ephemeral outer wall acts to protect the chlamydospores from the adverse activities of the surrounding soil microflora until the inner wall develops structural or chemical resistance against such degradation.

G. intraradices, in spite of the difficulty in preparing the chlamydospores for TEM, provided an opportunity to examine arbuscular

and intraradical hyphal ultrastructure, since these structures occur within the root cortex, along with abundant spores. Previous ultrastructural studies of mycorrhizae between several different plant symbionts and various species of Endogonaceae have been reviewed by Scannerini and Bonfante-Fasolo (1983) and Harley and Smith (1983). The observations made on the ultrastructure of arbuscules of G. intraradices in this study are similiar to those reported for other species of Glomus (Cooke, 1977; Harley and Smith, 1983; Scannerini and Bonfante-Fasolo, 1983; Bonfante-Fasolo, 1984). However, the occurrence of tannin bodies in the vacuoles of cortical cells colonized by VA mycorrhizal fungi has not been reported previously and is perhaps noteworthy in this study. These darkly pigmented structures in the cortical cells very likely cause the discoloration (slightly more yellowish appearance) of those portions of the root where the arbuscules occur.

Pigmentation is one of very few macroscopically detectable changes that occurs in colonized portions of roots of some VA mycorrhizal plants. Pigmented mycorrhizae have been reported previously in corn (Gerdemann, 1961), onions (Becker and Gerdemann, 1977), and star of Bethlehem (Scannerini and Bonfante-Fasolo, 1977). Gerdemann (1961) reported the yellow pigment to be soluble in water, but the specific location of the pigment within the root was not identified. Scannerini and Bonfante-Fasolo (1977), however, attributed the pigmentation to globular chromoplasts that occurred only in the cortical cells of the colonized root zones in their ultrastructural study of star of Bethlehem. Contrary to Gerdemann (1961), they found

the yellow pigment to be extractable with organic solvents. This indicates that the pigmentation may arise from more than one source in response to colonization of the plant by the fungal symbiont.

The occurrence of perforations in the young septa delimiting branches in the intraradical hyphae of G. intraradices is the first report of such septal elaboration in this genus. Scannerini *et al.* (1975) observed septa delimiting the moribund portions of arbuscules from the healthy areas in their ultrastructural study of the VA mycorrhiza of Ornithogalum umbellatum L. (Liliaceae) and an unidentified species of Glomus. However, the septa in their study appear to be simple, without perforations or any other obvious substructure.

The perforations reported here for G. intraradices are very similar to those demonstrated in the gametangial septa of Endogone pisiformis Lk. ex Fries in Chapter I. The lack of obvious pores in more mature septa may result from their occlusion by secondary wall material. Furthermore, these fine perforations contrast with the coarser septal pores observed in sporocarpic hyphae of S. coremioides, which are similar to the solitary pores reported in the septa of sporocarpic hyphae of E. pisiformis in Chapter I.

The occurrence of septal perforations in Sclerocystis and Glomus is perhaps significant in that it not only more closely associates these two important VA mycorrhiza-forming genera with each other, but also in that it indicates a closer relationship to the type genus Endogone, especially in conjunction with chlamydospore wall data. The outer wall that occurs in some of the species examined in this study

is similiar to the zygosporangium of Endogone as described in Chapter I. In particular, the ephemeral outer wall of Glomus etunicatum (Figs. 3.44, 3.45) stains with AMB very similarly to the zygosporangium of Endogone pisiformis (Fig. 1.15), although the silver proteinate post stain did not provide differential staining of the chlamydospore wall. The chlamydospore of Glomus (and Sclerocystis) may represent a reduced form of zygospore, with the azygospore of Gigaspora as an intermediate. However, there is admittedly no direct or conclusive evidence for this possible evolutionary lineage. Studies of chlamydospore wall and septal ultrastructure of additional species of Glomus and Sclerocystis are needed in order to determine the extent to which multiperforate septa and wall structure similiar to that of Endogone occur in these genera. Further such studies are especially needed for Sclerocystis, in order to verify the occurrence of septal perforations in very young sporocarp stages. Of course, the ability to culture and sporulate these fungi on artificial media would greatly facilitate such ultrastructural studies. Unfortunately, these fungi can not be cultured at the present time, although this is obviously a current goal of many mycorrhizal researchers (Hepper, 1984).

Figs. 3.1-3.6. *Glomus intraradices*. Figs. 3.1, 3.6. Light Microscopy (LM). Figs. 3.2-3.5. Scanning Electron Microscopy (SEM).

Fig. 3.1. Whole mount of two chlamydospores. (bar= 50  $\mu\text{m}$ ).

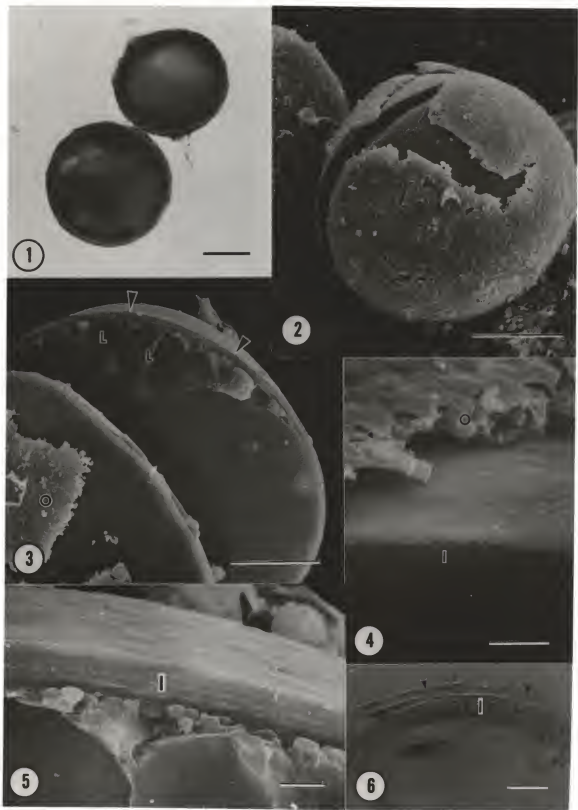
Fig. 3.2. Fractured chlamydospore showing ephemeral outer wall separated from persistant inner wall. (bar= 50  $\mu\text{m}$ ).

Fig. 3.3. Fractured chlamydospore showing lipid globules (L) enclosed by inner wall (arrowheads) and remnant of outer wall (O). (bar= 25  $\mu\text{m}$ ).

Fig. 3.4. Higher magnification of chlamydospore surface showing pitted and degraded outer wall (O) and multilayered inner wall (I). (bar= 2  $\mu\text{m}$ ).

Fig. 3.5. Fractured chlamydospore showing several layers of inner wall (I) enclosing spore contents. (bar= 2.5  $\mu\text{m}$ ).

Fig. 3.6. Thick, plastic section of chlamydospore showing outer wall (arrowheads) and multilayered inner wall (I). (bar= 25  $\mu\text{m}$ ).



Figs. 3.7-3.12. *Glomus intraradices*. Transmission Electron Microscopy (TEM).

Fig. 3.7. Transverse section of chlamydospore showing spherical lipid globules (L) of various sizes enclosed by multilayered inner (I) and partially degraded outer (arrowhead) walls. (bar= 10  $\mu\text{m}$ ).

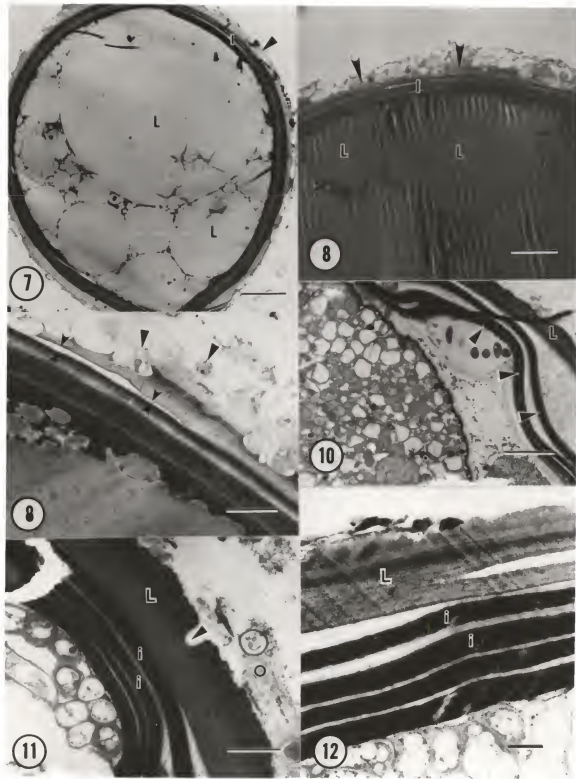
Fig. 3.8. Transverse section of chlamydospore showing lipid globules (L), multilayered inner wall (I), and outer wall degraded by bacteria (arrowheads). (bar= 5.0  $\mu\text{m}$ ).

Fig. 3.9. Chlamydospore showing inner wall partially separated (small arrowheads) from the outer wall with the latter extensively colonized by bacteria (large arrowheads). (bar= 2.0  $\mu\text{m}$ ).

Fig. 3.10. Portion of senescent chlamydospore showing inner layers (arrowheads) of inner wall separated partially from each other and from outer layer (L) of this wall. (bar= 5.0  $\mu\text{m}$ ).

Fig. 3.11. Chlamydospore as in Fig. 3.10 showing degraded outer wall (O) and inner wall consisting of a relatively thick outer layer (L) separated from several inner layers (i). Note degraded cavity in inner wall (arrowhead). (bar= 2.0  $\mu\text{m}$ ).

Fig. 3.12. Higher magnification of senescent chlamydospore showing thick outer layer (L) and four electron opaque inner layers (i) of inner wall. (bar= 0.5  $\mu\text{m}$ ).



Figs. 3.13-3.17. Glomus intraradices in roots of Paspalum notatum.  
Figs. 3.13-3.16. TEM. Fig. 3.17. LM.

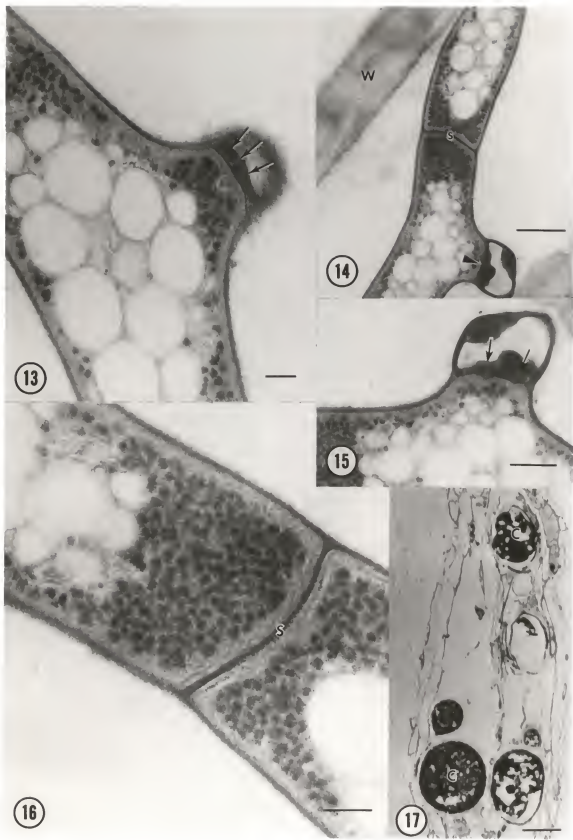
Fig. 3.13. Longitudinal section of intraradical hypha showing fine perforations (arrows) in septum at branching point. (bar= 0.1  $\mu\text{m}$ ).

Fig. 3.14. Longitudinal section of an intraradical hypha appressed to wall (W) of cortical cell showing a mature, apparently nonperforate septum (s) on main hypha and an immature septum (arrowhead) at branching point with fine, radial perforations. (bar= 0.5  $\mu\text{m}$ ).

Fig. 3.15. Higher magnification of Fig. 3.14 showing fine, radial perforations (arrows) in septum of hyphal branch. (bar= 0.2  $\mu\text{m}$ ).

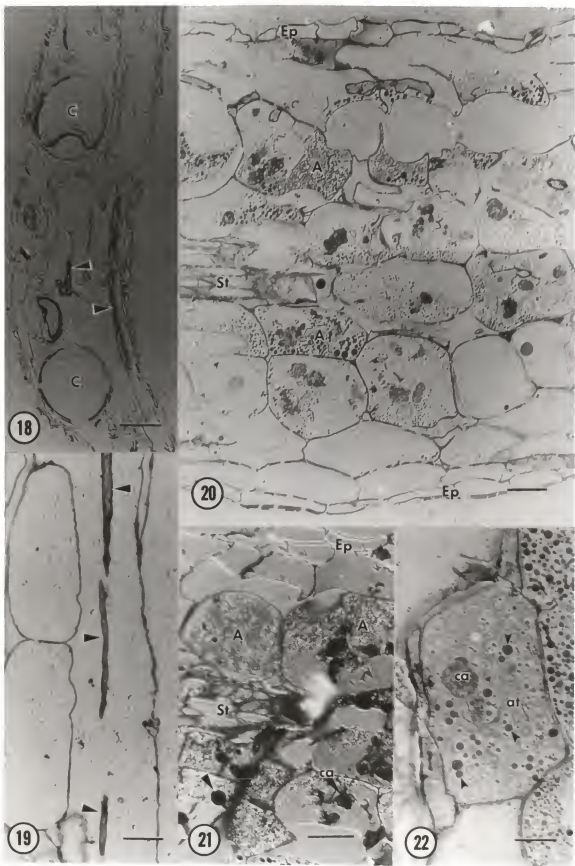
Fig. 3.16. Higher magnification of Fig. 3.14 showing mature septum (S) without any apparent perforations. (bar= 0.2  $\mu\text{m}$ ).

Fig. 3.17. Thick, plastic, longitudinal section of root showing several darkly stained chlamydospores (C) enclosed within. (bar= 50  $\mu\text{m}$ ).



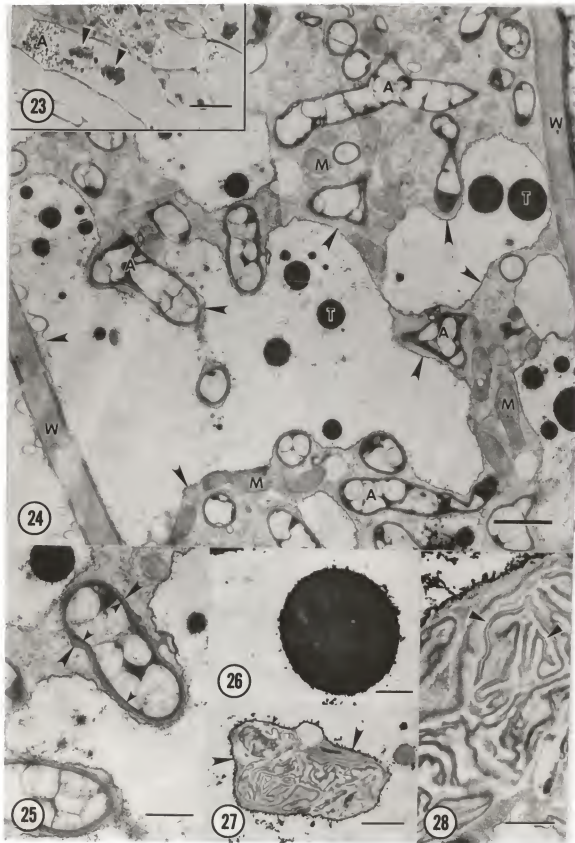
Figs. 3.18-3.22. Glomus intraradices in roots of Paspalum notatum L. Nomarski differential-interference contrast LM of thick, plastic sections.

- Fig. 3.18. Longitudinal section of root showing chlamydospores (C) and hyphae (arrowheads) embedded within. (bar= 100  $\mu\text{m}$ ).
- Fig. 3.19. longitudinal section of root showing hyphae (arrowheads) oriented longitudinally along the cortex. (bar= 50  $\mu\text{m}$ ).
- Fig. 3.20. Oblique longitudinal section of root showing a portion of stele (St), epidermis (Ep), and numerous cortical cells containing arbuscules (A). (bar= 50  $\mu\text{m}$ ).
- Fig. 3.21. Higher magnification of colonized root showing epidermis (Ep), stele (St), and several cortical cells containing finely branched arbuscules (A), tannin bodies (arrowheads), and portions of collapsed arbuscules (ca). (bar= 25  $\mu\text{m}$ ).
- Fig. 3.22. Cortical cell containing portion of collapsed arbuscule (ca), a main arbuscular trunk (at), and numerous tannin bodies (arrowheads). (bar= 10  $\mu\text{m}$ ).



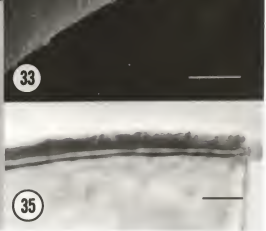
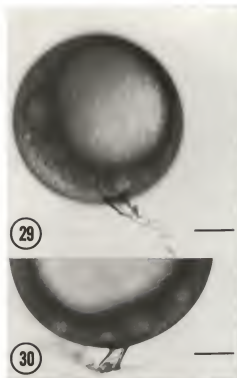
Figs. 3.23-3.28. Glomus intraradices in roots of Paspalum notatum.  
Fig. 3.23. LM. Figs. 3.24-3.28. TEM.

- Fig. 3.23. Thick, plastic, longitudinal section of root showing cortical cells containing finely branched arbuscules (A) and portions of collapsed arbuscular material (arrowheads). (bar= 50  $\mu\text{m}$ ).
- Fig. 3.24. Portion of cortical cell showing numerous vacuolate arbuscular branches (A), cortical cell wall (W), tonoplast (arrowheads) enclosing numerous tannin bodies (T), and mitochondria (M) of the cortical cell. (bar= 2.0  $\mu\text{m}$ ).
- Fig. 3.25. Higher magnification of Fig. 3.24 showing granular matrix between thin wall (small arrowheads) of arbuscular branch and host plasmalemma (large arrowheads). (bar= 1.0  $\mu\text{m}$ ).
- Fig. 3.26. Higher magnification of tannin body showing homogeneous, electron opaque contents. (bar= 0.25  $\mu\text{m}$ ).
- Fig. 3.27. Mass of collapsed arbuscular material enclosed by tonoplast (arrowheads). (bar= 2.0  $\mu\text{m}$ ).
- Fig. 3.28. Higher magnification of Fig. 3.27 showing collapsed arbuscular branches (arrowheads) compressed together within arbuscular mass. (bar= 1.0  $\mu\text{m}$ ).



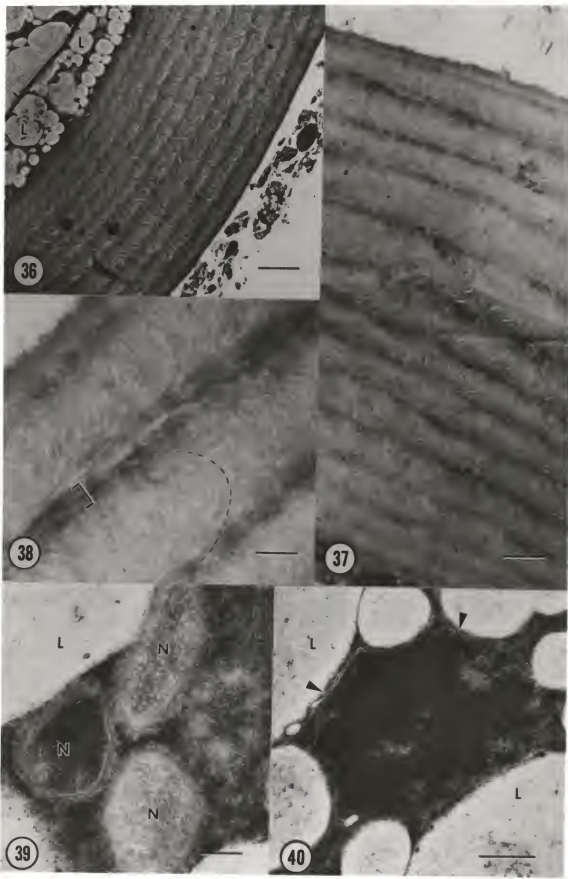
Figs. 3.29-3.35. Glomus constrictum. Figs. 3.29, 3.30, 3.34, 3.35.  
LM. Figs. 3.31-3.33. SEM.

- Fig. 3.29. Whole mount of chlamydospore. (bar= 100  $\mu\text{m}$ ).
- Fig. 3.30. Chlamydospore base showing constriction at hyphal connection. (bar= 100  $\mu\text{m}$ ).
- Fig. 3.31. Fractured chlamydospore showing smooth outer surface with adhering debris. (bar= 50  $\mu\text{m}$ ).
- Fig. 3.32. Higher magnification of chlamydospore showing a uniform, single wall. (bar= 5.0  $\mu\text{m}$ ).
- Fig. 3.33. Spore wall appearing split into two approximately equal sublayers. Note debris on spore surface. (bar= 5.0  $\mu\text{m}$ ).
- Fig. 3.34. Thick, plastic, oblique section of chlamydospore wall showing lamellate appearance. (bar= 2.0  $\mu\text{m}$ ).
- Fig. 3.35. Chlamydospore wall in optical section showing lamellate appearance. (bar= 25  $\mu\text{m}$ ).



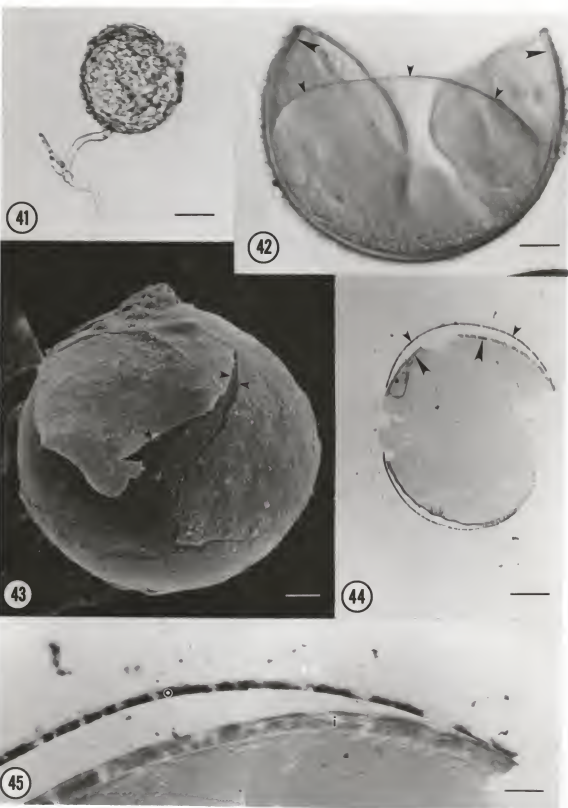
Figs. 3.36-3.40. Glomus constrictum. TEM.

- Fig. 3.36. Transverse section of chlamydospore showing lipid (L) of spore contents enclosed by single wall consisting of many lamellae or bands. (bar= 2.0  $\mu\text{m}$ ).
- Fig. 3.37. Chlamydospore wall showing lamellae as alternating light and dark zones of microfibrils. (bar= 1.0  $\mu\text{m}$ ).
- Fig. 3.38. Higher magnification of Fig. 3.37 showing each lamella as a band of microfibrils in an apparent arcuate orientation (dashed line) between thinner, darker bands of microfibrils (bracket) in parallel orientation. (bar= 0.3  $\mu\text{m}$ ).
- Fig. 3.39. Portion of chlamydospore cytoplasm showing cluster of apparent nuclei (N) enclosed by lipid globules (L). (bar= 0.3  $\mu\text{m}$ ).
- Fig. 3.40. Spore cytoplasm showing an apparently double membrane-bound nucleus (arrowheads) enclosed by lipid globules (L). (bar= 0.2  $\mu\text{m}$ ).



Figs. 3.41-3.45. Glomus etunicatum. Figs. 3.41, 3.42, 3.44, LM. Fig. 3.43. SEM. Fig. 3.45. Normarski differential-interference contrast LM. Fig. 3.41. Whole mount of chlamydospore showing debris-laden surface and hyphal connection. (bar= 100  $\mu\text{m}$ ).

- Fig. 3.42. Crushed chlamydospore showing outer wall (small arrowheads) separated from thick inner wall (large arrowheads). (bar= 50  $\mu\text{m}$ ).
- Fig. 3.43. Chlamydospore showing thin, roughened outer wall (arrowheads) separated from intact, smooth inner wall. (bar= 25  $\mu\text{m}$ ).
- Fig. 3.44. Thick, plastic, transverse section of crushed chlamydospore showing separation of outer wall (small arrowheads) from inner wall (large arrowheads). (bar= 50  $\mu\text{m}$ ).
- Fig. 3.45. Higher magnification of Fig. 3.44 showing thin, darkly stained outer wall (o) separated from thicker, less intensely stained inner wall (i). (bar= 10  $\mu\text{m}$ ).



Figs. 3.46-3.51. Glomus etunicatum. TEM of chlamydospore wall.

Fig. 3.46. Transverse section showing separation (arrowheads) of outer (o) and inner (i) walls. Note coarse, fibrous contents and uneven surface of outer wall. (bar= 0.5  $\mu\text{m}$ ).

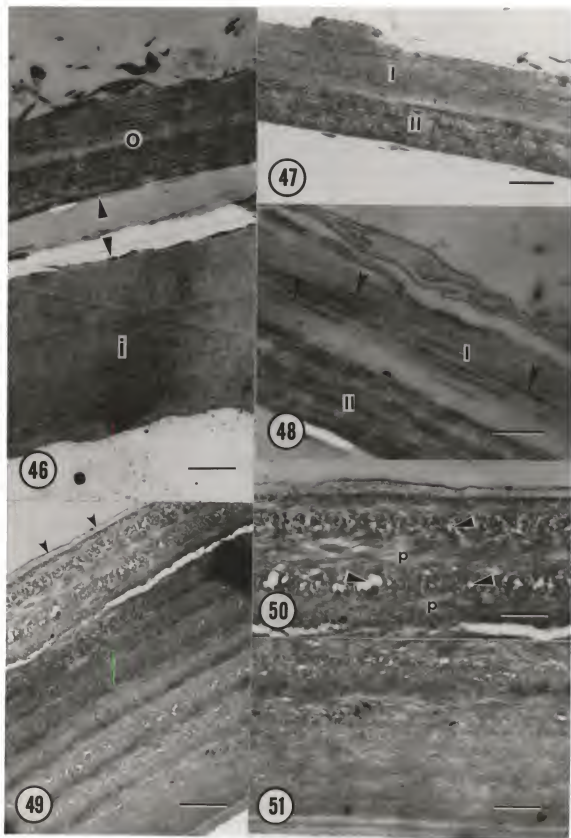
Fig. 3.47. Outer wall showing uneven surface and apparent outer (I) and inner (II) sublayers. (bar= 0.3  $\mu\text{m}$ ).

Fig. 3.48. Higher magnification of outer wall showing coarse, electron opaque, fibrillar material (arrowheads) embedded in granular matrix and oriented parallel to spore surface. Also note surface debris and subdivision into outer (I) and inner (II) layers. (bar= 0.3  $\mu\text{m}$ ).

Fig. 3.49. Inner wall of mature spore showing multilayered appearance of alternating light and dark bands from spore surface (arrowheads) inward. (bar= 1.0  $\mu\text{m}$ ).

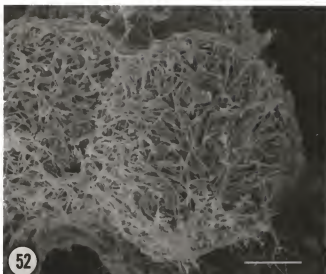
Fig. 3.50. Higher magnification of outer lamellae of inner spore wall showing bands of microfibrils in approximate parallel orientation (p) between zones containing irregular, open lacunae (arrowheads). (bar= 0.5  $\mu\text{m}$ ).

Fig. 3.51. Higher magnification of inner wall showing less distinct lamellae than in outer zone. (bar= 0.5  $\mu\text{m}$ ).



Figs. 3.52-3.56. Sclerocystis coremioides. Figs. 3.52-3.54, 3.56.  
SEM. Fig. 3.55. LM.

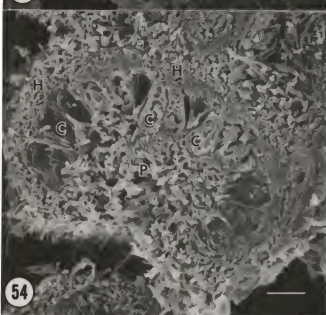
- Fig. 3.52. Typical sporocarps with peridia of interwoven hyphae. (bar= 100  $\mu$ m).
- Fig. 3.53. Higher magnification of sporocarp surface showing peridial hyphae in greater detail. (bar= 10  $\mu$ m).
- Fig. 3.54. Transverse section of sporocarp showing central plexus of sterile hyphae (P) enclosed by single layer of chlamydospores (C) and thick peridium of interwoven hyphae (H). (bar= 50  $\mu$ m).
- Fig. 3.55. Thick, plastic, transverse section of sporocarp showing central plexus (P), chlamydospores (C), and peridial hyphae (H). (bar= 50  $\mu$ m).
- Fig. 3.56. Higher magnification of sporocarp showing obovate chlamydospore (C) surrounded by thick-walled hyphae (arrowhead). (bar= 10  $\mu$ m).



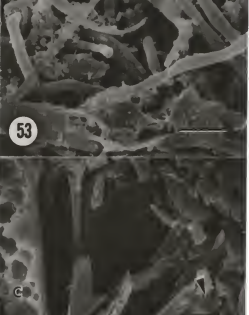
52



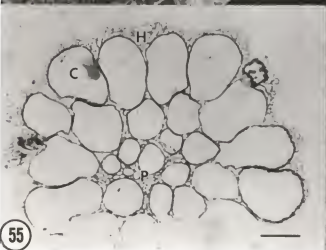
53



54



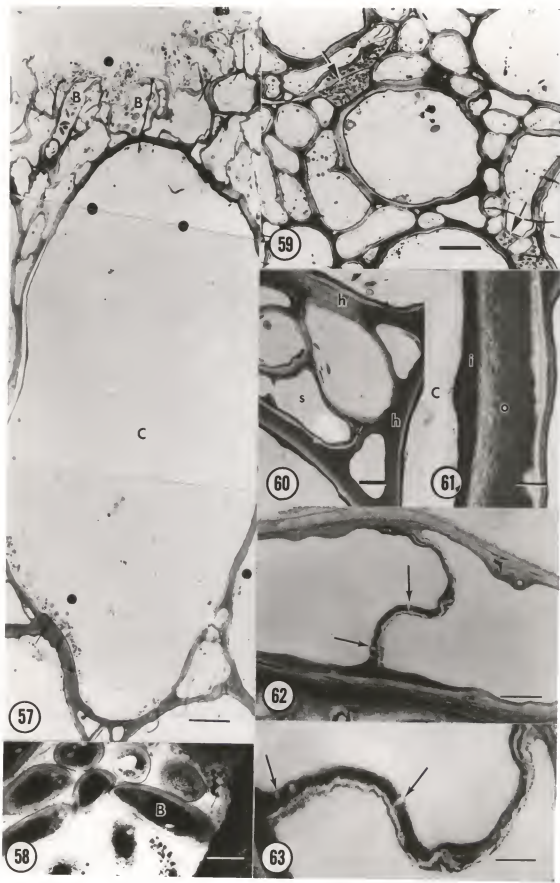
56



55

Figs. 3.57-3.63. Sclerocystis coremioides. TEM of sporocarp.

- Fig. 3.57. Longitudinal section of sporocarp showing chlamydospore (C) and associated hyphae of peridium, some enclosing colonies of bacteria (B). (bar= 5.0  $\mu\text{m}$ ).
- Fig. 3.58. Higher magnification of bacteria (B) enclosed within chambers of sporocarp. (bar= 0.3  $\mu\text{m}$ ).
- Fig. 3.59. Section of sporocarp showing numerous chambers within the central plexus, some enclosing dense colonies of bacteria (arrows). (bar= 2.0  $\mu\text{m}$ ).
- Fig. 3.60. Section of sporocarp showing open spaces (s) between chlamydospores and fused nature of contiguous hyphal walls (h). (bar= 1.0  $\mu\text{m}$ ).
- Fig. 3.61. Higher magnification of chlamydospore wall, with chlamydospore (C) at left and adjacent hypha lying to the right, showing an electron opaque inner spore wall (i) and no obvious demarcation between outer spore wall (o) and wall of adjacent hypha. (bar= 0.3  $\mu\text{m}$ ).
- Fig. 3.62. Transverse section of sporocarpic hypha showing septum with several perforations (arrows). (bar= 0.5  $\mu\text{m}$ ).
- Fig. 3.63. Higher magnification of Fig. 3.62 showing septal perforations (arrows) in greater detail. (bar= 0.25  $\mu\text{m}$ ).



CHAPTER IV  
GLAZIELLALES ORD. NOV. AND GLAZIELLACEAE FAM. NOV.:  
NEW TAXA BASED UPON LIGHT AND ELECTRON MICROSCOPIC  
OBSERVATIONS OF GLAZIELLA AURANTIACA

Introduction

The first specimen of Glaziella aurantiaca (Berk. & Curt.) Cooke was collected in Cuba in 1869 but was described mistakenly by Berkeley and Curtis as Xylaria aurantiaca. The genus Glaziella was erected a decade later by Berkeley (1879) for a specimen collected in Brazil. He named the fungus Glaziella vesiculosus and placed it in the Hypocreaceae due to the bright color and fleshy nature of the sporocarps, apparently unaware that the same fungus had been described by himself previously as X. aurantiaca. Cooke (1883), in a treatment of the Xylariaceae, transferred X. aurantiaca to Glaziella, apparently the first person to recognize that this species had been described erroneously as a species of Xylaria.

Von Höhnel (1913) first placed what is currently recognized as Glaziella in the Endogonaceae. However, he did not recognize that the fungus that he collected was previously described as Glaziella, and thus created the genus Endogonella for it. He considered the spores, embedded in the walls of the sporocarps, to be chlamydospores, not perithecia as previous workers had mistaken them. Furthermore, he considered this fungus properly placed in the Endogonaceae, since that family included other sporocarpic, chlamydosporic species.

Thaxter (1922), in a revision of the Endogonaceae, studied the type material of Berkeley and Curtis (1869), that of Berkeley (1879), and also the other specimens of Glaziella that had been described as

new species. He determined from this study that Glaziella is monotypic and that all other described species do not belong to the genus, most representing sterile forms of Entomaema liquescens Möller (Xylariaceae). Apparently no new species of Glaziella has been described since this revision of the family.

Boedijn (1930) discussed the history of classification of the genus, including its synonymy, and pointed out that Glaziella aurantiaca is the valid name for the species, not G. vesciculosa, as Thaxter (1922) had mistakenly assumed, since aurantiaca is the earliest used specific epithet for the fungus (as Xylaria aurantiaca Berk. & Curt., 1869). Boedijn (1930) also studied the morphological and anatomical features of two specimens collected in the Dutch East Indies. Although noting the extensively septate mycelium in the sporocarps, he nevertheless assumed the fungus to be in the Endogonaceae because of the presence of what he assumed to be chlamydospores.

In a recent monograph of the Endogonaceae, Gerdemann and Trappe (1974) included Glaziella as a monotypic genus. However, Gibson (1984), in an ultrastructural study of sporocarpic tissues of the fungus, found the septa to be typical of those of various ascomycete taxa and, on this basis, tentatively transferred it to the deuteromycetes due to lack of information regarding its teleomorphic stage.

The current study was undertaken in order to gain more information regarding the teleomorphic nature of this fungus by examining the sporocarpic tissues with both light and electron microscopy.

#### Materials and Methods

Since freshly collected material of Glaziella was not available for study, the following dried herbarium specimens, deposited in the Tulane University Herbarium, New Orleans, were examined with light and(or) electron microscopy: 1) GRENADE: ST. MARK PARISH, elev. 500-1000 ft., on ground, bright orange when fresh; coll. G. R. Proctor #2753, Nov. 21, 1957; det. J. M. Trappe; (NO 2753). 2) JAMAICA: ST. ANN PARISH, Mt. Diablo Forest Preserve; coll. T. H. Farr, July 3, 1960; det. J. M. Trappe; (NO 2751). 3) JAMAICA: ST. ELIZABETH PARISH, elev. 400 ft., near Maggoty Falls; coll A. L. Welden #501, July 31, 1957; det. J. M. Trappe; (NO 192). 4) JAMAICA: ST. THOMAS PARISH, Cherry Garden, under a mango tree, on gravelly bank; coll. Ellis #49, (no date given); det. J. M. Trappe; (NO 2752).

#### Light Microscopy (LM)

Small pieces of the dried sporocarp wall were rehydrated in 2.5% aqueous KOH for approximately 2 hr at room temperature, rinsed in three changes of deionized water, and allowed to soak in 40% aqueous mucilage for approximately 1 hr at room temperature before being frozen and sectioned in mucilage with a cryostat microtome (-20 C). Transverse sections approximately 12  $\mu\text{m}$  thick were mounted in

lacto-phenol cotton blue (Stevens, 1974) and examined with a Nikon compound light microscope equipped with Nomarski differential-interference contrast optics.

#### Scanning Electron Microscopy (SEM)

Cross sections of small pieces of the dried sporocarp walls were made with a razor blade under a dissecting microscope. These sections were placed on stubs with double-sticky cellophane tape, coated with gold in a Hummer Jr. sputter coater, and observed with a Hitachi S-450 scanning electron microscope.

#### Transmission Electron Microscopy (TEM)

Small, hand-sectioned pieces of the dried sporocarp wall were rehydrated with deionized water at 4 C overnight. These were then fixed at room temperature in 2% paraformaldehyde, 2.5% glutaraldehyde and 2 mM calcium chloride in 0.1 M sodium cacodylate buffer (pH 7.2) for ca. 2 hr at room temperature. The material was rinsed in 0.1 M sodium cacodylate buffer and postfixed in 1% osmium tetroxide in 0.1 M cacodylate buffer. It was then dehydrated in an ethanol series, which included en bloc staining with saturated uranyl acetate in 70% ethanol for ca. 2 hr at room temperature. The ethanol dehydration series was followed by acetone. The material was then embedded in ERL 4206 resin (Spurr, 1969) and ultrathin sectioned on a Sorvall MT-2 ultramicrotome with a diamond knife. The sections were collected on one-hole, formvar-coated copper grids, stained for 10 min in 2% (w/v) aqueous uranyl acetate followed by 10 min in Reynolds (1963) lead citrate, and examined at 75 kV on an Hitachi HU-11C or Philips EM-301 transmission electron microscope.

Cytochemistry

The method of Hoch (1977) was employed in an attempt to visualize, in better detail, the wall structure of sporocarpic hyphae and spores, or to obtain differential staining of the spore wall layering. Material prepared for TEM was ultrathin sectioned in the same manner as above. A drop of aqueous 1% barium permanganate was placed on the sections supported by formvar-coated copper grids. The stain was washed away after ca. 30 sec with a gentle stream of deionized water. To remove possible contaminants, a drop of 0.05% citric acid was placed on the sections for ca. 30 sec, after which they were rinsed again with deionized water. The sections were then stained with aqueous uranyl acetate for 2 min, rinsed with deionized water, and stained with Reynolds (1963) lead citrate. Both the uranyl acetate and lead citrate were placed, dropwise, directly on the sections, since staining times were relatively brief. The sections were then given a final deionized water rinse and dried for examination with TEM.

In order to localize carbohydrates in the sporocarpic tissues and spores, the silver proteinate stain was employed (Thiéry, 1967; McLaughlin, 1974). Material prepared for TEM was used, however, with the exclusion of the uranyl acetate en bloc treatment during the ethanol dehydration. Thin sections were obtained as described above, but were collected from the boat unmounted with small plastic rings in which the sections floated on the surface of a drop of liquid held in the center of the ring (Marinozzi, 1961). These sections were treated as follows: 1) incubated on 1% aqueous periodic acid for 30 min at

room temperature; 2) washed on deionized water, once briefly and three times for 10 min each; 3) incubated on 1% thiosemicarbazide in 10% aqueous acetic acid for 24 hr at room temperature; 4) washed on 10% aqueous acetic acid, twice briefly and three times for 20 min each; 5) washed on 5% aqueous acetic acid for 5 min; 6) washed on 1% aqueous acetic acid for 5 min; 7) washed on deionized water two times for 5 min each; 8) incubated on 1% aqueous silver proteinate for 30 min at room temperature in the dark; 9) washed on deionized water, three times briefly and once for 10 min. After this treatment the sections were mounted onto formvar-coated copper grids, dried, and observed with TEM. Control sections were treated as above, however, excluding the 1% periodic acid oxidation step.

#### Results

Certain evidence outlined below from both light and electron microscopy indicates that the spores of Glaziella, embedded in the sporocarp wall, arise from an ascogenous tissue system and represent ascospores. No evidence of a dual hyphal system of the type described by Boedijn (1930) was found.

#### General Features of the Sporocarps

The dried sporocarps of G. aurantiaca examined were tuber shaped, lobed, slightly elongate, hollow with an opening toward the base, pale orange in color, and ranged, in size by their greatest dimension, from 1.5 to 2.0 cm (Jamaica) to 3.5 to 4.5 cm (Grenada)(Figs. 4.1, 4.2). The fruiting bodies are assumed to have shrunken approximately one-third upon drying, since pieces of the wall rehydrated in deionized water generally increased in size by about that amount. The spores are

embedded within the middle layer of the wall and are often detectable as raised areas in the outer surface of the sporocarp (Figs. 4.3-4.5, 4.19). They are globose to widely ovoid and 300-450-(500)  $\mu\text{m}$  in diameter. The walls of the revived sporocarps are relatively thin (0.5-1.5 mm) and, when viewed in transverse section with light or electron microscopy, an inner and outer pseudoparenchymatous zone enclosing a region of relatively loose interwoven hyphae with many open spaces can be seen (Figs. 4.4, 4.5, 4.10, 4.19). The outer zone of pseudoparenchyma is somewhat wider than the inner one, 100-125  $\mu\text{m}$  for the former, versus 70-90  $\mu\text{m}$  for the latter (Figs. 4.4, 4.5). Both zones intergrade into the middle layer and do not produce sharply defined borders (Figs. 4.4, 4.5, 4.10). The tissue of these pseudoparenchymatous zones forms a textura angularis (Korf, 1958) with the constituent cells approximately 3-7  $\mu\text{m}$  in diameter (Fig. 4.11).

The individual hyphae of the middle layer are 3.0-4.5  $\mu\text{m}$  in diameter and are regularly septate (Figs. 4.6, 4.10, 4.21). A gelatinous matrix frequently cements the individual hyphae together (Fig. 4.4, 4.5, 4.40) and is probably responsible for the gelatinous nature of the fresh sporocarps (Thaxter, 1922; Boedijn, 1930).

#### Spore Ontogeny

Within the loosely interwoven mycelium of the middle layer are hyphae that are more darkly stained with lacto-phenol cotton blue than those surrounding. They often first appear appressed in pairs (Fig. 4.6) but, subsequently, proliferate and form densely stained pockets (Figs. 4.7, 4.8). These hyphae become more branched and intertwined than the surrounding mycelium and eventually form distinct pockets of

pseudoparenchyma that develop central locules or cavities (Figs. 4.9, 4.10). These pockets of pseudoparenchyma and the locules that develop within them usually occur in clusters and generally arise somewhat closer to the lower pseudoparenchymatous zone, although the position varies considerably from locule to locule within the middle layer.

Young asci develop within the pseudoparenchyma-lined locules. They are long clavate and have dense cytoplasm and relatively thick, hyaline walls (Figs. 4.12-4.15). The ascal attachments are difficult to distinguish, since they are embedded in a hyphal mass, but can be detected, in some instances, as arising from the densely stained cells of pseudoparenchyma lining the locules (Fig. 4.14). Young asci are typically centrally positioned in the locules (Figs. 4.15, 4.17) but are frequently dislodged during sectioning (Figs. 4.13, 4.14).

The more mature asci become distally inflated and usually produce a single ascospore (Fig. 4.16). At this point the ascus wall remains relatively thick and hyaline and is closely appressed to the young spore. However, as the ascospore increases in size, the ascus wall becomes structurally disorganized (Fig. 4.18) and disintegrates at an early stage in spore development. Consequently, the mature ascospores become individually embedded within the middle zone of the sporocarp wall. At this point the layer of pseudoparenchyma is crushed and the locule is typically completely filled by the much enlarged, mature ascospore (Figs. 4.5, 4.19-4.22).

Other than the possible hyphal fusion and various ascal stages referred to above, there was no evidence of ascogonia, trichogynes, antheridia or any other obvious mechanism of cross-fertilization.

Hyphal Characters

The loose, interwoven mycelium that comprises the bulk of the sporocarp consists of regularly septate hyphae (Figs. 4.6, 4.21, 4.23). The individual septa are quite typical of various ascomycete taxa with simple pores that become plugged with electron opaque material and are characteristically associated with one or more Woronin bodies (Figs. 4.21, 4.23-4.29). In the early development of the septum, the septal wall usually forms perpendicular to the hyphal wall, and plug formation is incomplete (Fig. 4.24). As the septum matures, the walls curve (Fig. 4.25), while the pore becomes more completely plugged. When fully mature, the septal walls are usually quite convoluted and the plugging extends completely through the simple, central pore (Figs. 4.26-4.29). At all stages of development the septal walls are electron translucent in comparison to the hyphal walls, and especially so in comparison to the plugs and Woronin bodies (Figs. 4.24-4.29). The electron opaque plugs have somewhat indistinct margins in younger septa (Figs. 4.24, 4.25), but at maturity the margin becomes quite well defined (Figs. 4.26, 4.28, 4.31). The Woronin bodies are uniformly electron opaque and are membrane bound, a condition which is especially evident in median sections (Fig. 4.30).

Structure of Mature Spores

Mature ascospores are visible, especially with the aid of a dissecting microscope, embedded in the thin walls of the sporocarp, usually in a position somewhat closer to the lower pseudoparenchymatous zone (Figs. 4.3-4.5, 4.19). The spores are almost

completely enclosed by the partially collapsed pseudoparenchymatous hyphae that once lined the locule (figs 4.21, 4.22). At the spore surface these hyphae are very dense and fuse or gelatinize into a single mass (Figs. 4.20-4.22). Spore cytoplasm was more or less preserved in the dried specimens. It is dense, homogeneous, and separated from the spore wall when observed with SEM (Figs. 4.19, 4.20).

The spore wall consists of a thin outer and thick inner wall, separated by a transition zone (Figs. 4.21, 4.34-4.36, 4.38). When observed with TEM both walls show a uniform granular consistency with little detectable sublayering (Fig. 4.38). The outer wall, however, is somewhat less electron opaque than the inner and frequently fused to the surrounding hyphae (Figs. 4.21, 4.37, 4.38). The two walls separate from each other at the transition zone (Figs. 4.34, 4.35).

The transition zone, more complex in structure than the two spore walls, consists of a thin, convoluted, membranous partition enclosed by wider, less electron opaque areas on both sides (Figs. 4.21, 4.32, 4.33, 4.38). The membranous partition is sinuous in outline in both SEM (Fig. 4.36) and TEM (Figs. 4.32, 4.33, 4.38, 4.39) and has fine radial striations within an electron translucent area between two, more electron dense borders (Figs. 4.33, 4.39).

#### Cytochemical Observations

Barium permanganate post staining results in an intense electron opacity of the gelatinous matrix between the hyphae of the middle layer of the sporocarp wall (Fig. 4.40). Neither the hyphal walls nor the septa are particularly well stained with barium permanganate

(Figs. 4.25, 4.31); also, the inner and outer spore walls show little affinity for this stain. The transition zone, however, does show evidence of differential staining. In contrast to standard uranyl acetate and lead citrate post staining (Figs. 4.32, 4.33), when stained with barium permanganate, the convoluted, membrane-like partition takes up less stain relative to the adjacent zones enclosing it (Fig. 4.39). The outer adjacent zone, in particular, was intensely stained.

Silver proteinate has little affinity for the gelatinous matrix material and the plugs and Woronin bodies are generally unstained (Fig. 4.41). The hyphal walls, however, show some deposition of silver (Fig. 4.42), and membranous fractions lining the septa and contained within the lumen of the hyphae are particularly well stained (Figs. 4.42). The silver proteinate is also quite specific for pockets of glycogen within the cytoplasm of the spores (Figs. 4.44-4.46). The surrounding lipid globules, in contrast, are completely unstained (Fig. 4.46). Controls for the silver proteinate stain that exclude the periodic acid oxidation step show only scattered, nonspecific depositon of silver randomly over the entire section.

#### Discussion

The genus Glaziella has had a quite confusing taxonomic history, apparently due in large part to the difficulties of various individuals in interpreting the nature of the spores. The mature spores are quite large and were believed by early workers to be perithecia, since they often bulge out the exterior wall of the sporocarp, frequently becoming broken open and hollow, and thus

appearing as ostiolate perithecia embedded within a stroma (Berkeley and Curtis, 1869; Berkeley, 1879; Boedijn, 1930). The inclusion of the genus in the Endogonaceae was originally based upon von Höhnel's (1913) assumption that the spores represent chlamydospores. Thaxter (1922) maintained the genus within the Endogonaceae, although he recognized only one species. He examined several specimens of Glaziella and apparently believed that the spores were chlamydospores. Interestingly, he also noted the regularly septate hyphae and believed that this character was anomalous for the family, and, furthermore, stated that this aspect of the fungus needed study.

Boedijn (1930), in his comprehensive treatment of the genus, also assumed the spores to be chlamydospores. He justified his placement of the genus in the Endogonaceae by suggesting the presence of two tissue systems within the sporocarps, one he describes as sparse, aseptate, and giving rise to the young spores, and the other as extensive, regularly septate, and representing the "vegetative" phase of the sporocarp. He stated that, since the spores arise from an aseptate mycelium, then perhaps Glaziella was a "phycomycete." However, no evidence was found in this study for such a dual tissue system. Some hyphae had relatively few septa; however, these were infrequent, random, and not necessarily associated with the sporogenous zones.

The data presented here indicate that Glaziella is an ascomycete. Perhaps the difficulty that earlier workers (von Höhnel, 1913; Thaxter, 1922; Boedijn, 1930) encountered in making this interpretation resulted from the presence of typically only a single spore per ascus. This difficulty is magnified by the existence of an

ascus that disintegrates at a relatively early stage in its development, leaving the individual spores embedded in the ascocarp walls.

Asci with single, large ascospores are not without precedence in the ascomycetes (Malloch and Cain, 1971; Uecker and Pollack, 1974). In these studies, however, the ascomycetous nature is perhaps less cryptic than in Glaziella, since obvious ascomycetous sporulating structures, such as perithecia and persistent ascal walls, are present.

The ambiguity of the mycorrhizal association of Glaziella provides little evidence for its inclusion in the Endogonaceae. Gerdemann and Trappe (1974) indicate that the mycorrhizal status of the genus is unknown. Trappe and Schenck (1982) presume Glaziella to be mycorrhizal, apparently because it has been reported on or in soil near various higher plant species in tropical lowlands. Studies of spore germination and culture of fresh material of Glaziella are obviously needed, especially for inoculation with suspected higher plant symbionts, in order to clarify the mycorrhizal status of the genus.

The data from this study clearly indicate that Glaziella should be transferred to the ascomycetes. The genus is so distinctive, however, that it can not to be accommodated in any existing

suprageneric taxon. Therefore, a new order and family are proposed to accomodate this monotypic genus:

Glaziellales ordo nov.

Ascocarpi cavi, lobati, cum orificio basale, aurantii ad sanguineos; muri tenues, gelatini; asci clavati ad subglobosos, unisporae, praecox deliquescentes, in muro inclusi; ascosporeae globosae ad subglobosas, magnae, laeves, aurantiae. Fam. typicum: Glaziellaceae.

Ascocarps hollow, lobed, with basal orifice, orange to red. Walls thin, gelatinous. Asci clavate to subglobose, unisored, early deliquescent, embedded within the sporocarp wall. Ascospores globose to subglobose, large, smooth, orange. Type family: Glaziellaceae.

Glaziellaceae fam. nov.

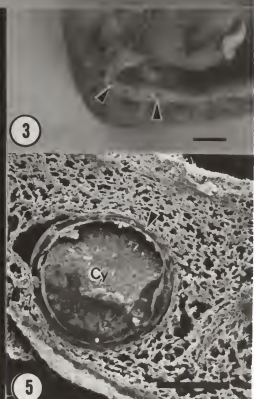
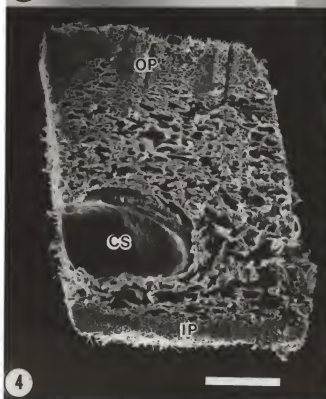
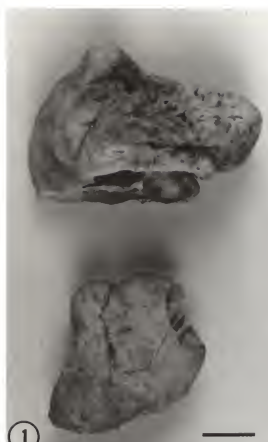
Ascocarpi usque ad 5.0 cm diametro, lobati, cavi, cum orificio versus humus, aurantii ad sanguineos; muri 0.5-1.5-(2.0) mm crassitudine, gelatini, ex hyphis implexis septatisque constantes, cum zonis pseudoparenchymatis interioribus exterioribusque; asci ab initio longiclavati, apice tumescenti, unisporae, praecox deliquescentes, in muro sporocarpo sparsi; sporae globosae ad late ellipticas, laeves, cum muris interioribus crassis ac cum muris exterioribus tenuibus. Gen. typicus: Glaziella.

Ascocarps up to 5.0 cm in diam., lobed, hollow, with an opening toward the soil, orange to dark red. Walls

0.5-1.5-(2.0) mm thick, gelatinous, composed of interwoven septate hyphae, with inner and outer pseudoparenchymatous zones. Asci initially long clavate, becoming apically inflated, unisored, early deliquescent, scattered within sporocarp wall. Spores globose to widely elliptical, smooth, with thick inner and thin outer walls. Type genus: Glaziella.

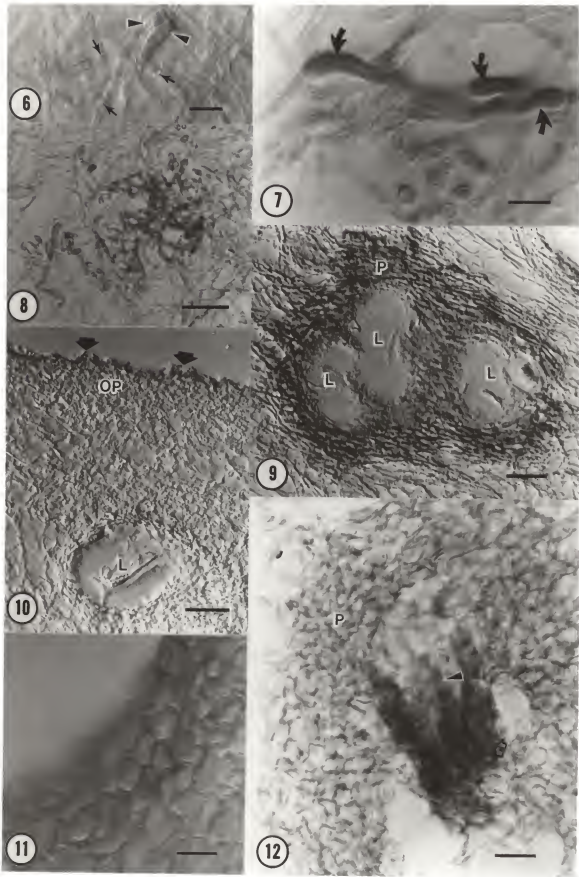
The Glaziellales appear to be related most closely to the Pezizales sensu Trappe (1979), the hypogeous species of which frequently have lobed, tuberous ascocarps, asci with reduced numbers of ascospores, and no forcible spore discharge mechanism. Obviously, further investigation of the growth habit of Glaziella is needed in order to gain more information about the general ecology of the fungus. In particular, additional data to determine if the fungus is initially hypogeous, as Thaxter (1922) believed it might be, would be helpful. Also, a closer examination of possible mycorrhizal host associations would be very helpful in elucidating the ecological niche of this fungus.

- Figs. 4.1-4.5. *Glaziella aurantiaca*. Figs. 4.1, 4.2, 4.3. macrophotography. Figs. 4.4, 4.5. Scanning electron microscopy (SEM).
- Fig. 4.1. Two typical dried sporocarps. (bar= 10.5 cm).
- Fig. 4.2. Sporocarp showing several lobes, one broken open exposing hollow interior (I) and thin wall (arrowhead). (bar= 0.5 cm).
- Fig. 4.3. Higher magnification of sporocarp showing individual spores (arrowhead) embedded within wall. (bar= 0.1 mm).
- Fig. 4.4. Sporocarp wall in cross section showing outer (OP) and inner (IP) pseudoparenchymatous zones with collapsed spore (CS) embedded within interwoven hyphae of middle layer. (bar= 150  $\mu$ m).
- Fig. 4.5. Sporocarp wall in cross section showing wall (arrowhead) and cytoplasm (CY) of mature spore embedded within. (bar= 150  $\mu$ m).



Figs. 4.6-4.12. *Glaziella aurantiaca*. Figs. 4.6-4.12. Cryostat, transverse sections of sporocarp wall stained with lacto-phenol cotton blue. Nomarski differential-interference contrast light microscopy.

- Fig. 4.6. Interwoven hyphae of middle layer of sporocarp wall showing two densely staining cells (arrowheads), possibly representing hyphal conjugation. Note regular septation (arrows) of surrounding hyphae. (bar= 5.0  $\mu\text{m}$ )
- Fig. 4.7. Higher magnification of sporocarp wall showing densely staining hyphae (arrows) at an early stage in development of pseudoparenchymatous pockets. (bar= 3.0  $\mu\text{m}$ ).
- Fig. 4.8. Later stage in development of pseudoparenchymatous pockets resulting from proliferation and intertwining of densely staining hyphae. (bar= 15  $\mu\text{m}$ ).
- Fig. 4.9. Pocket of densely staining pseudoparenchyma (P) enclosing three individual locules (L). (bar= 15  $\mu\text{m}$ ).
- Fig. 4.10. Portion of wall showing position of pseudoparenchyma-lined locule (L) relative to outer pseudoparenchymatous zone (OP) and outer surface (arrows) of sporocarp. (bar= 15  $\mu\text{m}$ ).
- Fig. 4.11. *Textura angularis* of outer pseudoparenchymatous zone of typical sporocarp wall, which is also typical of pseudoparenchyma lining locules and that of inner zone. (bar= 3.0  $\mu\text{m}$ ).
- Fig. 4.12. Young ascus (arrowhead) enclosed by densely staining cells (open arrows) within pocket of pseudoparenchyma (P) in middle layer of sporocarp wall. (bar= 7.5  $\mu\text{m}$ ).



Figs. 4.13-4.18. *Glaziella aurantiaca*. Cryostat transverse sections of sporocarp wall stained with lacto-phenol cotton blue. Nomarski differential-interference contrast LM.

Fig. 4.13. Young ascus, dislodged from the center of locule into the surrounding hyphae. Note thick hyaline wall (W) and densely staining cytoplasm (CY). (bar= 7.5  $\mu\text{m}$ ).

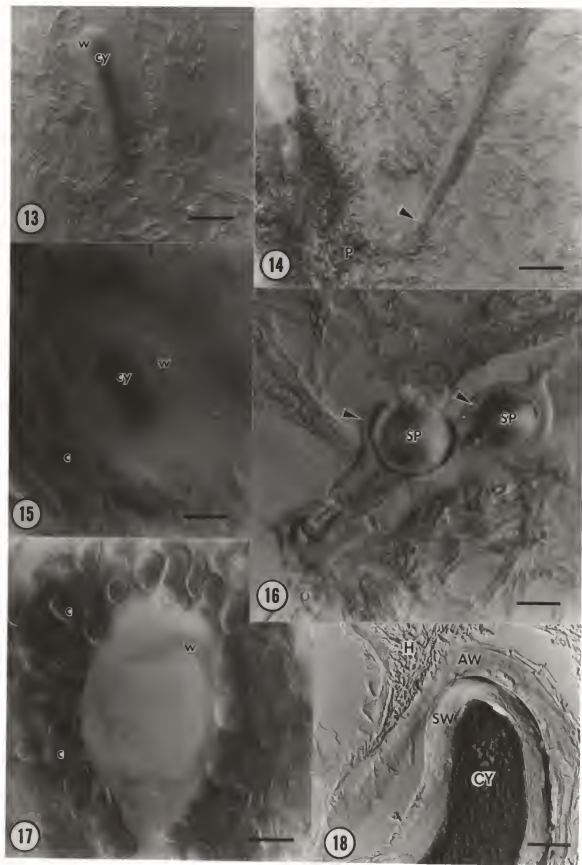
Fig. 4.14. Basal attachment (arrowhead), in densely staining pseudoparenchyma (P), of young ascus dislodged from locule. (bar= 15  $\mu\text{m}$ ).

Fig. 4.15. Pseudoparenchyma-lined locule containing a young ascus in cross section. Note hyaline wall (W) and dense cytoplasm (CY) of ascus and individual cells (C) of pseudoparenchyma. (bar= 3.0  $\mu\text{m}$ ).

Fig. 4.16. Two young, clavate asci within hyphae of middle wall layer. Note ascus walls (arrowheads) and young single ascospores (SP) enclosed within. (bar= 7.5  $\mu\text{m}$ ).

Fig. 4.17. Locule enclosed by darkly staining cells (C) of pseudoparenchyma showing wall (W) of ascus from which cytoplasm has been dislodged. (bar= 3.0  $\mu\text{m}$ ).

Fig. 4.18. More mature ascus with ascal wall (AW) enclosing young ascospore. Note wall (SW) and dense cytoplasm (CY) of spore, and hyphae (H) of surrounding middle layer. (bar= 15  $\mu\text{m}$ ).



Figs. 4.19-4.23. *Glaziella aurantiaca*. Figs. 4.19, 4.20, 4.22. SEM.  
Figs. 4.21, 4.23. TEM.

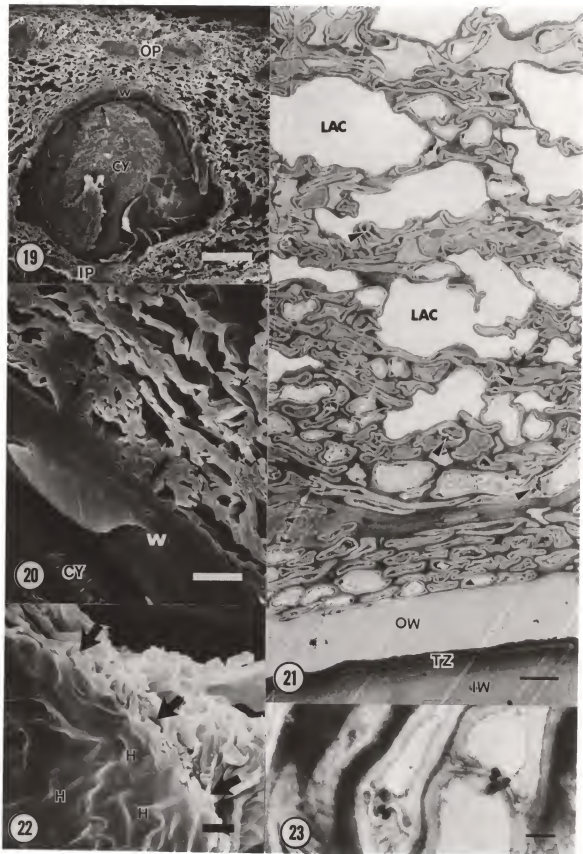
Fig. 4.19. Mature spore embedded between outer (OP) and inner (IP) pseudoparenchymatous zones within loosely interwoven hyphae of middle layer. Note spore wall (W) separated (arrows) from enclosed cytoplasm (CY). (bar= 100  $\mu$ m).

Fig. 4.20. Portion of sporocarp showing spore wall (W), outer layer of which is fused to crushed hyphae (large arrows) of pseudoparenchyma that once lined locule. Note spore wall separated from cytoplasm (CY) and collapsed hyphae further from spore surface (small arrows), both apparent artifacts of SEM preparation. (bar= 10  $\mu$ m).

Fig. 4.21. Outer wall (OW) of mature spore separated from inner wall (IW) by multipartite transition zone (TZ). Note spore embedded within loose, septate hyphae (arrowheads) of middle zone including numerous lacunae (LAC). (bar= 3.0  $\mu$ m).

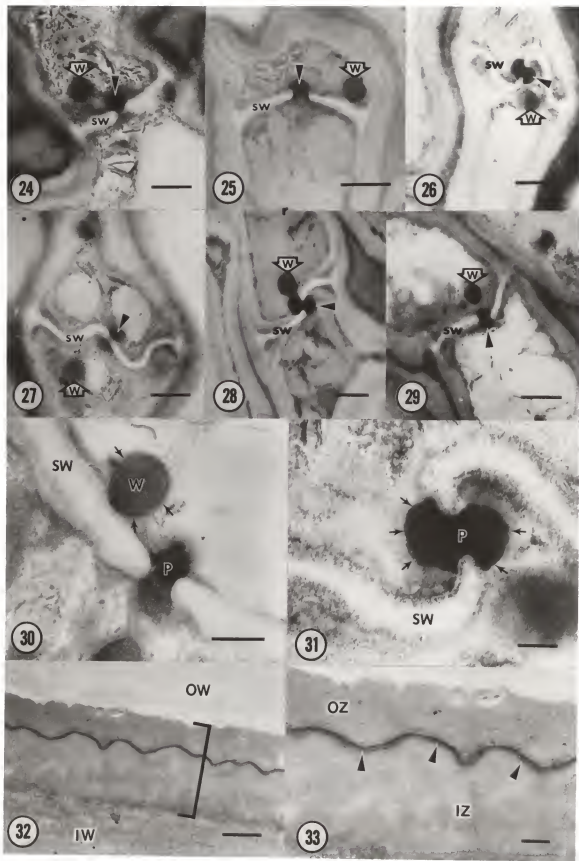
Fig. 4.22. Portion of sporocarp showing mass of fused hyphae (arrows) separated from spore surface leaving a large concavity in which individual hyphae (H), once appressed to outer spore wall surface, can be distinguished. (bar= 5.0  $\mu$ m).

Fig. 4.23. Two ascomycetous septa typical of hyphae of middle wall layer. (bar= 0.5  $\mu$ m).



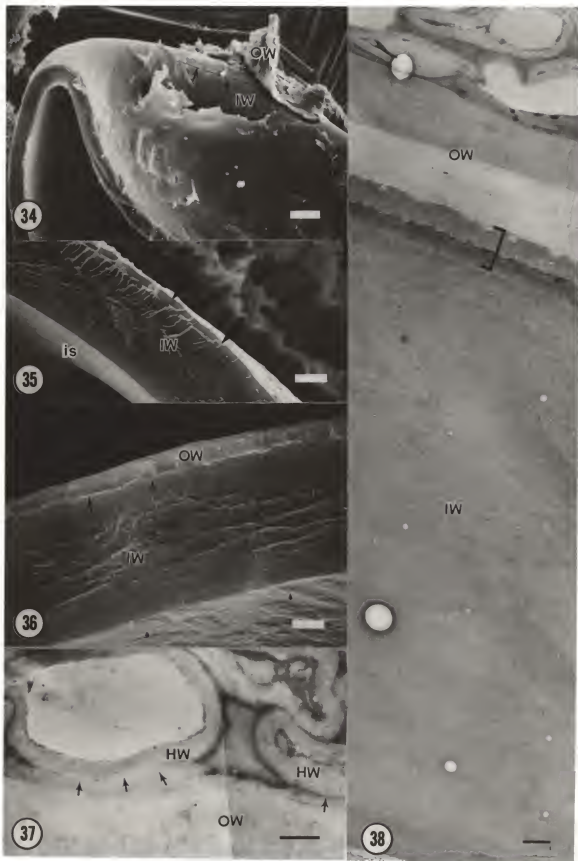
Figs. 4.24-4.33. *Glaziella aurantiaca*. Figs. 4.24-4.33. TEM.

- Fig. 4.24. Very young septum showing electron translucent septal wall (SW) more or less perpendicular to the hyphal wall, an electron dense Woronin body (W), and plug (arrowhead) just at opening of central pore. (bar= 0.5  $\mu$ m).
- Fig. 4.25. Moderately young septum showing electron translucent septal wall (SW) somewhat bowed, electron opaque plug (arrowhead) extending partially through pore, and associated Woronin body (W). (bar= 0.5  $\mu$ m).
- Fig. 4.26. Median section of mature septum, post stained with barium permanganate, showing convoluted, electron translucent septal wall (SW) with well-defined, electron opaque plug (arrowhead) extending through, and flaring out from both sides of, septal pore. Note Woronin body (W) evident in grazing section. (bar= 0.5  $\mu$ m).
- Fig. 4.27. Slightly nonmedian transverse section of mature septum showing convoluted, electron translucent septal wall (SW) with grazing sections of electron opaque Woronin body (W) and plug (arrowhead) traversing central pore. (bar= 0.5  $\mu$ m).
- Figs. 4.28, 4.29. Mature septa showing typical convoluted, electron translucent septal walls (SW) with complete pore plugs (arrowheads) and electron dense Woronin bodies (W). (bars= 0.5  $\mu$ m).
- Fig. 4.30. Septum at higher magnification showing membrane-bound (arrows) Woronin body (W) associated with septal wall (SW) and plug (P). (bar= 0.2  $\mu$ m).
- Fig. 4.31. Higher magnification of Fig. 4.26 showing plug (P) with well-defined margins (arrows) extending through central pore of septal wall (SW). (bar= 0.1  $\mu$ m).
- Fig. 4.32. Cross section of spore wall showing portions of outer (OW) and inner (IW) walls separated by relatively complex transition zone (bracket). (bar= 0.5  $\mu$ m).
- Fig. 4.33. Higher magnification of Fig. 4.32 showing transition zone consisting of thin, membranous partition (arrowheads) with fine radial striations, and less electron opaque outer (OZ) and inner (IZ) adjacent zones. (bar= 0.2  $\mu$ m).



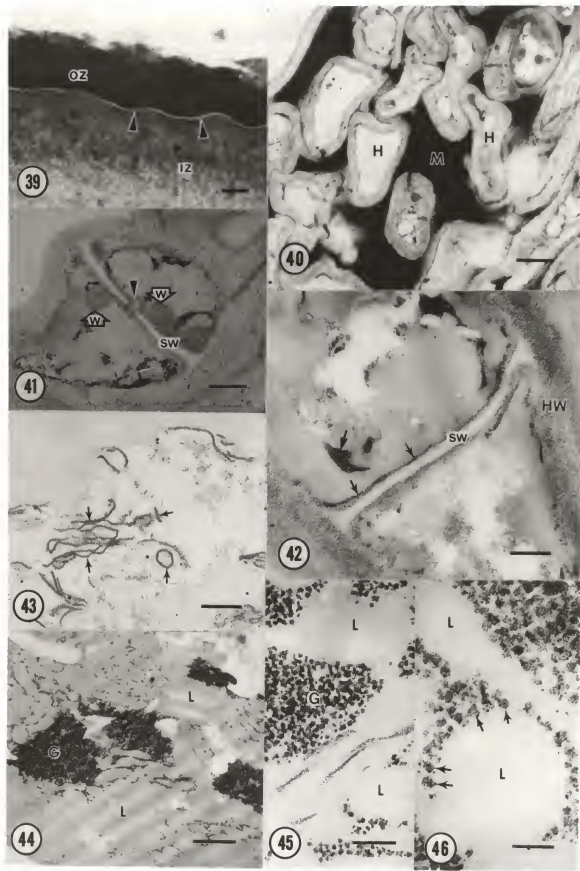
Figs. 4.34-4.38. Glaziella aurantiaca. Figs. 4.34-4.36. SEM. Figs. 4.37-4.38. TEM.

- Fig. 4.34. Collapsed spore with fragments of thin outer wall (OW) breaking away from thick inner wall (IW). Note crack in inner wall (arrows). (bar= 25  $\mu$ m).
- Fig. 4.35. Fractured spore with thick inner (IW) and thin outer (large arrows) walls separated by transition zone (small arrows). Note inner surface (IS) of inner wall. (bar= 5.0  $\mu$ m).
- Fig. 4.36. Higher magnification of Fig. 4.35 showing convoluted nature of thin, membranous partition (large arrows) of transition zone separating inner (IW) and outer (OW) walls (cf. Figs. 4.32, 4.33, and 4.38). Note wall deposits (small arrows) on inner surface of inner wall. (bar= 2.5  $\mu$ m).
- Fig. 4.37. Transverse section of outer spore wall (OW) appearing fused at points (arrows) with walls (HW) of appressed hyphae. (bar= 0.5  $\mu$ m).
- Fig. 4.38. Transverse section of spore wall showing thick inner wall (IW) separated by transition zone (bracket) from thin outer wall (OW), which is generally less electron opaque than inner wall. (bar= 1.0  $\mu$ m).



Figs. 4.39-4.46. *Glaziella aurantiaca*. Figs. 4.39-4.40. TEM with barium permanganate post stain. Figs. 4.41-4.46. TEM with silver proteinate post stain.

- Fig. 4.39. Transition zone of spore wall showing relatively electron translucent membranous partition (arrowheads) separating densely stained outer adjacent zone (OZ) from less intensely stained inner zone (IZ). (bar= 0.2  $\mu\text{m}$ ).
- Fig. 4.40. Constituent hyphae (H) of middle wall layer "cemented" together by intensely staining matrix (M). (bar= 1.0  $\mu\text{m}$ ).
- Fig. 4.41. Septum of hypha form middle layer showing little staining of septal wall (SW), plug (arrowhead), and Woronin bodies (W). (bar= 0.5  $\mu\text{m}$ ).
- Fig. 4.42. Nonmedian section of middle layer hypha showing an unstained septal wall (SW) lined with densely stained membranous material (small arrows). Note deposition of some stain (fine silver grains) on hyphal walls (HW) and clumps of apparent membranous material (large arrow) within hyphal lumen. (bar= 0.3  $\mu\text{m}$ ).
- Fig. 4.43. Intensely stained membranous fragments (arrows) within lumen of hypha of middle wall layer. (bar= 0.3  $\mu\text{m}$ ).
- Fig. 4.44. Transverse section of spore showing dense staining of apparent glycogen deposits (G) within cytoplasm between lipid globules (L). (bar= 1.0  $\mu\text{m}$ ).
- Fig. 4.45. Higher magnification of Fig. 4.44 showing glycogen (G) with individual rosettes evident between lipid globules (L). (bar= 0.2  $\mu\text{m}$ ).
- Fig. 4.46. Higher magnification of Fig. 4.44 showing rosettes of glycogen (arrows) enclosed between lipid globules (L). (bar= 0.1  $\mu\text{m}$ ).



CHAPTER V  
GENERAL CONCLUSIONS

The data from this study show a greater degree of coherence of certain genera of the Endogonaceae than was previously believed. The anomalous genus Glaziella is shown to be an ascomycete rather than a member of the Endogonaceae. The other genera of the family examined in this study (Endogone, Gigaspora, Glomus, and Sclerocystis) share certain characters that indicate close affinities with each other. The occurrence of septal perforations, a feature that has been shown for other zygomycetes, is a common theme in the genera examined, with the exception of Gigaspora for which septa were not examined. However, the outer walls of the Gigaspora species examined in this study are very similar to the zygosporangium of Endogone in staining properties, as is the outer wall of Glomus etunicatum, and thus may also be homologous to the zygosporangium.

As mentioned in Chapter III, the spore wall data, in conjunction with that of septal ultrastructure and germination mode, indicate that Gigaspora azygospores represent zygospores in which there is a reduction of one gametangium to form the peculiar, projecting hyphal appendage found in this genus. Furthermore, in this same scheme, the chlamydospores of Glomus then may represent a further reduction to a single gametangium (and possibly the loss of sexuality) with Sclerocystis representing an even further elaboration of chlamydospores into a highly organized sporocarpic configuration. Although there is no direct evidence for this particular evolutionary sequence in the Endogonaceae, at least there appears to be a greater

degree of coherence of this particular group of genera based upon these additional data.

In addition to the conclusions above, regarding the taxonomy and evolution of the Endogonaceae, the following general conclusions may be drawn regarding the individual genera and(or) species examined:

1. Endogone pisiformis is a typical zygomycete based upon the observed fusion of paired gametangia, autonomous zygosporangial and zygosporule walls, and multiperforate gametangial septa.
2. Gigaspora azygospores may be divided into two distinct groups: a) those possessing a membranous inner wall and intrawall germ chambers and, b) those without an inner membranous wall and producing germ tubes that directly penetrate all wall layers between thickenings of the innermost layer.
3. The separation of the membranous inner wall to form the germ chambers, in all the species of Gigaspora examined possessing them, occurs within a sublayer of the wall rather than at any preexisting partition.
4. The separation of species of Gigaspora based upon wall structure, especially ultrastructure, does not necessarily agree with traditional characters of separation, such as spore color.
5. Arcuate bands of microfibrils occur in the azygospore walls of Gigaspora species representing both spore types outlined above in No. 2; however, other species, also representing both spore types, do not possess these bands. Therefore, no obvious correlation exists between these bands and spore type.

6. Previous reports in the literature of cytological features such as nuclear clusters, membrane-bound phosphate granules, wall thickenings, etc. in Gigaspora are substantiated in this study; there are, however, differences in the interpretation of the data generated by this study on spore wall ultrastructure of Gigaspora margarita from that previously reported in the literature.
7. Several species of Gigaspora examined in this study have outer walls similar to the zygosporangium of Endogone pisiformis in their staining properties.
8. Although both possess septal perforations, there is no evidence from this study suggesting the synonymization of the chlamydosporic genera Glomus and Sclerocystis, since septal perforations are also reported for Endogone and represent a familial rather than a generic character.
9. The bands of microfibrils, which have been shown in the literature for Glomus epigaeus, are also shown in this study for other species of Glomus. They appear to be a common structural feature of the spore walls in species of this genus.
10. There is some degree of variation in the structure of the individual bands among the species of Glomus examined, although a high degree of similarity in the banding pattern still exists among the species possessing these bands.
11. The ephemeral outer walls of certain Glomus species are degraded by the activities of bacteria which also have been implicated in spore dormancy and germination.

12. The outer wall of Glomus etunicatum is similiar to, and possibly homologous with, the zygosporangium of Endogone in its structural and staining properties.
13. The presence of multiperforate septa in the intraradical hyphae of Glomus intraradicis associates Glomus with the type genus of the family, Endogone, which also has multiperforate septa.
14. Sclerocystis coremioides produces sporocarpic hyphae with coarse septal perforations which are similiar to the solitary perforations found in the sporocarpic hyphae of Endogone pisiformis.
15. The occurrence of septal perforations in Endogone, Glomus, and Sclerocystis indicates a closer phylogenetic association of these genera with each other and with other zygomycetes in which this type of septum is reported.
16. The ultrastructural features of the arbuscules of G. intraradicis on bahia grass shown in this study are very similiar to those reported previously in the literature for other species of Glomus, with the exception of the previously unreported vacuole membrane-bound tannin bodies.
17. Glaziella aurantiaca is an ascomycete, the ascospores of which have been mistaken in the past for chlamydospores. This taxon has no existing close relative among the ascomycetes. Its taxonomic isolation is sufficient to warrant the erection of a new order, the Glaziellales.

## BIBLIOGRAPHY

- Ames, R. N., and R. W. Schneider. 1979. Entrophospora, a new genus in the Endogonaceae. Mycotaxon 8: 347-352.
- Alexopoulos, C. J., and C. W. Mims. 1979. Introductory Mycology. Third Edition. John Wiley & Sons, New York. 632 pp.
- Atkinson, G. F. 1918. The genus Endogone. Mem. Brooklyn Bot. Gard. 1: 1-7.
- Bakerspigel, A. 1958. The structure and mode of division of the nuclei in the vegetative spores and hyphae of Endogone sphagnophila. Atk. Amer. J. Bot. 45: 404-410.
- Becker, W. N., and J. W. Gerdemann. 1977. Colorimetric quantification of vesicular-arbuscular mycorrhizal infection in onion. New Phytol. 78: 289-295.
- Becker, W. N., and I. R. Hall. 1976. Gigaspora margarita, a new species in the Endogonaceae. Mycotaxon 4: 155-160.
- Benjamin, R. K. 1966. The merosporangium. Mycologia 58: 1-42.
- Benjamin, R. K. 1979. Zygomycetes and their spores. Pp. 573-616 In: Bryce Kendrick (Ed.). The Whole Fungus, Vol. II. National Museums of Canada, Ottawa, Canada.
- Benjamin, R. K., and B. S. Mehrotra. 1963. Obligate azygospore formation in two species of Mucor (Mucorales). Aliso. 5: 235-245.
- Benny, G. L., and H. C. Aldrich. 1975. Ultrastructural observations on septal and merosporangial ontogeny in Linderina pennispora (Kickxellales; Zygomycetes). Canad. J. Bot. 53: 2325-2335.
- Benny, G. L., and K. L. O'Donnell. 1978. Syzygites melanocarpus. Pp. 127-128 In: M. S. Fuller (Ed.). Lower Fungi in the Laboratory. Palfrey Contributions in Botany No. 1, University of Georgia, Athens.
- Berch, S. M., and J. A. Fortin. 1982. Germination of zygospores of Endogone incrassata. Mycologia 74: 861-864.
- Berch, S. M., and J. A. Fortin. 1983a. Endogone pisiformis: axenic culture and associations with Sphagnum, Pinus sylvestris, Allium cepa and Allium porrum. Canad. J. Bot. 61: 899-905.
- Berch, S. M., and J. A. Fortin. 1983b. Germination of zygospores of Endogone pisiformis. Mycologia 75: 328-332.

- Berkeley, M. J. 1879. Fungi Brasiliensis in provincia Rio de Janeiro a clar. Dr. A. Glaziou lecti. Videnskabelige Meddeleser Naturh. Foren. Kjobenhaven. pp. 31.
- Berkeley, M. J., and C. E. Broome. 1873. J. Linn. Soc., Bot. 14: 137.
- Berkeley, M. J., and M. A. Curtis. 1869. Fungi Cubensis. J. Linn. Soc., Bot. 10: 280-392.
- Bessey, E. A. 1950. Morphology and Taxonomy of Fungi. McGraw-Hill, New York. 791 pp.
- Bezerra, J. L., and J. W. Kimbrough. 1982. Culture and cytological development of Rhytidhysterium rufulum on citrus. Canad. J. Bot. 60: 568-579.
- Bhattacharjee, K and K. G. Mukerji. 1982. Structure and hyperparasitism of a new species of Gigaspora. Trans. Brit. Mycol. Soc. 78: 184-188.
- Blakeslee, A. F. 1920. Sexuality in Mucors. Science 51: 375-382.
- Boedijn, K. B. 1930. Die gattung Glaziella Berkeley. Bull. Jard. Bot. Buitenzorg, Ser. 3. 11: 57-66.
- Bonfante-Fasolo, P. 1984. Anatomy and morphology of VA mycorrhizae. Pp. 5-23 In: C. L. Powell and D. J. Bagyaraj (Eds.) VA Mycorrhiza. CRC Press, Boca Raton, Florida
- Bonfante-Fasolo, P., and S. Scannerini. 1976. The ultrastructure of the zygospore in Endogone flammicorona Trappe & Gerdemann. Mycopathologia 59: 117-123.
- Bonfante-Fasolo, P., and S. Scannerini. 1977. Cytological observations on the mycorrhiza Endogone flammicorona-Pinus strobus. Allionia 22: 23-34.
- Bonfante-Fasolo, P., and B. Vian. 1984. Wall texture in the spore of a vesicular-arbuscular mycorrhizal fungus. Protoplasma 120: 51-60.
- Bucholtz F. 1912. Beitrage zur Kenntnis der Gattung Endogone Link. Beih. Bot. Centralbl., Abt.2. 29: 147-225.
- Chu-Chou, M., and L. J. Grace. 1979. Endogone flammicorona as a mycorrhizal symbiont of Douglas fir in New Zealand. New Zealand J. Forest. Sci. 9: 344-347.
- Cooke, M. C. 1883. On Xylaria and its allies. Grevillea 11: 81-94.
- Cooke, R. 1977. The Biology of Symbiotic Fungi. John Wiley & Sons, New York. 282 pp.

- Daniels, B. A., and S. O. Graham. 1976. Effects of nutrition and soil extracts on germination of Glomus mosseae spores. *Mycologia* 68: 108-116.
- Daniels, B. A., and J. M. Trappe. 1980. Factors affecting spore germination of the vesicular-arbuscular mycorrhizal fungus, Glomus epigaeus. *Mycologia* 72: 457-471.
- Danielson, R. M. 1982. Taxonomic affinities and criteria for identification of the common ectendomycorrhizal symbiont of pines. *Canad. J. Bot.* 60: 7-18.
- Fassi, B. 1965. Micorrize ectotrofiche Pinus strobus L. prodotte da un' Endogone (Endogone lactiflua Berk.). *Allionia* 11: 7-15.
- Fassi, B., A. Fontana, and J. M. Trappe. 1969. Ectomycorrhizae formed by Endogone lactiflua with species of Pinus and Pseudotsuga. *Mycologia* 61: 412-414.
- Fassi, B., and M. Palenzona. 1969. Sintesi micorrizicatra Pinus strobus, Pseudotsuga douglasii ed Endogone lactiflua. *Allionia* 15: 105-114.
- Ferrer, R. L., and R. A. Herrera. 1980. El genero Gigaspora Gerdemann et Trappe (Endogonaceae) en Cuba. *Rev. Jard. Bot. Nac., Univ. Habana* 1: 43-66.
- Gerdemann, J. W. 1955. Relation of a large soil-borne spore to phycomycetous mycorrhizal infections. *Mycologia* 47: 619-632.
- Gerdemann, J. W. 1961. A species of Endogone from corn causing vesicular-arbuscular type mycorrhiza. *Mycologia* 53: 254-261.
- Gerdemann, J. W. 1964. The effect of mycorrhizas on the growth of maize. *Mycologia* 56: 342-349.
- Gerdemann, J. W. 1975. Vesicular-arbuscular mycorrhizae. Pp. 575-591 In: J. G. Torrey and D. T. Clarkson (Eds.). *The Development and Function of Roots*. Academic Press, New York.
- Gerdemann, J. W., and B. K. Bakshi. 1976. Endogonaceae of India: Two new species. *Trans. Brit. Mycol. Soc.* 66: 340-343.
- Gerdemann, J. W., and T. H. Nicolson. 1963. Spores of mycorrhizal Endogone extracted from soil by wet sieving and decanting. *Trans. Brit. Mycol. Soc.* 46: 235-244.
- Gerdemann, J. W., and J. M. Trappe. 1970. Endogone incrassata: A zygomorphic species with hollow sporocarps. *Mycologia* 62: 1204-1208.

- Gerdemann, J. W., and J. M. Trappe. 1974. The Endogonaceae in the Pacific Northwest. *Mycologia Mem.* 5: 1-76.
- Gibson, J. L. 1984. Glaziella aurantiaca (Endogonaceae): zygomycete or ascomycete? *Mycotaxon* 20: 325-328.
- Godfrey, R. M. 1957a. Studies of British species of Endogone. I. Morphology and taxonomy. *Trans. Brit. Mycol. Soc.* 40: 136-144.
- Godfrey, R. M. 1957b. Studies of British species of Endogone. III. Germination of spores. *Trans. Brit. Mycol. Soc.* 40: 203-210.
- Hall, I. R. 1977. Species and mycorrhizal infections of New Zealand Endogonaceae. *Trans. Brit. Mycol. Soc.* 68: 341-356.
- Hall, I. R. 1984. Taxonomy of VA mycorrhizal fungi. Pp. 57-94 In: C. L. Powell and D. J. Bagyaraj (Eds.). *VA Mycorrhiza*. CRC Press, Boca Raton, Florida.
- Hall, I. R., and L. K. Abbott. 1984. Some Endogonaceae from South Western Australia. *Trans. Brit. Mycol. Soc.* 83: 203-208.
- Hall, I. R., and B. J. Fish. 1979. A key to the Endogonaceae. *Trans. Brit. Mycol. Soc.* 73: 261-270.
- Hawker, L. E., and A. Beckett. 1971. Fine structure and development of the zygospore of Rhizophorus sexualis (Smith) Callen. *Philos. Trans., Ser. B*, #263: 71-100.
- Hawksworth, D. L., B. C. Sutton, and G. C. Ainsworth. 1983. *Ainsworth & Bisby's Dictionary of the Fungi*. Seventh Edition. Commonwealth Mycological Institute. Kew, Surry. 445 pp.
- Harley, J. L., and S. E. Smith. 1983. *Mycorrhizal Symbiosis*. Academic Press, New York. 483 pp.
- Hepper, C. M. 1984. Isolation and culture of VA mycorrhizal (VAM) fungi. Pp. 95-112 In: C. L. Powell and D. J. Bagyaraj (Eds.). *VA Mycorrhiza*. CRC Press, Boca Raton, Florida.
- Hepper, C. M., and G. A. Smith. 1976. Observations on the germination of Endogone spores. *Trans. Brit. Mycol. Soc.* 66: 189-194.
- Hetrick, B. A. D., 1984. Ecology of VA mycorrhizal fungi. Pp. 35-55 In: C. L. Powell and D. J. Bagyaraj (Eds.). *VA Mycorrhiza*. CRC Press, Boca Raton, Florida.
- Hoch, H. C. 1977. Use of permanganate to increase electron opacity of fungal walls. *Mycologia* 69: 1209-1213.

- Höhnel, F. von. 1910. Sclerocystis coremioides Berk. et Br. Sitzungber. Kaiserl. Akad. Wiss. Wein Math.-Naturwiss. Kl. Abt. I. 119: 398-399.
- Höhnel F. von. 1913. Fragmente zur Mykologie. XV. Mitteilung Nr. 805. Endogonella n.g. (Endogoneae). Sitzungsber. Kaiserl. Acad. Wiss., Math.-Naturwiss. Kl., Abt. 1. Bd. CXXII. pp. 294-296.
- Jeffries, P., and T. W. K. Young. 1983. Light and electron microscopy of vegetative hyphae, septum formation, and yeast-mould dimorphism in Cokeromyces recurvatus. *Protoplasma* 117: 206-213.
- Jenkins, W. R. 1964. A rapid centrifugal-flotation technique for separating nematodes from soil. *Pl. Dis. Reporter* 48: 692.
- Kanouse, B. B. 1936. Studies of two species of Endogone in culture. *Mycologia* 28: 47-62.
- Korf, R. P. 1958. Japanese Discomycete Notes I-VIII. Sci. Rep. Yokohama Natl. Univ., Sec. 2, Biol. Ser. 7: 7-35.
- Koske, R. E., D. D. Miller, and C. Walker. 1983. Gigaspora reticulata: A newly described endomycorrhizal fungus from New England. *Mycotaxon* 16: 429-435.
- Malloch, D., and R. F. Cain. 1971. New cleistothelial Sordariaceae and a new family, Coniochaetaceae. *Canad. J. Bot.* 49: 869-880.
- MacDonald, R. M., and M. R. Chandler. 1981. Bacterium-like organelles in the vesicular-arbuscular mycorrhizal fungus Glomus caledonius. *New Phytol.* 89: 241-246.
- Marinozzi, V. 1961. Silver impregnation of ultrathin sections for electron microscopy. *J. Biophys. Biochem. Cytology* 9: 121.
- McLaughlin, D. J. 1974. Ultrastructural localization of carbohydrate in the hymenium and subhymenium of Coprinus. Evidence for the function of the Golgi apparatus. *Protoplasma* 84: 341-346.
- Menge, J. A. 1983. Utilization of vesicular-arbuscular mycorrhizal fungi in agriculture. *Canad. J. Bot.* 61: 1015-1024.
- Misra, P. C., N. N. Gupta, and K. Lata. 1979. A new species of Fennellomyces (Mucorales). *Mycotaxon* 10: 251-254.
- Mistry, A. 1977. Zygospore development in Absidia spinosa and Radiomyces spectabilis (Mucorales). *Microbiol. Lett.* 4: 35-39.
- Moreau, F. 1953. Les Champignons. Tome II. Systématique. Encycl. Mycol. 23: 941-2120. Lechevalier, Paris.

- Mosse, B. 1953. Fructifications associated with mycorrhizal strawberry roots. *Nature* 171: 974.
- Mosse, B. 1956. Fructifications of an Endogone species causing endotrophic mycorrhiza in fruit plants. *Ann. Bot. (London)* 20: 349-362.
- Mosse, B. 1957. Growth and chemical composition of mycorrhizal and non-mycorrhizal apples. *Nature* 179: 922-924.
- Mosse, B. 1959. The regular germination of resting spores and some observations on the growth requirements of an Endogone sp. causing vesicular-arbuscular mycorrhiza. *Trans. Brit. Mycol. Soc.* 42: 273-286.
- Mosse, B. 1970a. Honey-coloured, sessile Endogone spores. I. Life history. *Archiv Mikrobiol.* 70: 167-175.
- Mosse, B. 1970b. Honey-coloured, sessile Endogone spores. II. Changes in fine structure during spore development. *Archiv Mikrobiol.* 74: 129-145.
- Mosse, B. 1970c. Honey-coloured, sessile Endogone spores. III. Wall structure. *Archiv Mikrobiol.* 74: 146-159.
- Nicolson, T. H. 1967. Vesicular-arbuscular mycorrhiza--a universal plant symbiosis. *Sci. Prog., Oxford* 55: 561-581.
- Nicolson, T. H., and J. W. Gerdemann. 1968. Mycorrhizal Endogone species. *Mycologia* 60: 313-325.
- Nicolson, T. H., and N. C. Schenck. 1979. Endogonaceous mycorrhizal endophytes in Florida. *Mycologia* 71: 178-198.
- O'Donnell, K. L., J. J. Ellis, C. W. Hesseltine, and G. R. Hooper. 1977a. Azygosporogenesis in Mucor azygsporus. *Canad. J. Bot.* 55: 2712-2720.
- O'Donnell, K. L., J. J. Ellis, C. W. Hesseltine, and G. R. Hooper. 1977b. Morphogenesis of azygospores induced in Gilbertella persicaria (+) by imperfect hybridization with Rhizopus stolonifer (-). *Canad. J. Bot.* 55: 2721-2727.
- O'Donnell, K. L., S. L. Flegler, J. J. Ellis, and C. W. Hesseltine. 1978. The Zygorhynchus zygosporangium and zygospore. *Canad. J. Bot.* 56: 1061-1073.
- O'Donnell, K. L., G. R. Hooper, and W. G. Fields. 1976. Zygosporogenesis in Phycomyces blakesleeanus. *Canad. J. Bot.* 54: 2573-2586.

- Old, K. M., T. H. Nicolson and J. F. Redhead. 1973. A new species of mycorrhizal Endogone from Nigeria with a distinctive spore wall. New Phytol. 72: 817-823.
- Parke, J. L., and R. G. Linderman. 1980. Association of vesicular-arbuscular mycorrhizal fungi with the moss Funaria hygrometrica. Canad. J. Bot. 58: 1898-1904.
- Patouillard, N. 1902. Ackermannia Pat. Bull. Soc. Mycol. France 18: 180-181.
- Quattlebaum, E. C., and G. R. Carner. 1980. A technique for preparing Beauveria spp. for scanning electron microscopy. Canad. J. Bot. 58: 1700-1703.
- Reynolds, E. S. 1963. The use of lead citrate at high pH as an electron opaque stain in electron microscopy. J. Cell Biol. 17: 202-208.
- Richardson, K. C., L. Jarett, and E. H. Finke. 1960. Embedding in epoxy resins for ultrathin sectioning in electron microscopy. Stain Technol. 35: 313-323.
- Scannerini, S., and P. Bonfante-Fasolo. 1977. Unusual plastids in an endomycorrhizal root. Canad. J. Bot. 55: 2471-2474.
- Scannerini, S., and P. Bonfante-Fasolo. 1983. Comparative ultrastructural analysis of mycorrhizal associations. Canad. J. Bot. 61: 917-943.
- Scannerini, S., P. F. Bonfante, and A. Fontana. 1975. An ultrastructural model for the host-symbiont interaction in the endotrophic mycorrhizae of Ornithogalum umbellatum L. pp. 179-200 In: F. E. Sanders, B. Mosse, and P. B. Tinker (Eds.). Endomycorrhizas. Academic Press, New York.
- Schenck, N. C. 1983. Introduction. pp. ix-x In: N. C. Schenck (Ed.). Methods and Principles of Mycorrhizal Research. American Phytopathological Society, St. Paul, Minnesota.
- Schenck, N. C., and G. S. Smith. 1982. Additional new and unreported species of mycorrhizal fungi (Endogonaceae) from Florida. Mycologia 74: 77-92.
- Schenck, N. C., J. L. Spain, E. Sieverding, and R. H. Howeler. 1984. Several new and unreported vesicular-arbuscular mycorrhizal fungi (Endogonaceae) from Colombia. Mycologia 76: 685-699.
- Spurr, A. R. 1969. A low-viscosity epoxy resin embedding medium for electron microscopy. J. Ultrastruct. Res. 26: 31-43.

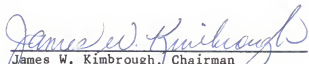
- Stevens, R. B. (Ed.). 1974. Mycology Guidebook. University of Washington Press, Seattle. 703 pp.
- Sward, R. J. 1981a. The structure of the spores of Gigaspora margarita. I. The dormant spore. New Phytol. 87: 761-768.
- Sward, R. J. 1981b. The structure of the spores of Gigaspora margarita. II. Changes accompanying germination. New Phytol. 88: 661-666.
- Sward, R. J. 1981c. The structure of the spores of Gigaspora margarita. III. Germ tube emergence and growth. New Phytol. 88: 667-674.
- Thaxter, R. 1922. A revision of the Endogoneae. Proc. Amer. Acad. Arts 57: 291-351.
- Thiéry, J.-P. 1967. Mise en evidence des polysaccharides sur coupes fines en microscopie electronique. J. Microscop. 6: 987-1018.
- Trappe, J. M. 1977. Three new Endogonaceae: Glomus constrictus, Sclerocystis clavispora, and Acaulospora scrobiculata. Mycotaxon 6: 359-366.
- Trappe, J. M. 1979. The orders, families, and genera of hypogeous Ascomycotina (truffles and their relatives). Mycotaxon 9: 297-340.
- Trappe, J. M. 1982. Synoptic keys to the genera and species of zygomycetous mycorrhizal fungi. Phytopathol. 72: 1102-1108.
- Trappe, J. M., and J. W. Gerdemann. 1972. Endogone flammicorona sp. nov., a distinctive segregate from Endogone lactiflua. Trans. Brit. Mycol. Soc. 59: 403-407.
- Trappe, J. M., and N. C. Schenck. 1982. Taxonomy of the fungi forming endomycorrhizae. Pp. 1-9 In: N. C. Schenck (Ed). Methods and Principles of Mycorrhizal Research. The American Phytopathological Society, St. Paul, Minnesota. 244 pp.
- Tulasne, L. R., and C. Tulasne. 1845. Fungi nonnulli hypogaei, novi v. minus cogniti act. Giorn. Bot. Ital. 2: 35-63.
- Tulasne, L. R., and C. Tulasne. 1851. Fungi Hypogaei. Histoire et monographie des champignons hypoges. pp. 181-183.
- Uecker, F. A., and F. G. Pollack. 1974. Development and cytology of Monosporascus cannonballus. Bot. Gaz. 136: 333-340.
- Walker, C. 1979. Complexipes moniliformis: a new genus and species tentatively placed in the Endogonaceae. Mycotaxon 8: 347-349.

- Walker, C. 1983. Taxonomic concepts in the Endogonaceae; spore wall characteristics in species descriptions. *Mycotaxon* 18: 443-455.
- Walker, C., and J. M. Trappe. 1981. Acaulospora spinosa sp. nov. with a key to the species of Acaulospora. *Mycotaxon* 12: 515-521.
- Warcup, J. H. 1975. A culturable Endogone associated with eucalypts. Pp. 53-63 In: F. E. Sanders, B. Mosse, and P. B. Tinker (Eds.). *Endomycorrhizas*. Academic Press, London. 626 pp.
- Watrud, L. S., J. J. Heithaus and E. G. Jaworski. 1978. Evidence of production of inhibitor by the vesicular-arbuscular mycorrhizal fungus Gigaspora margarita. *Mycologia* 70: 821-828.
- White, J. A., and M. F. Brown. 1979. Ultrastructure and X-ray analysis of phosphorus granules in a vesicular-arbuscular mycorrhizal fungus. 57: 2812-2818.
- Zycha, H. 1935. Mucorineae. *Kryptogamenflora Mark Brandenburg* 6a, Leipzig. 264 pp.
- Zycha, H., R. Siepmann, and G. Linnemann. 1969. Mucorales. *J. Cramer, Lehre*. 355 pp.

#### BIOGRAPHICAL SKETCH

Jack Lee Gibson was born in Ferndale, Michigan, on April 15, 1950, but his family soon moved to eastern Tennessee, where he attended elementary and middle school. His family then moved to Miami, Florida, where he graduated from high school. After service in the U.S. Navy he earned a Bachelor of Science degree in biology in 1975 from Florida International University, Miami, and subsequently earned a second Bachelor of Science degree in secondary education from the same institution before entering graduate school at the University of Florida in September, 1978. He completed the Master of Science in Teaching (botany) in 1980 and entered the Ph.D. program in botany. After completion of the doctorate, he will continue in the Department of Botany on a Post-doctoral Fellowship with Prof. James W. Kimbrough.

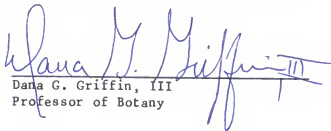
I certify that I have read this study and that in my opinion it conforms to acceptable standards of scholarly presentation, in scope and quality, as a dissertation for the degree of Doctor of Philosophy.

  
James W. Kimbrough, Chairman  
Professor of Botany

I certify that I have read this study and that in my opinion it conforms to acceptable standards of scholarly presentation, in scope and quality, as a dissertation for the degree of Doctor of Philosophy.

  
Henry C. Aldrich  
Professor of Microbiology  
and Cell Science

I certify that I have read this study and that in my opinion it conforms to acceptable standards of scholarly presentation, in scope and quality, as a dissertation for the degree of Doctor of Philosophy.

  
Dana G. Griffin, III  
Professor of Botany

I certify that I have read this study and that in my opinion it conforms to acceptable standards of scholarly presentation, in scope and quality, as a dissertation for the degree of Doctor of Philosophy.

  
Walter S. Judd  
Associate Professor of Botany

I certify that I have read this study and that in my opinion it conforms to acceptable standards of scholarly presentation and is fully adequate, in scope and quality, as a dissertation for the degree of Doctor of Philosophy.

Norman C. Schenck

Norman C. Schenck

Professor of Plant Pathology

This dissertation was submitted to the Graduate Faculty of the Department of Botany in the College of Liberal Arts and Sciences and to the Graduate School, and was accepted as partial fulfillment of the requirements for the degree of Doctor of Philosophy.

May, 1985

---

Dean for Graduate Studies  
and Research